Modeling structures with piezoelectric materials

Theory and SDT Tutorial

Etienne Balmes
Arnaud Deraemaeker

SDTools
44 rue Vergniaud
75013 Paris (France)
Tel. +33 1 44 24 63 71
General info http://www.sdtools.com
Support http://support.sdtools.com

Contents

Theory and reference

Contents

This chapter summarizes theoretical concepts associated with piezoelectricity and gives supporting examples. Release notes are given in the next section.

1.1 Release notes

This manual gives a more detailed set of examples for the use of SDT for the modeling of piezoelectric structures.
Major modifications for SDT 7.1 are

- Inclusion of new materials (Ferroperm, Sonox, MFCs) in the `m_piezo` database.
- Introduction of tutorials in `d_piezo('Tuto')`.
- New script for Macro Fiber Composites in `d_piezo('TutoPlate_mfc')`.
- Theory and new script for point load actuator using a shaped triangular piezoelectric transducer in `d_piezo('TutoPlate_triang')`.
- Theory and new script for vibration damping using RL shunt and piezoelectric patches in `d_piezo('TutoPz_shunt')`.
- Theory and new script for piezoelectric homogenization on RVEs of piezocomposites (application to MFCs) in `d_piezo('TutoPz_P1_homo')` and `d_piezo('TutoPz_P2_homo')` .
- Color visualization of stress and strain added to IDE patch script `d_piezo('TutoPatch_num_IDE')`.

Major modifications for SDT 6.6 were

- Writing of the present manual
- Significant generalization of `p_piezo('Electrode')` commands.
- Inclusion of elastic properties in the `m_piezo` database.
- Introduction of electrical and charge viewing illustrated in this manual.
- Specialized meshing capabilities and examples are grouped in `d_piezo('Mesh')`.

1.2 Basics of piezoelectricity

Polarization consists in the separation of positive and negative electric charges at different ends of the dielectric material on the application of an external electric field (Figure 1.1).

Spontaneous polarization is the phenomenon by which polarization appears without the application of an external electric field. Spontaneous polarization has been observed in certain crystals in which the centers of positive and negative charges do not coincide. Spontaneous polarization can occur more easily in perovskite crystal structures.

The level and direction of the polarization is described by the electric displacement vector D:

$$D = \varepsilon E + P \tag{1.1}$$

where P is the *permanent polarization* which is retained even in the absence of an external electric field, and εE represents the polarization induced by an applied electric field. ε is the dielectric permittivity. If no spontaneous polarization exists in the material, the process through which permanent polarization is induced in a material is known as *poling*.

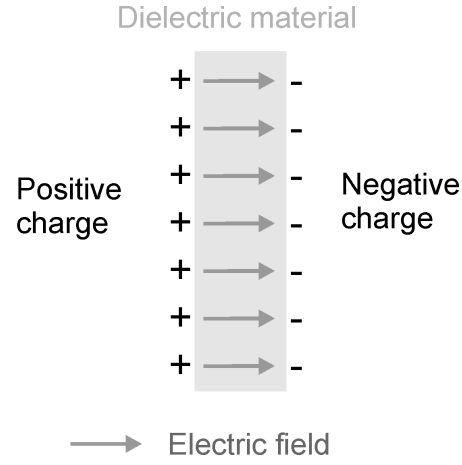

Figure 1.1: Polarization: separation of positive and negative electric charges on the two sides of a dielectric material

Ferroelectric materials have permanent polarization that can be altered by the application of an external electric field, which corresponds to poling of the material. As an example, perovskite structures are ferroelectric below the *Curie temperature*. In the ferroelectric phase, polarization can therefore be induced by the application of a (large) electric field.

Piezoelectricity was discovered by Pierre and Jacques Curie in 1880. The *direct piezoelectric effect* is the property of a material to display electric charge on its surface under the application of an external mechanical stress (i.e. to change its polarization). (Figure 1.2a). *The converse piezoelectric effect* is the production of a mechanical strain due to a change in polarization (Figure 1.2b).

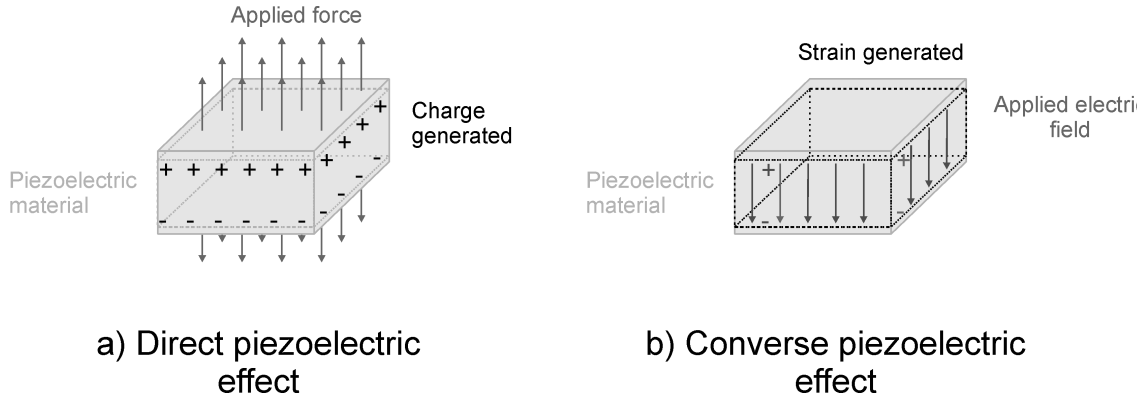

Figure 1.2: Direct and converse piezoelectric effect

Piezoelectricity occurs naturally in non ferroelectric single crystals such as quartz, but the effect is not very strong, although it is very stable. The direct effect is due to a distortion of the crystal lattice caused by the applied mechanical stress resulting in the appearance of electrical dipoles. Conversely, an electric field applied to the crystal causes a distortion of the lattice resulting in an induced mechanical strain. In other materials, piezoelectricity can be induced through *poling*. This can be achieved in *ferroelectric crystals, ceramics or polymers*.

A piezoelectric ceramic is produced by pressing ferroelectric material grains (typically a few micrometers in diameter) together. During fabrication, the ceramic powder is heated (sintering process) above Curie temperature. As it cools down, the perovskite ceramic undergoes phase transformation from the paraelectric state to the ferroelectric state, resulting in the formation of randomly oriented ferroelectric domains . These domains are arranged in grains, containing either 90ï¿½ or 180ï¿½ domains (Figure 1.3a). This random orientation leads to zero (or negligible) net polarization and piezoelectric coefficients (Figure 1.3b)).

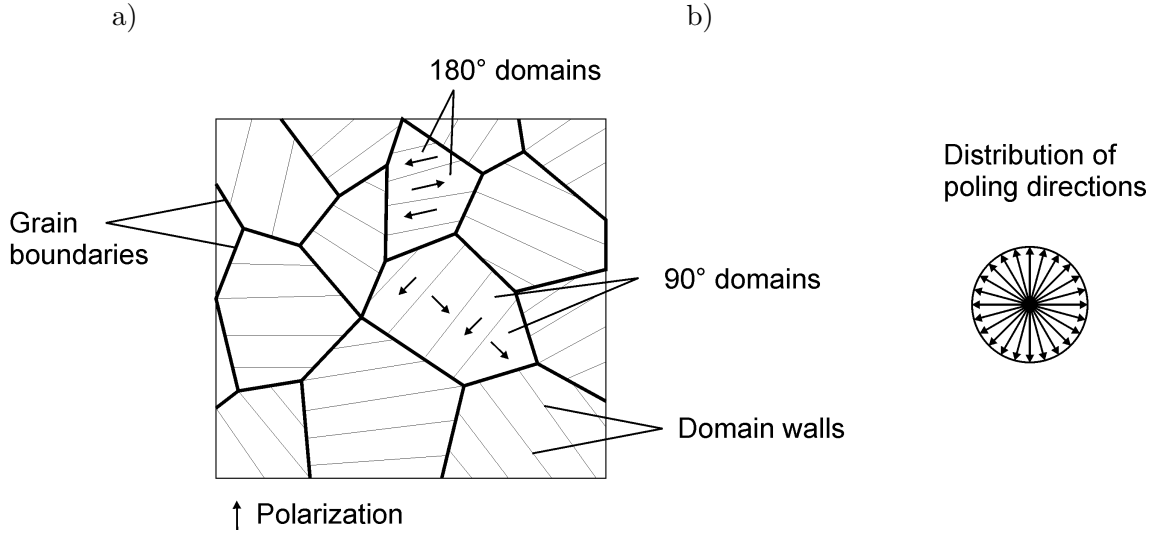

Figure 1.3: Piezoelectric ceramic : a) ferroelectric grains and domains, b) distribution of poling directions

The application of a sufficiently high electric field to the ceramic causes the domains to reorient in the direction of the applied electric field. Note however that the mobility of the domains is not such that all domains are perfectly aligned in the poling direction, but the total net polarization increases with the magnitude of the electric field (Figure 1.4). After removal of the applied electric field, the ferroelectric domains do not return in their initial orientation and a permanent polarization remains in the direction of the applied electric field (the poling direction). In this state, the application of a moderate electric field results in domain motions which are responsible for a deformation of the ceramic and are the source of the piezoelectric effect. The poling direction is therefore a very important material property of piezoelectric materials and needs to be known for a proper modeling.

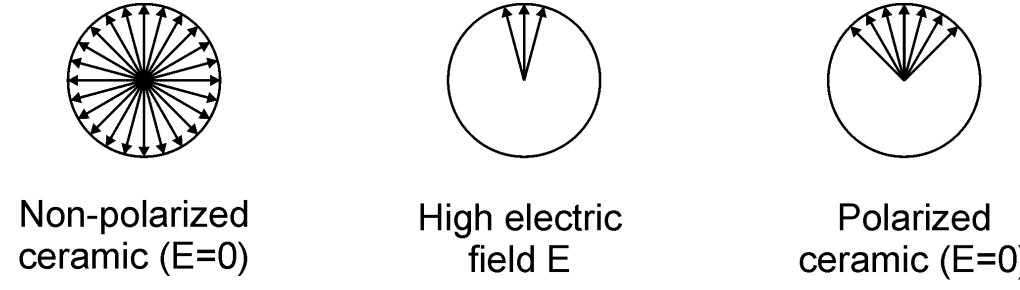

Figure 1.4: Orientation of the ferroelectric domains in non-polarized and polarized ceramics

Typical examples of simple perovskites are Barium titanate ($BaTiO3$) and lead titanate ($PbTiO3$). The most common perovskite alloy is lead zirconate titanate (PZT- PbZr TiO3). Nowadays, the most common ceramic used in piezoelectric structures for structural dynamics applications (active control, shape control, structural health monitoring) is PZT, which will be used extensively in the documented examples.

In certain polymers, piezoelectricity can be obtained by orienting the molecular dipoles within the polymer chain. Similarly to the ferroelectric domains in ceramics, in the natural state, the molecular dipole moments usually cancel each other resulting in an almost zero macroscopic dipole. Poling of the polymer is usually performed by stretching the polymer and applying a very high electric field, which causes the molecular dipoles to orient with the electric field, and remain orientated in this preferential direction after removal of the electric field (permanent polarization). This gives rise to piezoelectricity in the polymer. The technology of piezoelectric polymers has been largely dominated by ferroelectric polymers from the polyvinylidene fluoride (PVDF) family, discovered in 1969. The main advantage is the good flexibility, but their piezoelectric coefficients are much lower compared to ferroelectric ceramics.

1.2.1 Piezoelectric constitutive laws in 3D

Up to a certain level of electric field and strain, piezoelectric materials behave linearly. This tutorial is restricted to linear piezoelectricity, but the interested reader can refer to [1] for more details on non-linear piezoelectricity.

Assuming a linear piezoelectric material and adopting the notations of the IEEE Standards on piezoelectricity [2], the 3D constitutive equations are given by:

$$\begin{Bmatrix} T_1 \\ T_2 \\ T_3 \\ T_4 \\ T_5 \\ T_6 \\ D_1 \\ D_2 \\ D_3 \end{Bmatrix} = \begin{bmatrix} c_{11}^E & c_{12}^E & c_{13}^E & 0 & 0 & 0 & 0 & 0 & -e_{31} \\ c_{12}^E & c_{22}^E & c_{23}^E & 0 & 0 & 0 & 0 & 0 & -e_{32} \\ c_{13}^E & c_{23}^E & c_{33}^E & 0 & 0 & 0 & 0 & 0 & -e_{33} \\ 0 & 0 & 0 & c_{44}^E & 0 & 0 & 0 & -e_{24} & 0 \\ 0 & 0 & 0 & 0 & c_{55}^E & 0 & -e_{15} & 0 & 0 \\ 0 & 0 & 0 & 0 & 0 & c_{66}^E & 0 & 0 & 0 \\ 0 & 0 & 0 & 0 & e_{15} & 0 & \varepsilon_{11}^S & 0 & 0 \\ 0 & 0 & 0 & e_{24} & 0 & 0 & 0 & \varepsilon_{22}^S & 0 \\ e_{31} & e_{32} & e_{33} & & 0 & 0 & 0 & 0 & \varepsilon_{33}^S \end{bmatrix} \begin{Bmatrix} S_1 \\ S_2 \\ S_3 \\ S_4 \\ S_5 \\ S_6 \\ E_1 \\ E_2 \\ E_3 \end{Bmatrix} \tag{1.2}$$

where E_i and D_i are the components of the electric field vector and the electric displacement vector, and T_i and S_i are the components of stress and strain vectors, defined according to:

$$\left\{\begin{array}{c} T_1 \\ T_2 \\ T_3 \\ T_4 \\ T_5 \\ T_6 \end{array}\right\} = \left\{\begin{array}{c} T_{11} \\ T_{22} \\ T_{33} \\ T_{23} \\ T_{13} \\ T_{12} \end{array}\right\} \qquad \left\{\begin{array}{c} S_1 \\ S_2 \\ S_3 \\ S_4 \\ S_5 \\ S_6 \end{array}\right\} = \left\{\begin{array}{c} S_{11} \\ S_{22} \\ S_{33} \\ 2\,S_{23} \\ 2\,S_{13} \\ 2\,S_{12} \end{array}\right\} \tag{1.3}$$

Matrix notations are usually adopted leading to:

$$\begin{array}{l} \{T\} = \left[C^E\right]\{S\} - [e]^T\{E\} \\ \{D\} = [e]\{S\} + \left[\varepsilon^S\right]\{E\} \end{array} \tag{1.4}$$

A widely used alternative and equivalent representation consists in writing the constitutive equations in the following form:

$$\begin{array}{l} \{S\} = \left[s^E\right]\{T\} + [d]^T\{E\} \\ \{D\} = [d]\{T\} + \left[\varepsilon^T\right]\{E\} \end{array} \tag{1.5}$$

where the following relationships hold:

$$\left[s^E\right] = \left[c^E\right]^{-1} \tag{1.6}$$

$$[e] = [d]\left[c^E\right] \tag{1.7}$$

$$\left[\varepsilon^S\right] = \left[\varepsilon^T\right] - [d]\,[e]^T \tag{1.8}$$

There are also two additional possibilities to write these constitutive equations, which are less commonly used but are given here for completeness:

$$\begin{array}{l} \{S\} = \left[s^D\right]\{T\} + [g]^T\{D\} \\ \{E\} = -[g]\{T\} + \left[\beta^T\right]\{D\} \end{array} \tag{1.9}$$

$$\begin{array}{l} \{T\} = \left[c^D\right]\{S\} - [h]^T\{D\} \\ \{E\} = -[h]\{S\} + \left[\beta^S\right]\{D\} \end{array} \tag{1.10}$$

The following relationships hold:

$$\left[c^D\right]\left[s^D\right] = I_6 \tag{1.11}$$

$$\begin{array}{l} \left[\beta^S\right]\left[\varepsilon^S\right] = \left[\beta^T\right]\left[\varepsilon^T\right] = I_3 \\ \left[c^D\right] = \left[c^E\right] + [e]^T[h] \\ \left[s^D\right] = \left[c^D\right] - [d]^T[g] \\ \left[\beta^S\right] = \left[\beta^T\right] - [g]^T[h] \\ [d] = \left[\varepsilon^T\right][g] \\ [g] = [h]\left[s^D\right] \end{array} \tag{1.12}$$

$$[h] = \left[\varepsilon^S\right][e] \tag{1.13}$$

The piezoelectric coefficients are contained in the matrix $[d]$ whose structure is specific to each type of piezoelectric material. The typical structure for a z-polarized PZT material is

$$[d] = \begin{bmatrix} 0 & 0 & 0 & 0 & d_{15} & 0 \\ 0 & 0 & 0 & d_{24} & 0 & 0 \\ d_{31} & d_{32} & d_{33} & 0 & 0 & 0 \end{bmatrix} \tag{1.14}$$

Regular PZT ceramics are isotropic in the plane perpendicular to the poling direction ($d_{31} = d_{32}$, $d_{15} = d_{24}$), but piezoelectric composites can have orthotropic properties [3]. PVDF material does not exhibit piezoelectricity in the shear mode, so that the typical structure is:

$$[d] = \begin{bmatrix} 0 & 0 & 0 & 0 & 0 & 0 \\ 0 & 0 & 0 & 0 & 0 & 0 \\ d_{31} & d_{32} & d_{33} & 0 & 0 & 0 \end{bmatrix} \tag{1.15}$$

PVDF can be either isotropic or orthotropic in the plane perpendicular to the poling direction, depending on the fabrication process (uni-axial or bi-axial). Table 1.1 gives typical piezoelectric coefficients for PZT ceramics and PVDF films. Note that these properties can vary significantly from the figures in the table, as there are many different material types. The permittivity is usually given with its relative value which is the ratio of the permittivity by the permittivity of vacuum ($\varepsilon_0 = 8.854\,10^{-12} F/m$).

Material properties	PZT	PVDF (bi-axial)
Piezoelectric properties		
d_{33} (pC/N)	440	-25
d_{31} (pC/N)	-185	3
d_{32} (pC/N)	-185	3
Relative permittivity		
ε_r	1800	12
Young's Modulus		
$Y_1(GPa)$	54	3
$Y_2(GPA)$	54	3
$Y_3(GPA)$	48	10
ρ (kg/m^3)	7600	1800

Table 1.1: Typical piezoelectric properties of PZT ceramics and PVDF films

1.2.2 Piezoelectric constitutive laws in plates

When thin piezoelectric transducers are used with plate structures, the common plane stress hypothesis ($T_3 = 0$) must be used together with an hypothesis for the electric field. When the ceramic is poled through the thickness, the hypothesis commonly adopted is that the electric field is zero in the plane of the transducer ($E_1 = E_2 = 0$). The constitutive equations then reduce to:

$$\begin{Bmatrix} T_1 \\ T_2 \\ T_4 \\ T_5 \\ T_6 \\ D_3 \end{Bmatrix} = \begin{bmatrix} c_{11}^{E*} & c_{12}^{E*} & 0 & 0 & 0 & -e_{31}^{*} \\ c_{12}^{E*} & c_{22}^{E*} & 0 & 0 & 0 & -e_{32}^{*} \\ 0 & 0 & c_{44}^{E*} & 0 & 0 & 0 \\ 0 & 0 & 0 & c_{55}^{E*} & 0 & 0 \\ 0 & 0 & 0 & 0 & c_{66}^{E*} & 0 \\ e_{31}^{*} & e_{32}^{*} & 0 & 0 & 0 & \varepsilon_{33}^{S*} \end{bmatrix} \begin{Bmatrix} S_1 \\ S_2 \\ S_4 \\ S_5 \\ S_6 \\ E_3 \end{Bmatrix} \tag{1.16}$$

where the superscript * denotes the properties under the "piezoelectric plates" hypothesis ($T_3 = E_1 = E_2 = 0$). These properties are related to the 3D properties with the following relationships:

$$c_{11}^{E*} = \left[c_{11}^{E} - \frac{(c_{13}^{E})^2}{c_{33}^{E}} \right] \tag{1.17}$$

$$c_{12}^{E*} = \left[c_{12}^{E} - \frac{c_{13}^{E}\, c_{23}^{E}}{c_{33}^{E}} \right] \tag{1.18}$$

$$c_{22}^{E*} = \left[c_{22}^{E} - \frac{(c_{23}^{E})^2}{c_{33}^{E}} \right] \tag{1.19}$$

$$e^*_{31} = \left[e_{31} - \frac{c^E_{13}\, e_{33}}{c^E_{33}} \right] \tag{1.20}$$

$$e^*_{32} = \left[e_{32} - \frac{c^E_{23}\, e_{33}}{c^E_{33}} \right] \tag{1.21}$$

$$\varepsilon^{S*}_{33} = \left[\varepsilon^S_{33} + \frac{(e_{33})^2}{c^E_{33}} \right] \tag{1.22}$$

The distinction is very important, as it is often not well understood and many errors can arise from the confusion between plate and 3D properties of piezoelectric materials. Note however that the d_{ij}, s^E_{ij} and ε^T coefficients are equal for plate and 3D constitutive equations. It is therefore preferable to handle the material properties of piezoelectric materials in the form of (1.5).

Similarly to the 3D equations, the constitutive equations can be written in a matrix form, separating the mechanical and the electrical parts:

$$\begin{aligned} \{T\} &= \left[c^{E*}\right] \{S\} - [e^*]^T \{E\} \\ \{D\} &= [e^*] \{S\} + \left[\varepsilon^{S*}\right] \{E\} \end{aligned} \tag{1.23}$$

Using (1.7) in equations ((1.20),(1.21),(1.22)), one can further show that

$$[e^*] = [d^*] \left[c^{E*}\right] \tag{1.24}$$

and for the permittivity:

$$\varepsilon^{S*}_{33} = \varepsilon^T_{33} - [d^*] [e^*]^T \tag{1.25}$$

with

$$[d^*] = \begin{bmatrix} d_{31} & d_{32} & 0 & 0 & 0 \end{bmatrix} \tag{1.26}$$

and

$$[e^*] = \begin{bmatrix} e^*_{31} & e^*_{32} & 0 & 0 & 0 \end{bmatrix} \tag{1.27}$$

The values of e^*_{31}, e^*_{32} and ε^{S*}_{33} can therefore be computed knowing the elastic matrix $\left[c^{E*}\right]$ and the values of d_{31} and d_{32} and ε^T_{33}

1.2.3 Database of piezoelectric materials

`m_piezo Dbval` includes a number of material characteristics for piezoelectric materials. The properties are obtained from the datasheet of the material, but as we will illustrate, the data is not always sufficient to calculate all the material properties needed for the computations. Most of the

information in the datasheet is generally related to the constitutive equations written in the form of (1.5). For PZT, PVDF, or piezoelectric composites based on PZT and PVDF, the general form of these matrices is:

$$\begin{Bmatrix} S_1 \\ S_2 \\ S_3 \\ S_4 \\ S_5 \\ S_6 \\ D_1 \\ D_2 \\ D_3 \end{Bmatrix} = \begin{bmatrix} s_{11}^E & s_{12}^E & s_{13}^E & 0 & 0 & 0 & 0 & 0 & d_{31} \\ s_{12}^E & s_{22}^E & s_{23}^E & 0 & 0 & 0 & 0 & 0 & d_{32} \\ s_{13}^E & s_{23}^E & s_{33}^E & 0 & 0 & 0 & 0 & 0 & d_{33} \\ 0 & 0 & 0 & s_{44}^E & 0 & 0 & 0 & d_{24} & 0 \\ 0 & 0 & 0 & 0 & s_{55}^E & 0 & d_{15} & 0 & 0 \\ 0 & 0 & 0 & 0 & 0 & s_{66}^E & 0 & 0 & 0 \\ 0 & 0 & 0 & 0 & d_{15} & 0 & \varepsilon_{11}^T & 0 & 0 \\ 0 & 0 & 0 & d_{24} & 0 & 0 & 0 & \varepsilon_{22}^T & 0 \\ d_{31} & d_{32} & d_{33} & & 0 & 0 & 0 & 0 & \varepsilon_{33}^T \end{bmatrix} \begin{Bmatrix} T_1 \\ T_2 \\ T_3 \\ T_4 \\ T_5 \\ T_6 \\ E_1 \\ E_2 \\ E_3 \end{Bmatrix} \tag{1.28}$$

For an orthotropic material, the compliance matrix $\left[s^E\right]$ can be written as a function of the engineering constant E_i,ν_{ij} and G_{ij} as follows:

$$\left[s^E\right] = \begin{bmatrix} \frac{1}{E_x} & \frac{-\nu_{yx}}{E_y} & \frac{-\nu_{zx}}{E_z} & 0 & 0 & 0 \\ \frac{-\nu_{xy}}{E_x} & \frac{1}{E_y} & \frac{-\nu_{zy}}{E_z} & 0 & 0 & 0 \\ \frac{-\nu_{xz}}{E_x} & \frac{-\nu_{yz}}{E_y} & \frac{1}{E_z} & 0 & 0 & 0 \\ 0 & 0 & 0 & \frac{1}{G_{yz}} & 0 & 0 \\ 0 & 0 & 0 & 0 & \frac{1}{G_{xz}} & 0 \\ 0 & 0 & 0 & 0 & 0 & \frac{1}{G_{xy}} \end{bmatrix} \tag{1.29}$$

where z is aligned with the poling direction 3, and x, y with directions $1, 2$ respectively. Note that the matrix is symmetric so that:

$$\frac{\nu_{yx}}{E_y} = \frac{\nu_{xy}}{E_x}, \quad \frac{\nu_{zx}}{E_z} = \frac{\nu_{xz}}{E_x}, \quad \frac{\nu_{zy}}{E_z} = \frac{\nu_{yz}}{E_y} \tag{1.30}$$

A bulk piezoelectric ceramic exhibits transverse isotropic properties: the properties of the material are the same in the plane perpendicular to the poling direction. In this case, the compliance matrix reduces to:

$$\left[s^E\right] = \begin{bmatrix} \frac{1}{E_p} & \frac{-\nu_p}{E_p} & \frac{-\nu_{zp}}{E_z} & 0 & 0 & 0 \\ \frac{-\nu_p}{E_p} & \frac{1}{E_p} & \frac{-\nu_{zp}}{E_z} & 0 & 0 & 0 \\ \frac{-\nu_{pz}}{E_p} & \frac{-\nu_{pz}}{E_p} & \frac{1}{E_z} & 0 & 0 & 0 \\ 0 & 0 & 0 & \frac{1}{G_{zp}} & 0 & 0 \\ 0 & 0 & 0 & 0 & \frac{1}{G_{zp}} & 0 \\ 0 & 0 & 0 & 0 & 0 & \frac{2(1+\nu_p)}{E_p} \end{bmatrix} \tag{1.31}$$

and due to the symmetry we have:

$$\frac{\nu_{zp}}{E_z} = \frac{\nu_{pz}}{E_p} \tag{1.32}$$

where the subscript p refers to the in-plane properties. The matrix of piezoelectric coefficients is:

$$[d] = \begin{bmatrix} 0 & 0 & 0 & 0 & d_{15} & 0 \\ 0 & 0 & 0 & d_{15} & 0 & 0 \\ d_{31} & d_{31} & d_{33} & 0 & 0 & 0 \end{bmatrix} \tag{1.33}$$

and the matrix of dielectric permittivities:

$$\left[\varepsilon^T\right] = \begin{bmatrix} \varepsilon_{11}^T & 0 & 0 \\ 0 & \varepsilon_{11}^T & 0 \\ 0 & 0 & \varepsilon_{33}^T \end{bmatrix} \tag{1.34}$$

In order to use such a piezoelectric material in a 3D model, it is therefore necessary to have access to the 5 elastic constants E_p,E_z,ν_p,ν_{zp} and G_{zp}, 3 piezoelectric constants d_{31},d_{33}, and d_{15} and two dielectric constants ε_{11}^T,ε_{33}^T. Unfortunately, such constants are generally not given in that form, but can be calculated from the material properties found in the datasheet. It is important to introduce the electromechanical coupling factors which are generally given in the datasheet and are a function of the elastic, piezoelectric and dielectric properties of the material. They measure the effectiveness of the conversion of mechanical energy into electrical energy (and vice-versa). There is one coupling factor for each piezoelectric mode:

$$\begin{aligned} k_{31}^2 &= \frac{d_{31}^2}{\varepsilon_{33}^T s_{11}^E} \\ k_{33}^2 &= \frac{d_{33}^2}{\varepsilon_{33}^T s_{33}^E} \\ k_{15}^2 &= \frac{d_{15}^2}{\varepsilon_{11}^T s_{55}^E} \end{aligned} \tag{1.35}$$

In addition, coupling factors k_p for radial modes of thin discs, and k_t for thickness modes of arbitrary shaped thin plates are also commonly given in datasheet. k_p is related to k_{31} through:

$$k_p^2 = \frac{2k_{31}^2}{1 + \frac{s_{12}^E}{s_{11}^2}} \tag{1.36}$$

k_t is always lower than k_{33} but there does not seem to be a simple explicit expression of k_t as a function of the material properties. The fact that k_t is lower than k_{33} means that electrical energy conversion in the d_{33}-mode is less effective for a thin plate than for a rod. The definition of the coupling factors k_{33} and k_{15} also allows to write alternative expressions:

$$\begin{aligned} k_{33}^2 &= 1 - \frac{s_{33}^D}{s_{33}^E} \\ k_{15}^2 &= 1 - \frac{s_{55}^D}{s_{55}^E} = 1 - \frac{\varepsilon_{11}^S}{\varepsilon_{11}^T} \end{aligned} \tag{1.37}$$

We illustrate the use of these different relationships to form the full set of mechanical, piezoelectric and dielectric properties for the material *SONOX P502* from Ceramtec . The properties found in the datasheet are given in Table 1.2 (http://www.ceramtec.com/).

Material property	value	unit
Piezoelectric properties		
d_{33}	440	$10^{-12}m/V$
d_{31}	-185	$10^{-12}m/V$
d_{15}	560	$10^{-12}m/V$
e_{33}	16.7	$C/m^2 = As/m^2$
g_{33}	$26.9\ 10^{-3}$	Vm/N
Permittivity		
ε_{33}^T	$1850\ \varepsilon_0$	F/m
ε_{33}^S	$875\ \varepsilon_0$	F/m
ε_{11}^T	$1950\ \varepsilon_0$	F/m
ε_{11}^S	$1260\ \varepsilon_0$	F/m
Elastic properties		
s_{11}^E	$18.5\ 10^{-12}$	m^2/N
s_{33}^E	$20.7\ 10^{-12}$	m^2/N
c_{33}^D	$15.7\ 10^{10}$	N/m^2
c_{55}^D	$6.5\ 10^{10}$	N/m^2
Coupling coefficients		
k_{33}	0.72	
k_{15}	0.74	
k_{31}	0.33	
k_p	0.62	
k_t	0.48	
Density		
ρ	7740	kg/m^3

Table 1.2: Properties of *SONOX P502* from the datasheet

E_p and E_z are computed directly from the definitions of s_{11}^E and s_{33}^E:

$$E_p = \frac{1}{s_{11}^E} = 54.05GPa \tag{1.38}$$

$$E_z = \frac{1}{s_{33}^E} = 48.31GPa \tag{1.39}$$

Knowing the value of s_{11}^E, d_{31}, ε_{33}^T and k_p, s_{12}^E can be computed:

$$s_{12}^E = -s_{11}^E + 2\frac{d_{31}^2}{k_p^2 \varepsilon_{33}^T} = -7.6288\,10^{-12} m^2/N$$

allowing to compute the value of ν_p:

$$\nu_p = -E_p s_{12}^E = 0.4124$$

and the value of G_p

$$G_p = \frac{E_p}{2(1+\nu_p)} = 19.17GPa$$

From the value c_{55}^D and k_{15}, we compute

$$s_{55}^E = \frac{1}{c_{55}^D(1-k_{15}^2)} = 34\,10^{-12} m^2/N$$

from which the the value of G_{zp} is computed:

$$G_{zp} = \frac{1}{s_{55}^E} = 29.41GPa$$

The value of ν_{zp} cannot be calculated from the datasheet information. We therefore assume that, as for most PZT ceramics:

$$\nu_{zp} = 0.39$$

The value of ν_{pz} is calculated as:

$$\nu_{pz} = \frac{E_p}{E_z}\nu_{zp} = 0.44$$

The complete set of values is summarized in Table 1.3. These are the values used in `m_piezo`. Note that there is some redundancy in the data from the datasheet, which allows to check for consistency. The two following coupling factors are computed from the data available and checked against the tabulated values.

$$k_{31} = \sqrt{\frac{d_{31}^2}{\varepsilon_{33}^T s_{11}^E}} = 0.3361$$

$$k_{33} = \sqrt{\frac{d_{33}^2}{\varepsilon_{33}^T s_{33}^E}} = 0.7556$$

The values are close to the values in Table 1.2. In addition, the value of g_{33} is given by:

$$g_{33} = \frac{d_{33}}{\varepsilon_{33}^T} = 0.0269 Vm/N$$

and corresponds exactly to the value tabulated. The value of e_{33} can be computed using Equation (1.7), leading to:

$$e_{33} = 19.06 C/m^2$$

where there is a difference of about 15% with the tabulated value of $e_{33} = 16.7 C/m^2$. Using (1.37) to compute k_{15} with the values from the datasheet, one gets:

$$k_{15} = \sqrt{1 - \frac{\varepsilon_{11}^S}{\varepsilon_{11}^T}} = 0.5948$$

which shows the non-consistency of the value of ε_{11}^S in the datasheet. In fact, when computed using (1.8), one gets:

$$\varepsilon_{11}^S = 908 \varepsilon_0$$

Material property	value	unit
Piezoelectric properties		
d_{33}	440	$10^{-12} m/V$
d_{31}	-185	$10^{-12} m/V$
d_{15}	560	$10^{-12} m/V$
Permittivity		
ε_{33}^T	1850 ε_0	F/m
ε_{11}^T	1950 ε_0	F/m
Mechanical properties		
E_p	54.05	GPa
E_z	48.31	GPa
G_{zp}	29.41	GPa
G_p	19.17	GPa
ν_p	0.4124	
ν_{zp}	0.39	
ν_{pz}	0.44	
ρ	7740	kg/m^3

Table 1.3: Properties of *SONOX P502* to be used in 3D finite element models

From the input values used in `m_piezo`, it is possible to compute the mechanical, piezoelectric and permittivity matrices used in the four different forms of the constitutive equations (1.4),(1.5),(1.9),(1.10) using the relationships (1.6)-(1.8)) and (1.11)-(1.13). The command `p_piezo('TabDD')` can be used in order to have access to all the matrices from the input values in `m_piezo`. This will be illustrated in section 1.2.5.

As the mechanical properties of PZT are not strongly orthotropic, a simplification can be done by considering that the material is isotropic (for the mechanical and dielectric properties, not the piezoelectric properties). An isotropic version of *SONOX P502* is included in `m_piezo` under the name of *SONOX_P502_iso* whose properties are given in Table 1.4.

Material property	value	unit
Piezoelectric properties		
d_{33}	440	$10^{-12}m/V$
d_{31}	-185	$10^{-12}m/V$
d_{15}	560	$10^{-12}m/V$
Permittivity		
ε^T	1850 ε_0	F/m
Mechanical properties		
E	54.05	GPa
ν	0.41	
ρ	7740	kg/m^3

Table 1.4: Simplified material properties for *SONOX P502* considering mechanical isotropy

The second example is the *PIC 255* PZT from PI ceramics. The properties found in the datasheet are given in Table 1.5 (http://www.piceramic.com/pdf/piezo_material.pdf). Note that C_{33}^D is not given in the datasheet, therefore we estimated it from the value of *PIC 155* given in the same datasheet, which is just slightly stiffer.

Material property	value	unit
Piezoelectric properties		
d_{33}	400	$10^{-12} m/V$
d_{31}	-180	$10^{-12} m/V$
d_{15}	550	$10^{-12} m/V$
g_{31}	-11.3 10^{-3}	Vm/N
g_{33}	25 10^{-3}	Vm/N
Permittivity		
ε_{33}^T	1750 ε_0	F/m
ε_{11}^T	1650 ε_0	F/m
Elastic properties		
s_{11}^E	16.1 10^{-12}	m^2/N
s_{33}^E	20.7 10^{-12}	m^2/N
c_{33}^D	11 10^{10}	N/m^2
Coupling coefficients		
k_{33}	0.69	
k_{15}	0.66	
k_{31}	0.35	
k_p	0.62	
k_t	0.47	
Density		
ρ	7800	kg/m^3

Table 1.5: Properties of *PIC 255* from the datasheet

E_p and E_z are computed directly from the definitions of s_{11}^E and s_{33}^E:

$$E_p = \frac{1}{s_{11}^E} = 62.11\, GPa$$

$$E_z = \frac{1}{s_{33}^E} = 48.31\, GPa$$

Knowing the value of s_{11}^E, d_{31}, ε_{33}^T and k_p, s_{12}^E can be computed:

$$s_{12}^E = -s_{11}^E + 2\frac{d_{31}^2}{k_p^2 \varepsilon_{33}^T} = -5.22\, 10^{-12}\, m^2/N$$

allowing to compute the value of ν_p:

$$\nu_p = -E_p s_{12}^E = 0.3242$$

and the value of G_p

$$G_p = \frac{E_p}{2(1+\nu_p)} = 23.53\,GPa$$

The value of s_{55}^E can be computed as:

$$s_{55}^E = \frac{d_{15}^2}{\varepsilon_{11}^T k_{15}^2} = 4.75\,10^{-11}\,m^2/N$$

which leads to:

$$G_{zp} = \frac{1}{s_{55}^E} = 21.03\,GPa$$

Again, the value of ν_{zp} cannot be calculated from the datasheet information. We cannot assume a value of 0.39 as previously, as it would lead to a non-physical value of ν_{pz}. As ν_p is in the range of 0.32 and ν_{zp} is typically slightly lower, we assume that :

$$\nu_{zp} = 0.30$$

The value of ν_{pz} is calculated as:

$$\nu_{pz} = \frac{E_p}{E_z}\nu_{zp} = 0.39$$

The complete set of values is summarized in Table 1.6. These are the values used in `m_piezo`. Note that there is some redundancy in the data from the datasheet, which allows to check for consistency. The two following coupling factors are computed from the data available and checked against the tabulated values.

$$k_{31} = \sqrt{\frac{d_{31}^2}{\varepsilon_{33}^T s_{11}^E}} = 0.36$$
$$k_{33} = \sqrt{\frac{d_{33}^2}{\varepsilon_{33}^T s_{33}^E}} = 0.70$$

The values are very close to the values in Table 1.5. In addition, the value of g_{33} and g_{31} are given by:

$$g_{31} = \frac{d_{31}}{\varepsilon_{33}^T} = -11.6\,10^{-3}\,Vm/N$$
$$g_{33} = \frac{d_{33}}{\varepsilon_{33}^T} = 25.8\,10^{-3}\,Vm/N$$

and are also very close to the values tabulated.

Material property	value	unit
Piezoelectric properties		
d_{33}	400	$10^{-12}m/V$
d_{31}	-180	$10^{-12}m/V$
d_{15}	550	$10^{-12}m/V$
Permittivity		
ε_{33}^T	1750 ε_0	F/m
ε_{11}^T	1650 ε_0	F/m
Mechanical properties		
E_p	62.11	GPa
E_z	48.31	GPa
G_{zp}	21.03	GPa
G_p	23.53	GPa
ν_p	0.3242	
ν_{zp}	0.30	
ν_{pz}	0.39	
ρ	7800	kg/m^3

Table 1.6: Properties of *PIC 255* to be used in 3D finite element models

As shown in the derivations above, the datasheet for PZT material typically do not contain the full information to derive all the coefficients needed for computations, and some hypothesis need to be made. In addition, it is usual to have a variation of 10 % or more on these properties from batch to batch, and the datasheet are not updated for each batch. Note also that the properties are given at 20 ï¿½C and are temperature dependant. The variations with temperature are rarely given in the datasheet. This may also account for inaccuracies in the computations.

1.2.4 Illustration of piezoelectricity in statics: patch example

Consider a thin piezoelectric patch of dimensions b x h x w. The poling direction, noted 3 in the IEEE Standards on piezoelectricity is perpendicular to the plane of the piezoelectric patch. Continuous electrodes are present on the top and bottom surfaces ($z = 0$, $z = h$) so that the electric potential is constant on these surfaces and denoted by V_1 and V_2 respectively. We assume that a difference of potential is applied between the electrodes, resulting in an electric field parallel to the poling direction and equal to

$$E_3 = -\frac{dV}{dz} = \frac{-(V_2 - V_1)}{h} = \frac{V_1 - V_2}{h}$$

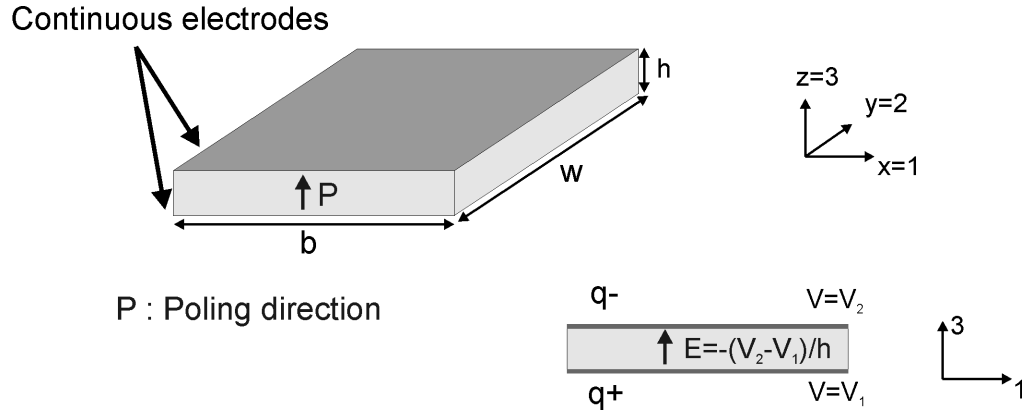

Figure 1.5: A piezoelectric patch poled through the thickness with continuous electrodes on the top and bottom surfaces

Assume that a constant difference of electric potential is applied to the two electrodes of the piezoelectric patch, as illustrated in Figure 1.5. We adopt the following expression for the constitutive equations:

$$\begin{aligned} \{S\} &= \left[s^E\right]\{T\} + [d]^T\{E\} \\ \{D\} &= [d]\{T\} + \left[\varepsilon^T\right]\{E\} \end{aligned} \tag{1.40}$$

The patch is assumed to be unconstrained so that it can expand freely, leading to $\{T\} = 0$, so that we have :

$$\{S\} = \begin{Bmatrix} S_1 \\ S_2 \\ S_3 \\ S_4 \\ S_5 \\ S_6 \end{Bmatrix} = [d]^T\{E\} = \begin{Bmatrix} d_{31}\frac{V_1-V_2}{h} \\ d_{32}\frac{V_1-V_2}{h} \\ d_{33}\frac{V_1-V_2}{h} \\ 0 \\ 0 \\ 0 \end{Bmatrix} \tag{1.41}$$

We have taken into account the fact that the electric field is in the z-direction only. This shows that when applying a difference of potential across the thickness (in the poling direction), strains will be induced in the directions 1,2, and 3. The magnitude of these different strains is proportional to the d_{3i} coefficients of the piezoelectric material. For a ceramic PZT material, $d_{31} = d_{32} < 0$, and $d_{33} > 0$ and is generally between 2 and 3 times larger in magnitude than d_{31} and d_{32}.

The second equation can be used in order to assess the amount of charge that is accumulated on

both electrodes. We have :

$$\{D\} = \begin{Bmatrix} D_1 \\ D_2 \\ D_3 \end{Bmatrix} = \left[\varepsilon^T\right] \{E\} \tag{1.42}$$

The only non-zero component of the D vector is D_3 given by :

$$D_3 = \varepsilon_{33}^T \frac{V_1 - V_2}{h} \tag{1.43}$$

The charge accumulated on the electrode is given by :

$$q = -\int_S \{D\} \{n\} \, dS$$

where $\{n\}$ is the normal to the electrode. For the top electrode, this leads to :

$$q = -\frac{\varepsilon_{33}^T A}{h}(V_1 - V_2)$$

where A is the surface of the electrode. For the bottom electrode

$$q = \frac{\varepsilon_{33}^T A}{h}(V_1 - V_2)$$

When $(V_1 - V_2)$ is positive, the electric field is in the direction of poling and the charge on the top electrode is negative, while the charge accumulated on the bottom electrode is positive (Figure 1.5). Note that this equation corresponds to the equation linking the charge to the difference of potential for a capacitor ($q = C\Delta V$). The value of the capacitance is therefore :

$$C^T = \frac{\varepsilon_{33}^T A}{h}$$

which corresponds to the capacitance of the free piezoelectric patch ($\{T\} = 0$).

If we now consider the case where the piezoelectric patch is fully mechanically constrained ($\{S\} = 0$), we have:

$$\begin{aligned} \{T\} &= -\left[e\right]^T \{E\} = -\left[e\right]^T \{E\} \\ \{D\} &= \left[\varepsilon^S\right] \{E\} \end{aligned} \tag{1.44}$$

leading to :

$$\{T\} = \begin{Bmatrix} T_1 \\ T_2 \\ T_3 \\ T_4 \\ T_5 \\ T_6 \end{Bmatrix} = \begin{Bmatrix} -e_{31}\frac{V_1 - V_2}{h} \\ -e_{32}\frac{V_1 - V_2}{h} \\ -e_{33}\frac{V_1 - V_2}{h} \\ 0 \\ 0 \\ 0 \end{Bmatrix} \tag{1.45}$$

$$D_3 = \varepsilon_{33}^S \frac{V_1 - V_2}{h}$$

In this case, the capacitance is given by:

$$C^S = \frac{\varepsilon_{33}^S A}{h}$$

which corresponds to the capacitance of the constrained piezoelectric patch ($\{S\} = 0$). This illustrates the fact that the capacitance of a piezoelectric patch depends on the mechanical boundary conditions. This is not the case for other types of dielectric materials in which the piezoelectric effect is not present, and for which therefore the capacitance is independent on the mechanical strain or stress.

1.2.5 Numerical illustration : rectangular patch in statics

In this very simple example, the electric field and the strains are all constant, so that the electric potential and the displacement field are linear. It is therefore possible to obtain an exact solution using a single volumic 8-node finite element (with linear shape functions, the nodal unknowns being the displacements in x,y and z and the electric potential ϕ). Consider a piezoelectric patch whose dimensions and material properties are given in Table 1.7. The material properties correspond to the material *SONOX_P502_iso* in `m_piezo`.

Property	Value
b	10 mm
w	10 mm
h	2 mm
E	54 GPa
ν	0.44
$d_{31} = d_{32}$	-185 $10^{-12} pC/N$ (or m/V)
d_{33}	440 $10^{-12} pC/N$ (or m/V)
$d_{15} = d_{24}$	560 $10^{-12} pC/N$ (or m/V)
$\varepsilon_{33}^T = \varepsilon_{22}^T = \varepsilon_{11}^T$	1850 ε_0
ε_0	8.854 $10^{-12} Fm^{-1}$

Table 1.7: Geometrical and material properties of the piezoelectric patch

We first produce the mesh, associate the material properties and define the electrodes with `d_piezo('TutoPatch-s1')` . The default material is *SONOX_P502_iso*. The number of elements in the x, y and z directions are given by n_x,n_y and n_z.

```
% See full example as MATLAB code in d_piezo('ScriptPatch')
%% Step 1 Build mesh - Define electrodes
```

```
% Meshing script can be viewed with sdtweb d_piezo('MeshPatch')
model=d_piezo('MeshPatch lx=1e-2 ly=1e-2 h=2e-3 nx=1 ny=1 nz=1');
% Define electrodes
model=p_piezo('ElectrodeMPC Top -ground',model,'z==2e-3');
model=p_piezo('ElectrodeMPC Bottom -Input "Free patch"',model,'z==0');
```

The information about the nodes associated to each electrode can be obtained through the following call:

```
p_piezo('TabInfo',model)
```

The material can be changed for example to PIC_255 with the following call, and the full set of mechanical, piezoelectric and permittivity matrices can be obtained in order to check consistency with the datasheet (`d_piezo('TutoPatch-s2')`):

```
%% Step 2 Define material properties
model.pl=m_piezo('dbval 1 -elas 2 PIC_255');
p_piezo('TabDD',model) % creates the table with full set of matrices
```

The next step consists in defining the boundary conditions and load case using `d_piezo('TutoPatch-s3')` . We consider here two cases, the first one where the patch is free to expand, and the second one where it is mechanically constrained (all mechanical degrees of freedom are equal to 0).

```
%% Step 3 Compute static response
% to avoid rigid body mode
model=stack_set(model,'info','Freq',10);
def=fe_simul('dfrf',model); def.lab={'Free patch, axial'};
def.fun=[0 1]; def=feutil('rmfield',def,'data','LabFcn');

% Append mechanically constrained structure
%    can't call fe_simul because no free DOF
%    see code with sdtweb d_piezo('scriptFullConstrain')
def=d_piezo('scriptFullConstrain',model,def);
def.lab{2}='Constrained patch, axial';
```

We can look at the deformed shape, and plot the electric field for both cases.
(`d_piezo('TutoPatch-s4')`

```
%% Step 4 Visualize deformed shape
cf=feplot(model,def);
% Electric field representation
p_piezo('viewElec EltSel "matid1" DefLen 20e-4 reset',cf);
fecom('colormap',[1 0 0]);fecom('undef line');iimouse('resetview');
```

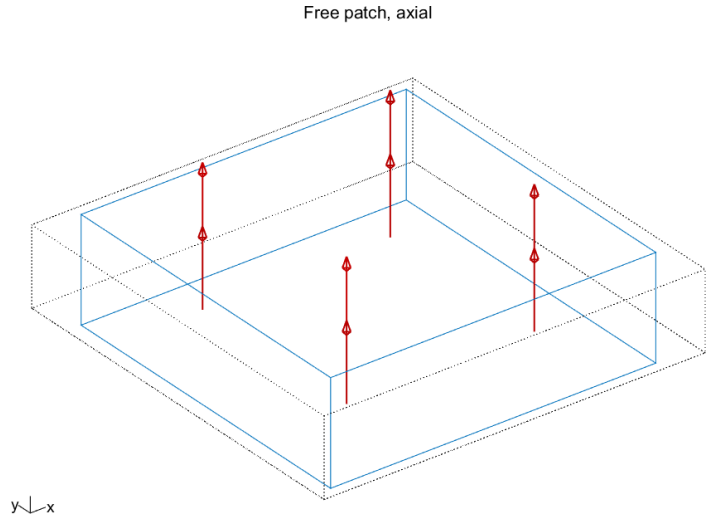

Figure 1.6: Vizualisation of the electric field and deformed shape for the free patch under unit voltage excitation

For the free patch deformed shape, we compute the mean strains from which d_{31}, d_{32} and d_{33} are deduced. The values are found to be equal to the analytical values used in the model. Note that the parameters of the constitutive equations can be recovered using (`d_piezo('TutoPatch-s5')`):

```
%% Step 5 : check constitutive law
% Decompose constitutive law
CC=p_piezo('viewdd -struct',cf); %
```

where the fields of CC are self-explanatory. The parameters which are not directly defined are computed from the equations presented in Section 1.2.1.

```
% Display and compute mean strains
a=p_piezo('viewstrain -curve -mean',cf); % Strain S
fprintf('Relation between mean strain on free structure and d_3i\n');
E3=a.Y(9,1); disp({'E3 mean' a.Y(9,1)  1/2e-3 'E3 analytic'})

disp([a.X{1}(1:3) num2cell([a.Y(1:3,1)/E3 CC.d(3,1:3)']) ...
     {'d_31';'d_32';'d_33'}])
```

For the constrained patch, we compute the mean stress from which we can compute the e_{31}, e_{32} and e_{33} values which are found to be equal to the analytical values used in the model:

```
% Display and compute mean stresses
b=p_piezo('viewstress -curve -mean',cf); % Stress T
fprintf('Relation between mean stress on pure electric and e_3i\n');
disp([b.X{1}(1:3) num2cell([b.Y(1:3,2)/-E3 CC.e(3,1:3)']) ...
     {'e_31';'e_32';'e_33'}])

% Mean stress/strain
disp([b.X{1} num2cell(b.Y(:,2)) num2cell(a.Y(:,1)) a.X{1}])
```

We can also compute the charge and the charge density (in pC/m^2) accumulated on the electrodes, and compare with the analytical values (d_piezo('TutoPatch-s6')):

```
%% Step 6 Check capacitance values
% Theoretical values of Capacitance and charge density - free patch
CT=CC.epst_r(3,3)*8.854e-12*1e-2*1e-2/2e-3; %% Capacitance - free patch
CdensT=CC.epst_r(3,3)*8.854e-12/2e-3*1e12; %% charge density - free patch

% Theoretical values of Capacitance and charge density - constrained patch
CS=CC.epss_r(3,3)*8.854e-12*1e-2*1e-2/2e-3; %% Capacitance - free patch
CdensS=CC.epss_r(3,3)*8.854e-12/2e-3*1e12; %% charge density - free patch

% Represent charge density (C/S) value on the electrodes
%   - compare with analytical values
cut=p_piezo('electrodeviewcharge',cf,struct('EltSel','matid 1'));
b=fe_caseg('stressobserve',cut,cf.def);b=reshape(b.Y,[],2);
disp([{'','CdensT','CdensS'};{'Numeric';'Theoretical'} ...
  num2cell([mean(abs(b));CdensT CdensS])])
  iimouse('zoom reset');

% Compute the value of the total charge (from reaction at electrical dof)
% Compare with analytical values
p_piezo('electrodeTotal',cf) %
disp('Theoretical values of capacitance')
disp([{'CT';'CS'} num2cell([CT;CS])])
```

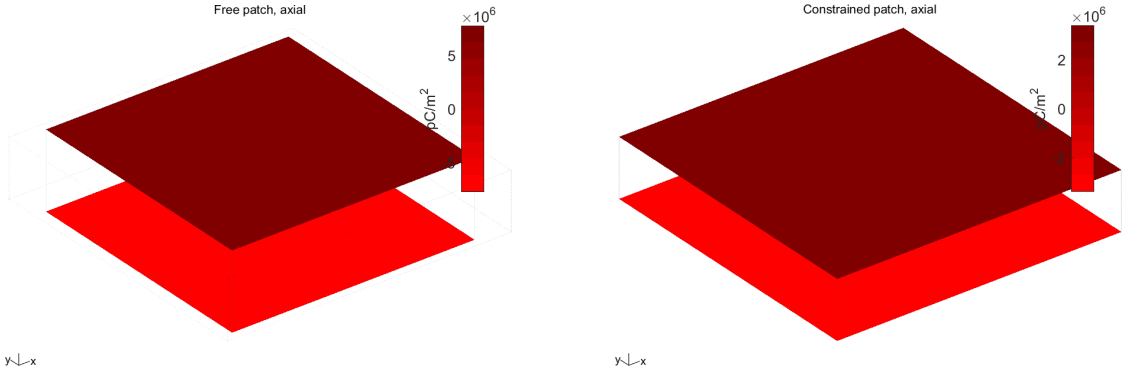

Figure 1.7: Vizualisation of the total charge on the electrodes for the unconstrained and constrained patch under unit voltage excitation

The results clearly show the very large difference of charge density between the two cases (free patch or constrained patch).

For this simple static example, a finer mesh can be used, but it does not lead to more accurate results (this can be done by changing the values in the call of $d\_piezo('mesh')$) for example:

```
% Build mesh with refinement
model=d_piezo('MeshPatch lx=1e-2 ly=1e-2 h=2e-3 nx=5 ny=5 nz=2');
% Now a model with quadratic elements
model=d_piezo('MeshPatch lx=1e-2 ly=1e-2 h=2e-3 Quad');
```

1.2.6 Piezoelectric shear actuation

We now consider the same patch but where the polarization is in the plane of the actuator, as represented in Figure 1.8. As in the previous example, continuous electrodes are present on the top and bottom surfaces ($z = 0$, $z = h$) so that the electric potential is constant on these surfaces and denoted by V_1 and V_2 respectively. We assume that a difference of potential is applied between the electrodes, resulting in an electric field perpendicular to the poling direction and equal to

$$E_2 = -\frac{dV}{dz} = \frac{-(V_2 - V_1)}{h} = \frac{V_1 - V_2}{h}$$

The electric field is now applied in direction 2, so that it will activate the shear $d_{24} = d_{15}$ mode of the piezoelectric material.

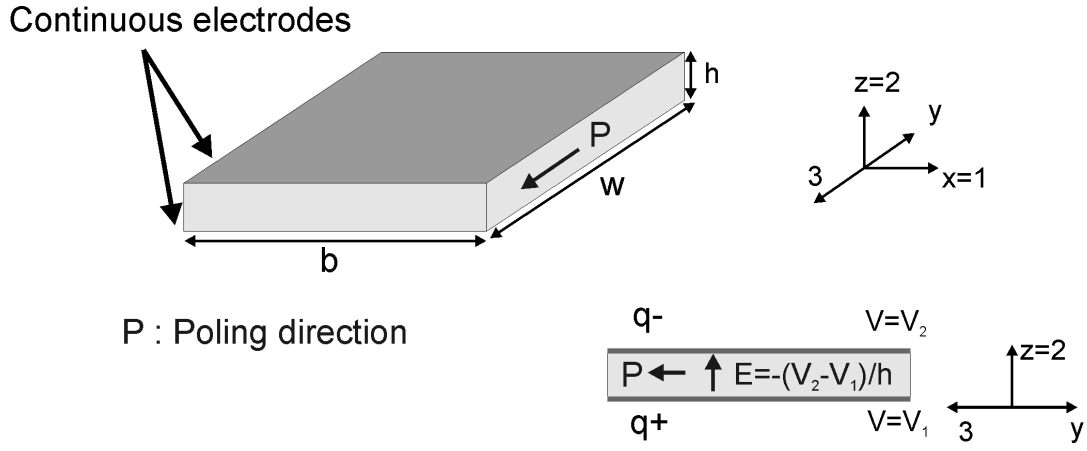

Figure 1.8: A piezoelectric patch poled in the plane with continuous electrodes on the top and bottom surfaces

The patch is assumed to be unconstrained so that it can expand freely, leading to $\{T\} = 0$, so that we have :

$$\{S\} = \left\{ \begin{array}{c} S_1 \\ S_2 \\ S_3 \\ S_4 \\ S_5 \\ S_6 \end{array} \right\} = [d]^T \{E\} = \left\{ \begin{array}{c} 0 \\ 0 \\ 0 \\ d_{24} \frac{V_1 - V_2}{h} \\ 0 \\ 0 \end{array} \right\} \tag{1.46}$$

We have taken into account the fact that the electric field is in the z-direction only, corresponding to direction 2 in the local axis of the piezoelectric material (direction 3 is the poling direction by convention). This shows that when the patch is poled in the plane, when applying a difference of potential across the thickness, a shear strain in the local 23 plane will be induced. The magnitude of this strain is proportional to the d_{24} coefficient of the piezoelectric material.
The second equation can be used in order to assess the amount of charge that is accumulated on both electrodes. We have :

$$\{D\} = \left\{ \begin{array}{c} D_1 \\ D_2 \\ D_3 \end{array} \right\} = \left[\varepsilon^T\right] \{E\} \tag{1.47}$$

The only non-zero component of the D vector is D_2 given by :

$$D_2 = \varepsilon_{22}^T \frac{V_1 - V_2}{h} \tag{1.48}$$

The charge accumulated on the electrode is given by :

$$q = -\int_S \{D\}\{n\}\, dS$$

where $\{n\}$ is the normal to the electrode. For the top electrode, this leads to :

$$q = -\frac{\varepsilon_{22}^T A}{h}(V_1 - V_2)$$

where A is the surface of the electrode. For the bottom electrode

$$q = \frac{\varepsilon_{22}^T A}{h}(V_1 - V_2)$$

When $(V_1 - V_2)$ is positive, the charge on the top electrode is negative, while the charge accumulated on the bottom electrode is positive (Figure 1.5). The value of the capacitance is therefore:

$$C^T = \frac{\varepsilon_{22}^T A}{h}$$

which corresponds to the capacitance of the free piezoelectric patch ($\{T\} = 0$) and is equal to the capacitance when the poling is out of the plane of the transducer because we have assumed $\varepsilon_{22}^T = \varepsilon_{33}^T$ (in reality, there is typically a difference of 5% between these two values so that the capacitance will be slightly different).

If we now consider the case where the piezoelectric patch is fully mechanically constrained ($\{S\} = 0$), we have:

$$\begin{array}{c} \{T\} = -[e]^T \{E\} = -[e]^T \{E\} \\ \{D\} = \left[\varepsilon^S\right] \{E\} \end{array} \tag{1.49}$$

leading to :

$$\begin{array}{c} \{T\} = \left\{ \begin{array}{c} T_1 \\ T_2 \\ T_3 \\ T_4 \\ T_5 \\ T_6 \end{array} \right\} = \left\{ \begin{array}{c} 0 \\ 0 \\ 0 \\ -e_{24}\frac{V_1 - V_2}{h} \\ 0 \\ 0 \end{array} \right\} \\ D_2 = \varepsilon_{22}^S \frac{V_1 - V_2}{h} \end{array} \tag{1.50}$$

In this case, the capacitance is given by:

$$C^S = \frac{\varepsilon_{22}^S A}{h}$$

which corresponds to the capacitance of the constrained piezoelectric patch ($\{S\} = 0$). Note that this capacitance is clearly different from C^S when the poling is out of the plane, because the value of ε_{22}^S is very different from the value of ε_{33}^S, due to the different values of stiffness and piezoelectric coefficients in shear and extensional mode.

1.2.7 Numerical illustration : rectangular patch in statics: shear mode

The following scripts illustrates the shear actuation using a single 8-node element as in the extension example. The patch is meshed and then the poling is aligned with the $-y$ axis by performing a rotation of 90^o around the x-axis (d_piezo('TutoPatchShear-s1')).

```
% See full example as MATLAB code in d_piezo('ScriptPatchShear')
%% Step 1 Build mesh and define electrodes
%Meshing script can be viewed with sdtweb d_piezo('MeshPatch')
model=d_piezo('MeshPatch lx=1e-2 ly=1e-2 h=2e-3 nx=1 ny=1 nz=1');

% Define electrodes
model=p_piezo('ElectrodeMPC Top -ground',model,'z==2e-3');
model=p_piezo('ElectrodeMPC Bottom -Input "Free patch"',model,'z==0');

% Rotate basis to align poling direction with y (-90ï¿½ around x)
model.bas=basis('rotate',[],'rx=-90',1); %create local basis with id=1
model=feutil('setpro 1 COORDM=1',model); % assign basis with id=1 to pro=1
```

Then the response is computed both for the free case and the fully constrained case (Figure 1.9): (d_piezo('TutoPatchShear-s2'))

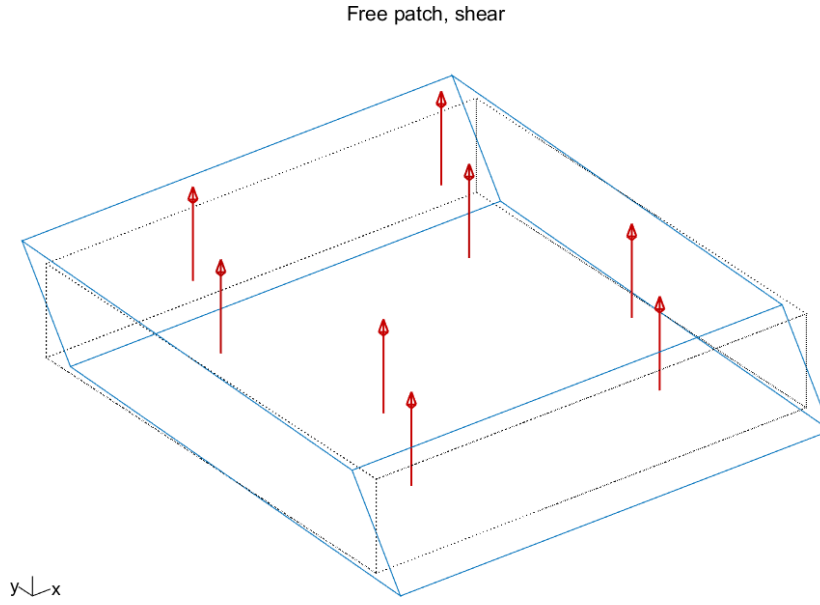

Figure 1.9: Deformed shape of a piezoelectric patch poled in the plane with an electric field applied in the out-of-plane direction

```
%% Step 2 Compute static response
% to avoid rigid body mode
model=stack_set(model,'info','Freq',10);
def=fe_simul('dfrf',model); def.lab={'Free patch, shear'};
def.fun=[0 1]; def=feutil('rmfield',def,'data','LabFcn');

% Append mechanically constrained structure
%    can't call fe_simul because no free DOF
%    see code with sdtweb d_piezo('scriptFullConstrain')
def=d_piezo('scriptFullConstrain',model,def);
def.lab{2}='Constrained patch, shear';

(d_piezo('TutoPatchShear-s3') )

%% Step 3 Vizualise deformed shape
cf=feplot(model,def); fecom('undef line');

% Electric field representation
```

```
p_piezo('viewElec EltSel "matid1" DefLen 20e-4 reset',cf);
iimouse('zoom reset')
```

The mean of shear strain and stress is evaluated and compared to the d_{24} piezo coefficient. Note that the mean values are computed in the global yz axis for which a negative strain corresponds to a positive strain in the local 23 axis. Finally the capacitance is evaluated and compared to the theoretical values, showing a perfect agreement, and demonstrating the difference with the extension case for C^S.
(d_piezo('TutoPatchShear-s4'))

```
%% Step 4 : Check constitutive law
% Decompose constitutive law
CC=p_piezo('viewdd -struct',cf); %

% Display and compute mean strains
a=p_piezo('viewstrain -curve -mean',cf); % Strain S
fprintf('Relation between mean strain on free structure and d_24\n');
E3=a.Y(9,1); disp({'E3 mean' a.Y(9,1)  1/2e-3 'E3 analytic'})

disp([a.X{1}(4) num2cell([a.Y(4,1)/E3 CC.d(2,4)']) ...
     {'d_24'}])

% Display and compute mean stresses
b=p_piezo('viewstress -curve -mean',cf); % Stress T
fprintf('Relation between mean stress on pure electric and e_24 \n');
disp([b.X{1}(4) num2cell([b.Y(4,2)/-E3 CC.e(2,4)']) ...
     {'e_24'}])


% Mean stress/strain
disp([b.X{1} num2cell(b.Y(:,2)) num2cell(a.Y(:,1)) a.X{1}])

% Theoretical values of Capacitance and charge density - free patch
CT=CC.epst_r(2,2)*8.854e-12*1e-2*1e-2/2e-3; %% Capacitance - free patch
CdensT=CC.epst_r(2,2)*8.854e-12/2e-3*1e12; %% charge density - free patch

% Theoretical values of Capacitance and charge density - constrained patch
CS=CC.epss_r(2,2)*8.854e-12*1e-2*1e-2/2e-3; %% Capacitance - constrained patch
CdensS=CC.epss_r(2,2)*8.854e-12/2e-3*1e12; %% charge density - constrained patch

% Represent charge density (C/S) value on the electrodes
```

```
%   - compare with analytical values
cut=p_piezo('electrodeviewcharge',cf,struct('EltSel','matid 1'));
b=fe_caseg('stressobserve',cut,cf.def);b=reshape(b.Y,[],2);
disp([{'','CdensT','CdensS'};{'Numeric';'Theoretical'} ...
  num2cell([mean(abs(b));CdensT CdensS])])
    iimouse('zoom reset');


(d_piezo('TutoPatchShear-s5') )

%% Step 5 Check capacitance
% Compute the value of the total charge (from reaction at electrical dof)
% Ccompare with analytical values
p_piezo('electrodeTotal',cf) %
disp('Theoretical values of capacitance')
disp([{'CT';'CS'} num2cell([CT;CS])])
```

1.3 Discrete equations of piezoelectric structures

Hamilton's principle is used to derive the dynamic variational principle [1]:

$$\int_{t_1}^{t_2} \left(\int_V \left[-\rho \{\ddot{u}\}^T \{\delta u\} - \{S\}^T \left[c^E\right] \{\delta S\} + \{E\}^T [e] \{\delta S\} \right.\right.$$
$$\left. + \{S\}^T [e]^T \{\delta E\} + \{E\}^T \left[\varepsilon^S\right] \{\delta E\} + \{f\}^T \{\delta u\} - \{\rho_e\}^T \{\delta \phi\} \right] dV$$
$$\left. + \int_{\Omega_1} \{t\}^T \{\delta u\}\, d\Omega - \int_{\Omega_2} \{\sigma\}^T \{\delta \phi\}\, d\Omega \right) dt = 0$$

where V is the volume of the piezoelectric structure, ρ is the mass density, $\{u\}$ is the displacement field and $\{\delta u\}$ its variation, $\{\phi\}$ is the elecctric pontential and $\{\delta\phi\}$ its variation. $\{f\}$ is the volumic force, $\{\rho_e\}$ the volumic charge density, $\{t\}$ the vector of applied surface forces on Ω_1 and $\{\sigma\}$ the charge density applied on Ω_2. The variational principle is the starting point for all discrete finite element formulations. 3D and shell approximations are detailed below.

1.3.1 Piezoelectric solid finite elements

For 3D solids, the discretized strain and electric fields are linked to the discretized displacement vector (u, v, w) and electric potential ϕ by:

$$\left\{ \begin{array}{c} S \\ E \end{array} \right\} = \left\{ \begin{array}{c} \epsilon_x \\ \epsilon_y \\ \epsilon_z \\ \gamma_{yz} \\ \gamma_{zx} \\ \gamma_{xy} \\ E_x \\ E_y \\ E_z \end{array} \right\} = \left[\begin{array}{cccc} N,x & 0 & 0 & 0 \\ 0 & N,y & 0 & 0 \\ 0 & 0 & N,z & 0 \\ 0 & N,z & N,y & 0 \\ N,z & 0 & N,x & 0 \\ N,y & N,x & 0 & 0 \\ 0 & 0 & 0 & -N,x \\ 0 & 0 & 0 & -N,y \\ 0 & 0 & 0 & -N,z \end{array} \right] \left\{ \begin{array}{c} u \\ v \\ w \\ \phi \end{array} \right\} \tag{1.51}$$

where $N,x\ u$ is a short notation for

$$\sum_i \frac{\partial N_i}{\partial x} u_i$$

and $N_i(x, y, z)$ are the finite element shape functions. Plugging (1.51) in (1.51) leads to the discrete set of equations which are written in the matrix form:

$$\left[\begin{array}{cc} M_{qq} & 0 \\ 0 & 0 \end{array} \right] \left\{ \begin{array}{c} \ddot{q_{mech}} \\ \ddot{V} \end{array} \right\} + \left[\begin{array}{cc} K_{qq} & K_{qV} \\ K_{Vq} & K_{VV} \end{array} \right] \left\{ \begin{array}{c} q_{mech} \\ V \end{array} \right\} = \left\{ \begin{array}{c} F_{mech} \\ Q \end{array} \right\} \tag{1.52}$$

where $\{q_{mech}\}$ contains the mechanical degrees of freedom (3 per node related to u, v, w), and $\{V\}$ contains the electrical degrees of freedom (1 per node, the electric potential ϕ). $\{F_{mech}\}$ is the vector of applied external mechanical forces, and $\{Q\}$ is the vector of applied external charges.

1.3.2 Piezoelectric shell finite elements

Shell strain is defined by the membrane, curvature and transverse shear as well as the electric field components. In the piezoelectric multi-layer shell elements implemented in SDT, it is assumed that in each piezoelectric layer $i = 1...n$, the electric field takes the form $\vec{E} = (0 \quad 0 \quad E_{zi})$. E_{zi} is assumed to be constant over the thickness h_i of the layer and is therefore given by $E_{zi} = -\frac{\Delta\phi_i}{h_i}$ where $\Delta\phi_i$ is the difference of potential between the electrodes at the top and bottom of the piezoelectric layer i. It is also assumed that the piezoelectric principal axes are parallel to the structural orthotropy axes.

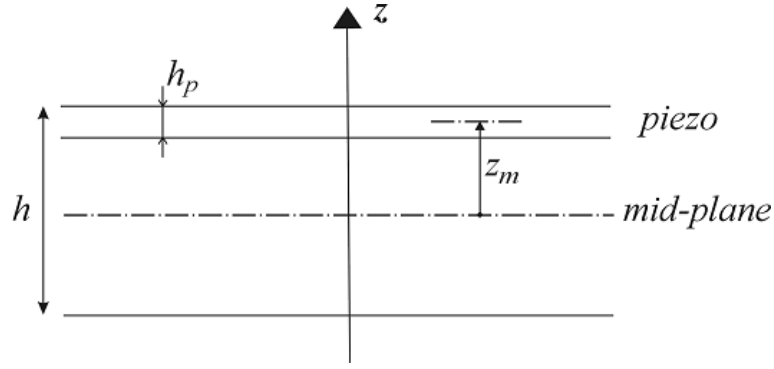

Figure 1.10: Multi-layer shell piezoelectric element

The discretized strain and electric fields of a piezoelectric shell take the form

$$\begin{Bmatrix} \epsilon_{xx} \\ \epsilon_{yy} \\ 2\epsilon_{xy} \\ \kappa_{xx} \\ \kappa_{yy} \\ 2\kappa_{xy} \\ \gamma_{xz} \\ \gamma_{yz} \\ -E_{z1} \\ ... \\ -E_{zn} \end{Bmatrix} = \begin{bmatrix} N,x & 0 & 0 & 0 & 0 & 0 & ... & 0 \\ 0 & N,y & 0 & 0 & 0 & 0 & ... & 0 \\ N,y & N,x & 0 & 0 & 0 & 0 & ... & 0 \\ 0 & 0 & 0 & 0 & -N,x & 0 & ... & 0 \\ 0 & 0 & 0 & N,y & 0 & 0 & ... & 0 \\ 0 & 0 & 0 & N,x & -N,y & 0 & ... & 0 \\ 0 & 0 & N,x & 0 & N & 0 & ... & 0 \\ 0 & 0 & N,y & -N & 0 & 0 & ... & 0 \\ 0 & 0 & 0 & 0 & 0 & -\frac{1}{h_1} & ... & 0 \\ ... & ... & ... & ... & ... & 0 & ... & -\frac{1}{h_n} \end{bmatrix} \begin{Bmatrix} u \\ v \\ w \\ ru \\ rv \\ \Delta\phi_1 \\ ... \\ \Delta\phi_n \end{Bmatrix} \tag{1.53}$$

There are thus n additional degrees of freedom $\Delta\phi_i$, n being the number of piezoelectric layers in the laminate shell. The constitutive laws are obtained by using the "piezoelectric plates" hypothesis (2.19) and the definitions of the generalized forces N, M, Q and strains $\varepsilon, \kappa, \gamma$ for shells:

$$\left\{ \begin{array}{c} N \\ M \\ Q \\ D_{z1} \\ ... \\ D_{zn} \end{array} \right\} = \left[\begin{array}{cccccc} A & B & 0 & G_1^T & ... & G_n^T \\ B & D & 0 & z_{m1}G_1^T & ... & z_{mn}G_n^T \\ 0 & 0 & F & 0 & ... & 0 \\ G_1 & z_{m1}G_1 & 0 & -{\varepsilon_1}^S & ... & 0 \\ ... & ... & ... & 0 & ... & 0 \\ G_n & z_{mn}G_n & 0 & 0 & ... & -{\varepsilon_n}^S \end{array} \right] \left\{ \begin{array}{c} \epsilon \\ \kappa \\ \gamma \\ -E_{z1} \\ ... \\ -E_{zn} \end{array} \right\} \tag{1.54}$$

D_{zi} is the electric displacement in piezoelectric layer , z_{mi} is the distance between the midplane of the shell and the midplane of piezoelectric layer i (Figure 1.10), G_i is given by

$$G_i = \left\{ \begin{array}{ccc} e_{31}^* & e_{32}^* & 0 \end{array} \right\}_i [R_s]_i \tag{1.55}$$

where * refers to the piezoelectric properties under the piezoelectric plate assumption as detailed in section 1.2.2 and $[R_s]_i$ are rotation matrices associated to the angle θ of the principal axes $1, 2$ of the piezoelectric layer given by:

$$[R_s] = \left[\begin{array}{ccc} \cos^2\theta & \sin^2\theta & \sin\theta\cos\theta \\ \sin^2\theta & \cos^2\theta & -\sin\theta\cos\theta \\ -2\sin\theta\cos\theta & 2\sin\theta\cos\theta & \cos^2\theta - \sin^2\theta \end{array} \right] \tag{1.56}$$

Plugging (1.53) into (1.51) leads again to:

$$\left[\begin{array}{cc} M_{qq} & 0 \\ 0 & 0 \end{array} \right] \left\{ \begin{array}{c} \ddot{q_{mech}} \\ \ddot{V} \end{array} \right\} + \left[\begin{array}{cc} K_{qq} & K_{qV} \\ K_{Vq} & K_{VV} \end{array} \right] \left\{ \begin{array}{c} q_{mech} \\ V \end{array} \right\} = \left\{ \begin{array}{c} F_{mech} \\ Q \end{array} \right\} \tag{1.57}$$

where $\{q_{mech}\}$ contains the mechanical degrees of freedom (5 per node corresponding to the displacements u, v, w and rotations rx, ry), and $\{V\}$ contains the electrical degrees of freedom. The electrical dofs are defined at the element level, and there are as many as there are active layers in the laminate. Note that the electrical degree of freedom is the difference of the electric potential between the top and bottom electrodes $\Delta\phi$.

1.3.3 Full order model

Piezoelectric models are described using both mechanical q_{mech} and electric potential DOF V. As detailed in sections section 1.3.1 and section 1.3.2 , one obtains models of the form

$$\left[\begin{array}{cc} Z_{CC}(s) & Z_{CV} \\ Z_{VC} & Z_{VV} \end{array} \right] \left\{ \begin{array}{c} q_{mech} \\ V \end{array} \right\} = \left\{ \begin{array}{c} F_{mech} \\ Q \end{array} \right\} \tag{1.58}$$

for both piezoelectric solids and shells, where $Z_{CC}(s)$ is the dynamic stiffness expressed as a function of the Laplace variable s.
For piezoelectric shell elements, electric DOF correspond to the difference of potential on the electrodes of one layer, while the corresponding load is the charge Q. In SDT, the electric DOFs for shells are unique for a single shell property and are thus giving an implicit definition of electrodes (see `p_piezo Shell`). Note that a common error is to fix all DOF when seeking to fix mechanical DOFs, calls of the form `'x==0 -DOF 1:6'` avoid this error.

For volume elements, each volume node is associated with an electric potential DOF and one defines multiple point constraints to enforce equal potential on nodes linked by a single electrode and sets one of the electrodes to zero potential (see `p_piezo ElectrodeMPC` and section 2.5 for a tutorial on how to set these contraints). During assembly the constraints are eliminated and the resulting model has electrical DOFs that correspond to differences of potential and loads to charge.

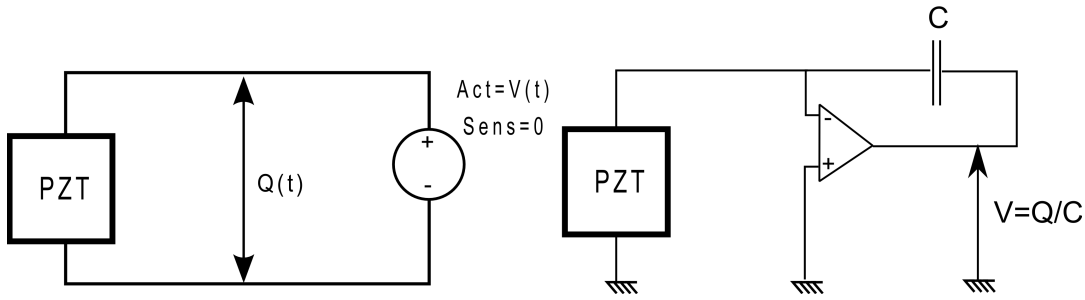

Figure 1.11: Short circuit: voltage actuator, charge sensor

Short circuit (SC), charge sensors configurations correspond to cases where the potential is forced to zero (the electrical circuit is shorted). In (1.58), this corresponds to a case where the potential (electrical DOF) is fixed and the charge corresponds to the resulting force associated with this boundary condition.
A **voltage actuator** corresponds to the same problem with $V = V_{In}$ (built in SDT using `fe_load DofSet` entries). The closed circuit charge is associated with the contraint on the enforced voltage and can be computed by extracting the second row of (1.58)

$$\{Q\} = [Z_{VC}]\{q_{mech}\} + [Z_{VV}]\{V_{In}\} \tag{1.59}$$

`p_piezo ElectrodeSensQ` provides utilities to build the charge sensors, including sensor combinations.
SC is the only possibly boundary condition in a FEM model where voltage is the unknown. The alternative is to leave the potential free which corresponds to not specifying any boundary condition.

When computing modes under voltage actuation, the proper boundary condition is a short circuit.

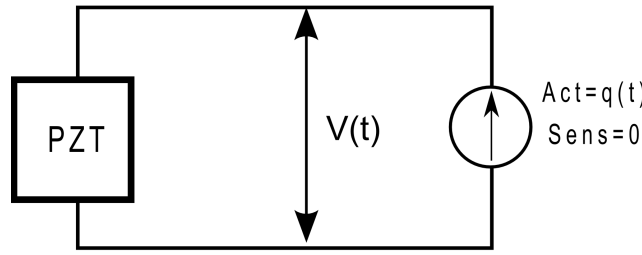

Figure 1.12: Open circuit (voltage sensor, charge actuator)

Open circuit (OC), voltage sensor, configurations correspond to cases where the charge remains zero and a potential is created on the electrodes due to mechanical deformations. A piezoelectric actuator driven using a charge source also would correspond to this configuration (but the usual is voltage driving).
The voltage DOF $\{V\}$ associated to open-circuits are left free in (1.58). Since electrostatics are normally considered, Z_{vv} is actually frequency independent and the voltage DOFs could be condensed exactly

$$\{V\} = [Z_{VV}]^{-1} \left(Q_{in} - [Z_{VC}] \{q_{mech}\}\right) \tag{1.60}$$

Since voltage is an explicit DOF, it can be observed using `fe_case SensDOF` sensor entries. Similarly charge is dual to the voltage, so a charge input would be a simple point load on the active DOF associated to an electrode. Note that specifying a charge distribution does not make sense since you cannot both enforce the equipotential condition and specify a charge distribution that results from this constraint.
It is possible to observe charge in an OC condition, but this is of little interest since this charge will remain at 0.

1.3.4 Using the Electrode stack entry

SDT 6.6 underwent significant revisions to get rid of solver strategies that were specific to piezo applications. The `info,Electrodes` of earlier releases is thus no longer necessary. To avoid disruption of user procedures, you can still use the old format with a `.ver=0` field.

`p_piezo ElectrodeInit` is used to build/verify a data structure describing master electric DOFs associated with electrodes defined in your model. The `info,Electrode` stack entry is a structure with fields

`.data` rows `NodeId IsOpen` gives the electrode nodes and for each one `1` if the circuit is open (voltage free), and `0` if it is closed (voltage enforced or fixed, actuator).

`.ver=1` is used to specify that the more general piezoelectric strategies of SDT >= 6.6 are used. This is the combined with the `p_piezo Electrode2Case` command which builds piezo loads and sensors. For SDT 6.5 strategies, use `.ver=0`.

`.def` `.DOF`, `.lab_in` **only needed** when combining multiple electrodes into a single input. The `.lab_in` is a cell array of strings, you should end the string with `V` so that it shows Q for associated charge sensors.

Each column gives the weighting coefficients associated with each electrode. Thus `def=[1;0;1]` corresponds to a single equal input on electrodes 1 and 3. Note that it does not make sense to combine electrical DOFs that are of mixed nature (actuator/sensor).

The `.DOF` field should contain `NodeId+.21` since the potential corresponds to DOF `.21`.

The `.lab_in` field can be used to provide labels associated with each actuator/sensor defined as a column of def. You should end the label with `V` so that the collocated sensor ends with a `Q` label.

`.cta` `.lab` (optional) can be used to combine electrodes into sensors / actuators. Each row of `.cta` defines a sensor (with matching `.lab`). Each column corresponds to an electrode declared in the `.data` field. You cannot combine open and closed circuit electrodes. It is possible to use both a `.cta` and a `.def` field.

`[model,data]=p_piezo('ElectrodeInit',model);` generates a default value for the electrode stack entry. Combination of actuators and sensors (both charge and voltage) is illustrated in section 2.1.3.

1.3.5 Model reduction

When building reduced or state-space models to allow faster simulation, the validity of the reduction is based on assumptions on bandwidth, which drive modal truncation, and considered loads which lead to static correction vectors.
Modes of interest are associated with boundary conditions in the absence of excitation. For the electric part, these are given by potential set to zero (grounded or shorted electrodes) and enforced by actuators (defined as `DofSet` in SDT) which in the absence of excitation is the same as shorting. Excitation can be mechanical F_{mech}, charge on free electric potential DOF Q_{In} and enforced voltage V_{In}. One thus seeks to solve a problem of the form

$$\begin{bmatrix} Z_{CC}(s) & Z_{CV} \\ Z_{VC} & Z_{VV} \end{bmatrix} \begin{Bmatrix} q_{mech} \\ V \end{Bmatrix} = \begin{Bmatrix} F_{mech} \\ Q_{In} \end{Bmatrix} - \begin{bmatrix} Z_{CV_{In}} \\ Z_{V_{In}} \end{bmatrix} \{V_{In}\} \tag{1.61}$$

Using the classical modal synthesis approach (implemented as `fe2ss('free')`), one builds a Ritz basis combining modes with grounded electrodes ($V_{In} = 0$), static responses to mechanical and charge loads and static response to enforced potential

$$\begin{Bmatrix} q_C \\ V \\ V_{In} \end{Bmatrix} = \left[\begin{bmatrix} \phi_q \\ \phi_V \\ 0 \end{bmatrix} \begin{bmatrix} Z(0)^{-1} \begin{Bmatrix} F_{mech} \\ Q_{In} \end{Bmatrix} \\ 0 \end{bmatrix} \begin{bmatrix} Z(0)^{-1} \begin{bmatrix} Z_{CV_{In}} \\ Z_{V_{In}} \end{bmatrix} \\ I \end{bmatrix} \right] \begin{Bmatrix} q_{mode} \\ q_{stat} \\ V_{In} \end{Bmatrix} \tag{1.62}$$

In this basis, one notes that the static response associated with enforced potential V_{In} does not verify the boundary condition of interest for the state-space model where $V_{In} = 0$. Since it is desirable to retain the modes with this boundary condition as the first vectors of basis (1.62) and to include static correction as additional vectors, the strategy used here is to rewrite reduction as

$$\{q\} = \left[\begin{bmatrix} \phi_q \\ \phi_V \\ 0 \end{bmatrix} \begin{bmatrix} Z(0)^{-1} \begin{bmatrix} F_m & Z_{CV_{In}} \\ Q_{In} & Z_{V_{In}} \end{bmatrix} \\ 0 \end{bmatrix} \right] \{q_R\} + \begin{Bmatrix} 0 \\ 0 \\ V_{In} \end{Bmatrix} \tag{1.63}$$

where the response associated with reduced DOFs q_R verifies $V_{In} = 0$ and the total response is found by adding the enforced potential on the voltage DOF only. The presence of this contribution corresponds to a D term in state-space models. The usual SDT default is to include it as a residual vector as shown in (1.62), but to retain the shorted boundary conditions, form (1.63) is prefered.

Tutorial

Contents

SDT supports piezoelectric constitutive laws for all 3D volume elements and composite shells. The main steps of an analysis are

- define/import mesh. This is a typical SDT process and is described in the SDT manual.
- define piezoelectric material properties, see `m_piezo Database`.
- define electrodes through an MPC for volumes, see `p_piezo ElectrodeMPC`, or the element property for shells, see `p_piezo Shell`.
- define electric boundary conditions, loading, and sensors, this has been discussed in section 1.3.3 and will be illustrated in the examples below.
- compute the response using full order (static or direct frequency response, calling `fe_simul`) or reduced order models (calling `fe2ss`, following the theory given in section 1.3.5).
- visualize the response in more detail.

2.1 Composite plate with 4 piezoelectric patches

2.1.1 Benchmark description

This example deals with a multi-layer composite plate with 4 piezoceramic patches. The geometry is represented in Figure 2.1. It corresponds to a cantilevered composite plate with 4 piezoelectric patches modeled using the `p_piezo Shell` formulation.
The material properties of the composite plate and the piezoceramic patches are given in Table 2.1. The composite material is made of 6 identical layers (total thickness of $1.3mm$), and the piezoelectric material corresponds to the *Sample_ULB* material in `m_piezo Database`.

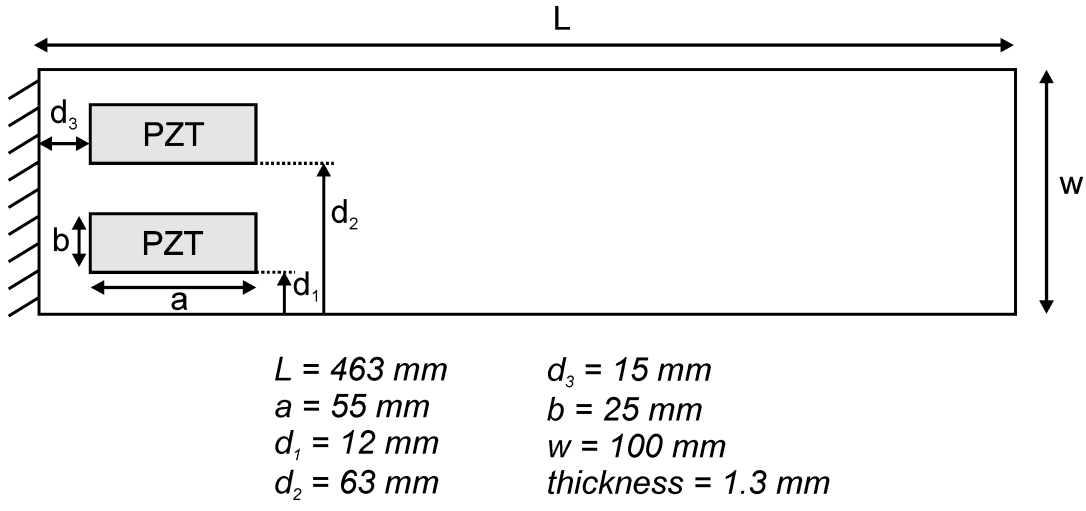

Figure 2.1: Geometric details of the composite plate with 4 piezoceramic patches

Property	Value
Composite layers	
E_x	$41.5GPa$
E_y	$41.5GPa$
G_{xy}	$3.35GPa$
ν_{xy}	0.042
ρ	$1490kg/m^3$
Piezoceramic patches	
E	$65GPa$
ν	0.3
ρ	$7800kg/m^3$
thickness	$0.25mm$
d_{31}	-205 $10^{-12}pC/N$ (or m/V)
d_{32}	-205 $10^{-12}pC/N$ (or m/V)
ε_{33}^T	2600 ε_0
ε_0	8.854 $10^{-12}Fm^{-1}$

Table 2.1: Material properties of the plate and the piezoceramic patches

2.1.2 Sample script

The first step consists in the creation of the model, the definition of the boundary conditions, and the definition of the default damping coefficient. (`d_piezo('TutoPlate_4pzt_single-s1')`) The resulting mesh is shown in Figure 2.2

```
% See full example as MATLAB code in d_piezo('ScriptPz_plate_4pzt_single')
%% Step 1 - Build model and visualize
model=d_piezo('MeshULBplate');  % creates the model
model=fe_case(model,'FixDof','Cantilever','x==0');
% Set modal default zeta based on loss factor of material 1
model=stack_set(model,'info','DefaultZeta',feutilb('getloss',1,model)/2);


cf=feplot(model); fecom('colordatagroup'); set(gca,'cameraupvector',[0 1 0])
```

One can have access to the piezoelectric material properties and the list of nodes associated to each pair of electrodes. Here nodes 1682 to 1685 are associated to the four pairs of electrodes defined in the model. The corresponding degree of freedom is the difference of potential between the electrodes in each pair corresponding to a specific piezoelectric layer. In this models, layers 1 and 8 are piezoelectric in groups 1 and 2 (the 6 internal layers correspond to the 6 layers of the supporting composite plate). Therefore only .21 (electrical) DOF is associated to nodes 1682-1685.

```
p_piezo('TabDD',model)   % List piezo constitutive laws
p_piezo('TabInfo',model) % List piezo related properties
```

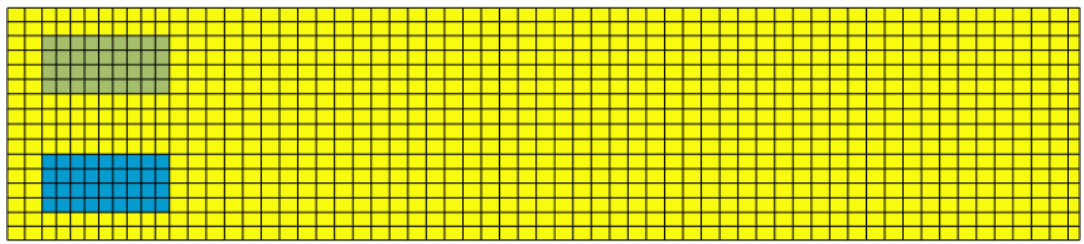

Figure 2.2: Mesh of the composite plate. The different colours represent the different groups

The next step consists in the definition of the actuators and sensors in the model. Here, we consider one actuator on Node 1682 (layer 1 of group 1), the four piezoelectric patches are used as charge sensors, and the tip displacement of the cantilever beam is measured at node 1054. Note that in order for Q-S1, Q-S2 and Q-S3 to measure resultant charge, the corresponding electrical difference of potential needs to be set to zero. If this is not done, then the charge sensors will measure a

charge close to zero (round-off errors) as there is no charge when the difference of potential across the electrodes is free. For Q-Act, the electrical dof is already fixed due to the fact that the patch is used as a voltage actuator.
(d_piezo('TutoPlate_4pzt_single-s2'))

```
%% Step 2 - Define actuators and sensors
model=fe_case(model,'SensDof','Tip',1054.03); % Displ sensor
model=fe_case(model,'DofSet','V-Act',struct('def',1,'DOF',1682.21)); %Act
model=p_piezo('ElectrodeSensQ  1682 Q-Act',model); % Charge sensors
model=p_piezo('ElectrodeSensQ  1683 Q-S1',model);
model=p_piezo('ElectrodeSensQ  1684 Q-S2',model);
model=p_piezo('ElectrodeSensQ  1685 Q-S3',model);
% Fix dofs 1683-1685 to measure resultant (charge)
model=fe_case(model,'FixDof','SC*1683-1685',[1683:1685]+.21);
sens=fe_case(model,'sens');
```

In order to check the effect of the actuator, we compute the static response using the full model and represent the deformed shape (Figure 2.3).
(d_piezo('TutoPlate_4pzt_single-s3'))

```
%% Step 3 Compute static and dynamic response
d0=fe_simul('dfrf',stack_set(model,'info','Freq',0)); % direct refer frf at 0Hz
cf.def=d0; fecom(';view3;scd .1;colordatagroup;undefline')
```

We can now compute the transfer function between the actuator and the four charge sensors, as well as the tip sensor using the full model. The result is stored in the variable $C1$.

```
% Compute frequency response function (full model)
if sdtkey('cvsnum','mklserv_client')>=126;ofact('mklserv_utils -silent')
    f=linspace(1,100,400); % in Hz
else;
  f=linspace(1,100,100); % in Hz (just 100 points to make it fast)
end

d1=fe_simul('dfrf',stack_set(model,'info','Freq',f(:))); % direct refer frf
% Project response on sensors
C1=fe_case('SensObserve',sens,d1);C1.name='DFRF';C1.Ylab='V-Act';
C1.Xlab{1}={'Frequency','Hz'};
```

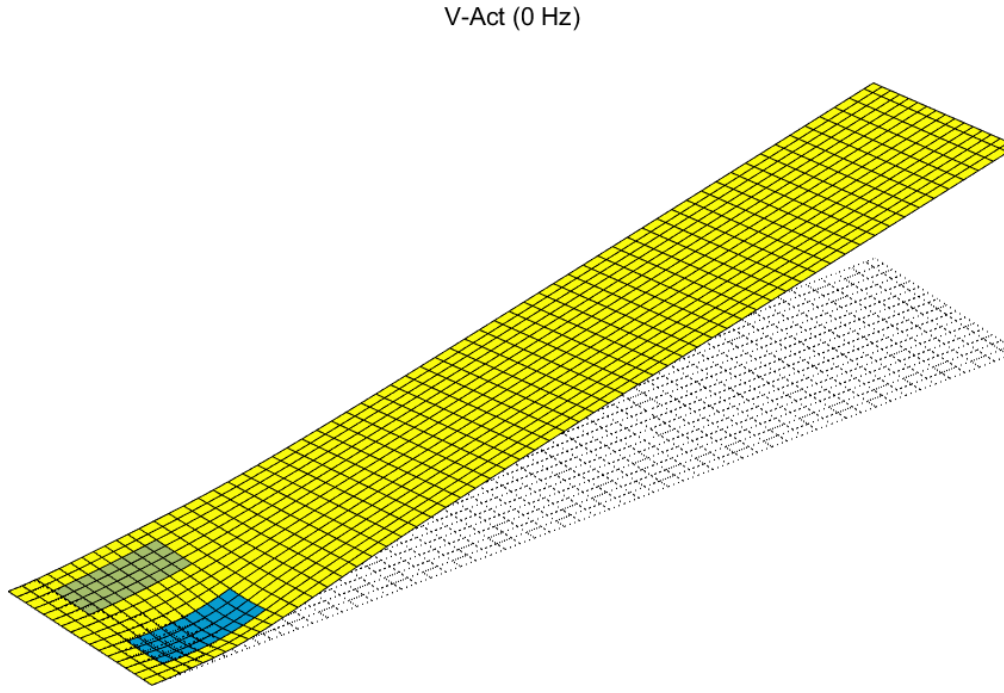

Figure 2.3: Deformed shape under voltage actuation on one of the bottom piezoelectric patches

A reduced state-space model can be built and the frequency response function calculated, and stored in the variable $C2$. The two curves obtained are compared to show the accuracy of the reduced state-space model in Figure 2.4.
(d_piezo('TutoPlate_4pzt_single-s4'))

```
%% Step 4 - Build state-space model
[s1,TR1]=fe2ss('free 5 10 0',model); %
C2=qbode(s1,f(:)*2*pi,'struct');C2.name='SS';

% Compare the two curves
C2.X{2}=sens.lab; C1.X{3}=nor2ss('lab_in',s1);C2.X{3}=nor2ss('lab_in',s1);%
C2=feutil('rmfield',C2,'lab'); C1.Ylab=C2.Ylab;
ci=iiplot;
iicom(ci,'curveinit',{'curve',C1.name,C1;'curve',C2.name,C2});
iicom('submagpha');
```

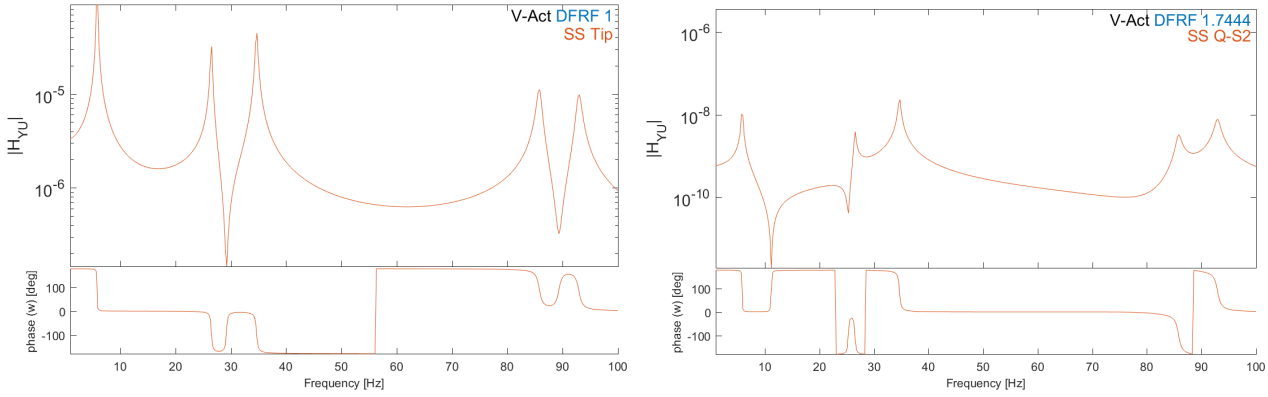

Figure 2.4: Comparison of FRF due to voltage actuation with the bottom piezo: full (DFRF) and reduced (SS) state-space models. Tip displacement and charge corresponding to electrical node 1682

2.1.3 Using combined electrodes

Combination of electrodes can be used in order to build a variety of actuators and sensors. For example, using the four piezoelectric patches, it is possible to induce a pure bending in the cantilever plate by using the following combination: the two actuators on one side of the plate are combined (the same voltage is applied to both simultaneously), while the two actuators on the opposite side are combined and driven out of phase. This allows to cancel the in-plane effect of the patches and

to induce a pure bending. If all 4 actuators are driven in phase, then it only induces in-plane forces causing displacements only in the plane of the plate (Figure 2.5).

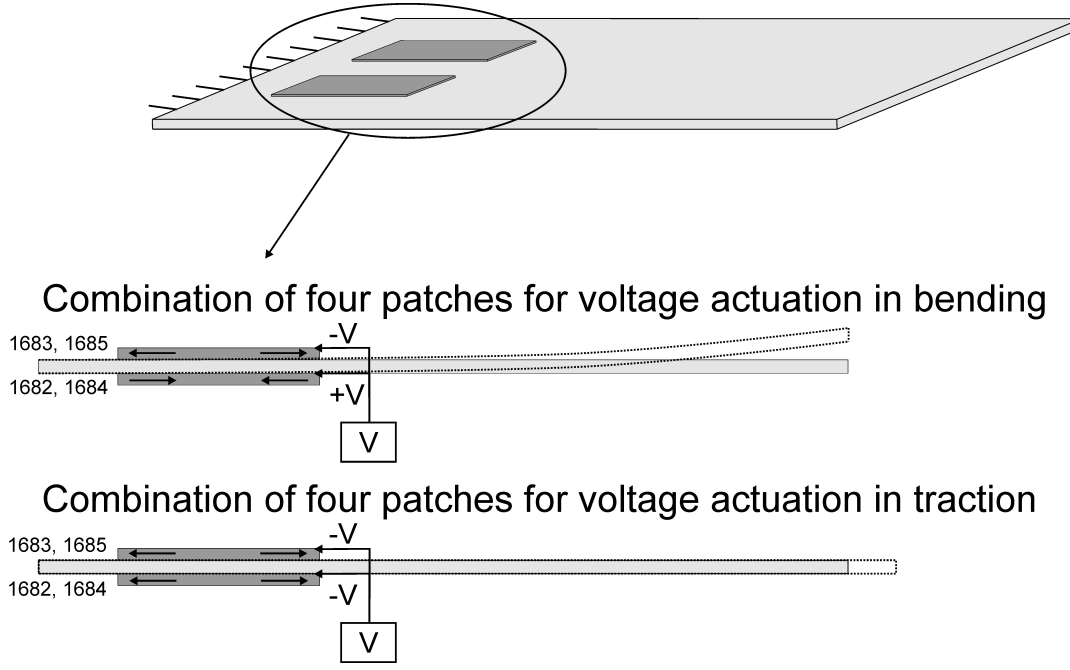

Figure 2.5: Example of combination of voltage actuators to induce bending or traction

The corresponding script to combine all four patches for bending and traction is:
(d_piezo('TutoPlate_4pzt_comb-s1'))

```
% See full example as MATLAB code in d_piezo('ScriptPz_plate_4pzt_comb')
%% Step 1 - Build model and define actuator combinations
model=d_piezo('MeshULBplate -cantilever');  % creates the model

% combine electrodes to generate pure bending / pure traction
data.def=[1 -1 1 -1;1 1 1 1]'; % Define combinations for actuators
data.lab={'V-bend';'V-Tract'};
data.DOF=p_piezo('electrodeDOF.*',model);
model=fe_case(model,'DofSet','V_{In}',data);
```

(d_piezo('TutoPlate_4pzt_comb-s2'))

```
%% Step 2 Compute static response
d0=fe_simul('dfrf',stack_set(model,'info','Freq',0)); % direct refer frf
cf=feplot(model); cf.def=d0;
fecom(';view3;scd .02;colordataEvalZ;undefline')
```

The resulting static deflections of the plate are shown in Figure 2.6.

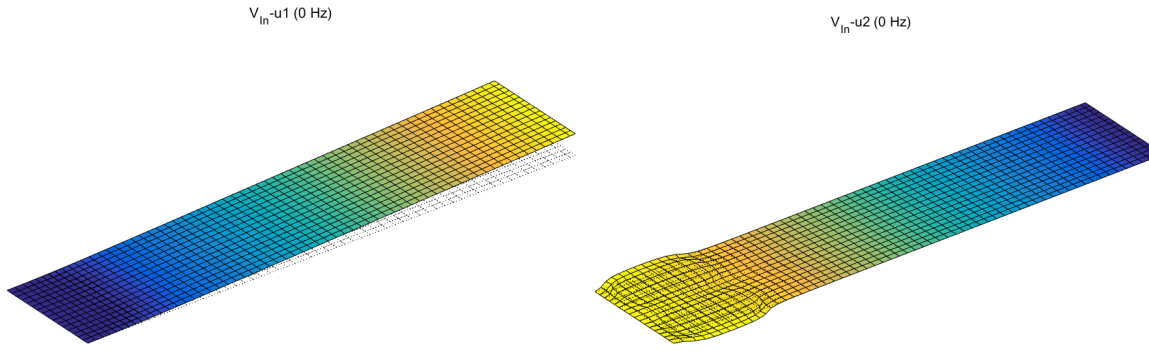

Figure 2.6: Static responses using a combination of actuators in order to induce pure bending or pure in-plane motion

We can now define two displacements sensors at the tip in the z and x directions and compute the FRFs between the bending actuator and the two displacements as well as the traction actuator and the two displacement sensors (Figure 2.7). The bending actuator/'Tip-z' FRF show three resonances corresponding to the first three bending mode shapes, while the traction actuator/'Tip-x' FRF shows no resonance due to the fact that the traction mode shape has a frequency much higher than the frequency band of the calculations. The FRFs show clearly the possibility to excite either bending or traction independently on the plate. The two other FRFs are close to zero.
(d_piezo('TutoPlate_4pzt_comb-s3'))

```
%% Step 3 - Dynamic response and state-space model
% Add tip displacement sensor in x and z
model=fe_case(model,'SensDof','Tip-z',1054.03); % Z-disp
model=fe_case(model,'SensDof','Tip-x',1054.01); % X-disp

% Make SS model and display FRF
[sys,TR]=fe2ss('free 5 30 0 -dterm',model);
C1=qbode(sys,linspace(1,100,400)'*2*pi,'struct');
C1.name='Bend-tract combination'; % Force name
C1.X{2}={'Tip-z';'Tip-x'}; % Force input labels
```

```
C1.X{3}={'V-bend';'V-tract'}; % Force output labels
iicom('CurveReset');iicom('curveinit',C1)
```

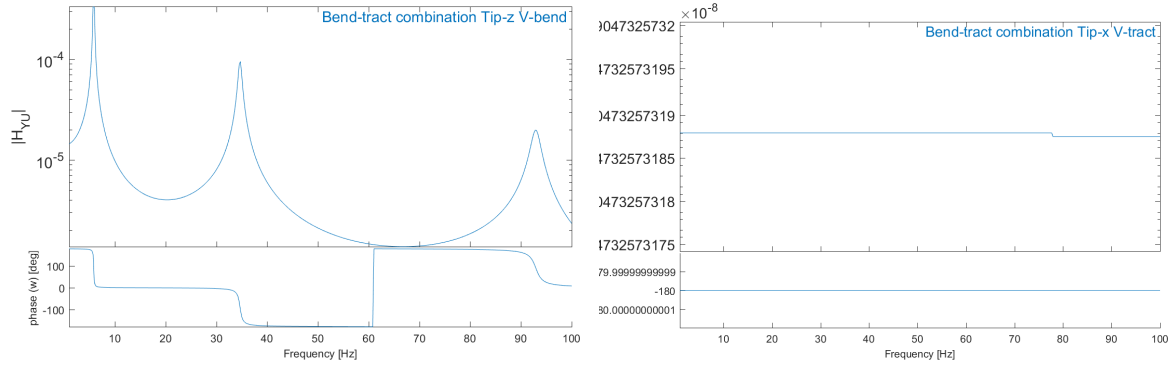

Figure 2.7: Bending actuator/'Tip-z' FRF (left) and traction actuator/'Tip-x' FRF (right)

Voltage and charge sensors can also be combined. Let us consider a voltage combination of nodes 1682 and 1683 for actuation, which will result in bending and a slight torsion of the plate due to the unsymmetrical bending actuation.
(d_piezo('TutoPlate_pzcomb_2-s1'))

```
% See full example as MATLAB code in d_piezo('ScriptPz_plate_pzcomb_2')
%% Step 1 - Build model and define actuator combinations
model=d_piezo('MeshULBplate cantilever');  % creates the model
model=fe_case(model,'DofSet','V*1683-1682', ...
    struct('def',[1;-1],'DOF',[1682;1683]+.21));
```

(d_piezo('TutoPlate_pzcomb_2-s2'))

```
%% Step 2 - Compute static response
d0=fe_simul('dfrf',stack_set(model,'info','Freq',0)); % direct refer frf
cf=feplot(model); cf.def=d0;
fecom(';view3;scd .1;colordatagroup;undefline')
```

We now define two sensors, consisting in charge combination with opposite signs for nodes 1684 and 1685 and voltage combination with opposite signs for the same nodes (Figure 2.8 shows the case of charge combination).

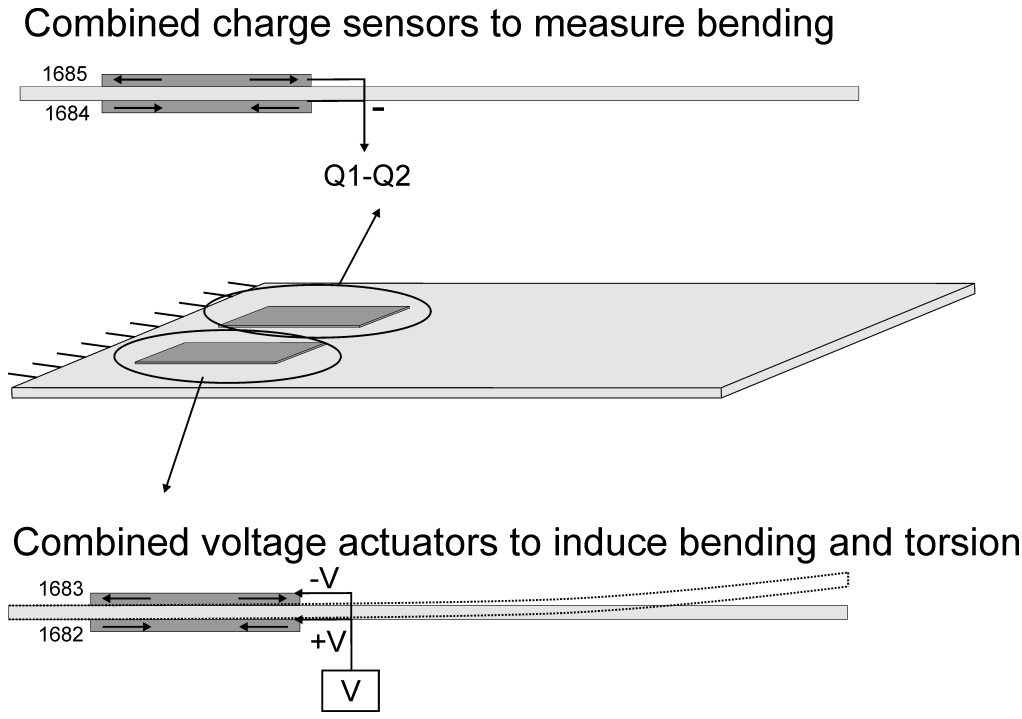

Figure 2.8: Example of combination of charge sensors to measure bending or traction

```
(d_piezo('TutoPlate_pzcomb_2-s3') )

%% Step 3 - Define sensor combinations
% Combined charge output (SC electrodes) % difference of charge 1684-1685
r1=struct('cta',[1 -1],'DOF',[1684;1685]+.21,'name','QS3+4');
model=p_piezo('ElectrodeSensQ',model,r1);
% Combined voltage output (OC electrodes) % difference of voltage 1684-1685
r1=struct('cta',[1 -1],'DOF',[1684;1685]+.21,'name','VS3+4');
model=fe_case(model,'SensDof',r1.name,r1);
```

By default, the electrodes are in 'open-circuit' condition for sensors, except if the sensor is also used as voltage actuator which corresponds to a 'short-circuit' condition. Therefore, as the voltage is left 'free' on nodes 1684 and 1685, the charge is zero and the combination will also be zero. If we wish to use the patches as charge sensors, we need to short-circuit the electrodes, which will result in a zero voltage and in a measurable charge. This is illustrated by computing the response in both configurations (open-circuit by default, and short-circuiting the electrodes for nodes 1684 and 1685):

```
(d_piezo('TutoPlate_pzcomb_2-s4') )
%% Step 4 - Compute dynamic response with state-space model
[sys,TR]=fe2ss('free 5 10 0 -dterm',model);
 C1=qbode(sys,linspace(1,100,400)'*2*pi,'struct'); C1.name='OC';

% Now you need to SC 1684 and 1685 to measure charge resultant
model=fe_case(model,'FixDof','SC*1684-1685',[1684;1685]+.21);
[sys2,TR2]=fe2ss('free 5 10 0 -dterm',model);
C2=qbode(sys2,linspace(1,100,400)'*2*pi,'struct');C2.name='SC';

% invert channels and scale
C1.Y=fliplr(C1.Y); C1.X{2}= flipud(C1.X{2});
C2.Y(:,1)=C2.Y(:,1)*C1.Y(1,1)/C2.Y(1,1);
iicom('curvereset'),iicom('curveinit',{'curve',C1.name,C1;'curve',C2.name,C2 });
```

The FRF for the combination of charge sensors is not exactly zero but has a negligible value in the 'open-circuit' condition, while the voltage combination is equal to zero in the 'short-circuit' condition. Charge sensing in the short-circuit condition and voltage sensing in the open-circuit condition are compared by scaling the two FRFs to the static response ($f = 0Hz$) and the result is shown on Figure 2.9. The FRFs are very similar but the eigenfrequencies are slightly lower in the case of charge sensing. This is due to the well-known fact that open-circuit always leads to a stiffening of the piezoelectric material. The effect on the natural frequency is however not very strong due to the small size of the piezoelectric patches with respect to the full plate.

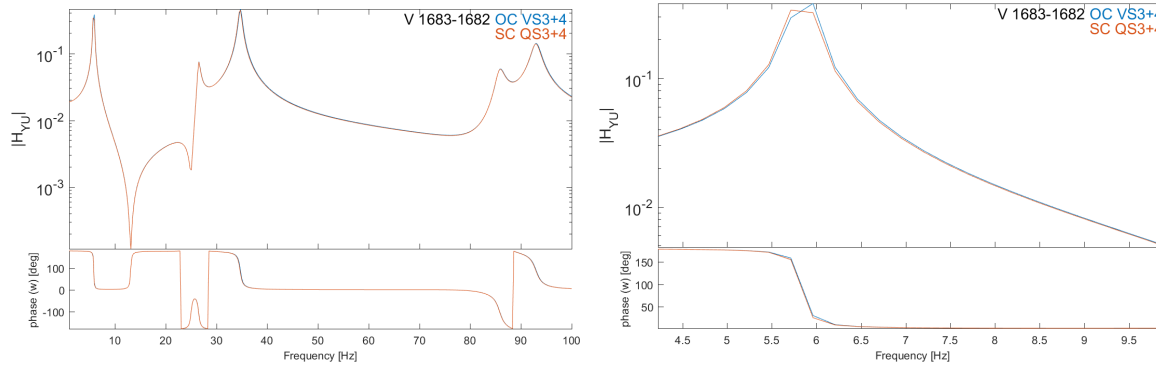

Figure 2.9: Comparison of FRFs (scaled to the static response) for voltage (green) and charge (blue) sensing. Zoom on the third eigenfrequency (right)

The stiffening effect due to the presence of an electric field in the piezoelectric material when the

electrodes are in the open-circuit condition is a consequence of the piezoelectric coupling. One can look at the level of this piezoelectric coupling by comparing the modal frequencies with the electrodes in open and short-circuit conditions.

```
(d_piezo('TutoPlate_pzcomb_2-s5') )
```

```
%% Step 5 - Compute OC and SC frequencies
model=d_piezo('MeshULBplate -cantilever');
% Open circuit : do nothing on electrodes
d1=fe_eig(model,[5 20 1e3]);
% Short circuit : fix all electric DOFs
DOF=p_piezo('electrodeDOF.*',model);
d2=fe_eig(fe_case(model,'FixDof','SC',DOF),[5 20 1e3]);
r1=[d1.data(1:end)./d2.data(1:end)];
plot(r1,'*','linewidth',2);axis tight
xlabel('Mode number');ylabel('f_{OC}/f_{SC}');
```

Figure 2.10 shows the ratio of the eigenfrequencies in the open-circuit vs short-circuited conditions. The difference depends on the mode number but is always lower than 1%. Higher stiffening effects occur when more of the strain energy is contained in the piezoelectric elements, and the coupling factor is higher.

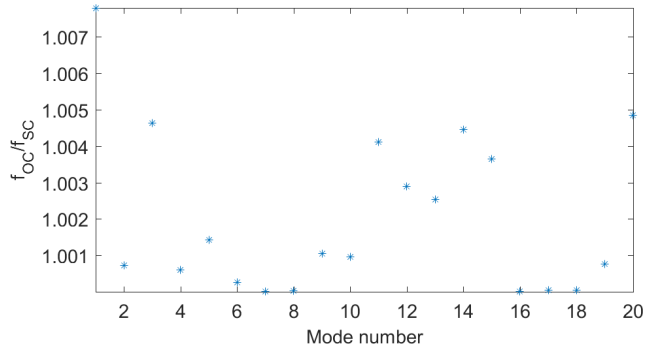

Figure 2.10: Ratio of the natural frequencies of modes 1 to 20 in open-circuit vs short-circuit conditions illustrating the stiffening of the piezoelectric material in the open-circuit condition

2.2 Integrating thin piezocomposite transducers in plate models

2.2.1 Introduction

PZT ceramics are commonly used due to their good actuation capability and very wide bandwidth. The major drawbacks of these ceramics are their brittle nature, and the fact that they cannot be easily attached to curved structures. In order to overcome these drawbacks, several packaged PZT composites have appeared on the market. A typical piezocomposite transducer is made of an active layer sandwiched between two soft thin encapsulating layers (Figure 2.11).

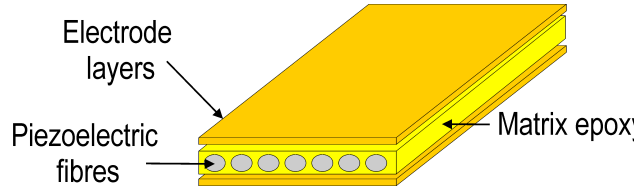

Figure 2.11: General layout of a piezoelectric composite transducer

The packaging plays two different roles : (i) applying prestress to the active layer in order to avoid cracks, and (ii) bringing the electric field to the active layer through the use of a specific surface electrode pattern. Due to the difficulty to ensure contact between cylindrical fibers and the electrodes, rectangular fibers have been developed, leading to the 'Macro Fiber Composite' transducers initially developed by the NASA [4] and currently manufactured by the company Smart Material (http://www.smart-material.com). As this type of transducer is widely used in the research community, this section shows how to integrate MFCs in piezoelectric plate models in SDT. Note however that all types of piezocomposites can be modeled, providing sufficient material data is available, which is rarely the case, as highlighted in the following for the case of MFCs.

Both d_{31} and d_{33} MFCs have been developed. The d_{31} MFCs are based on the same concept as the bulk ceramic patches where poling is made through the thickness (Figure 2.12a). The d_{33} MFCs

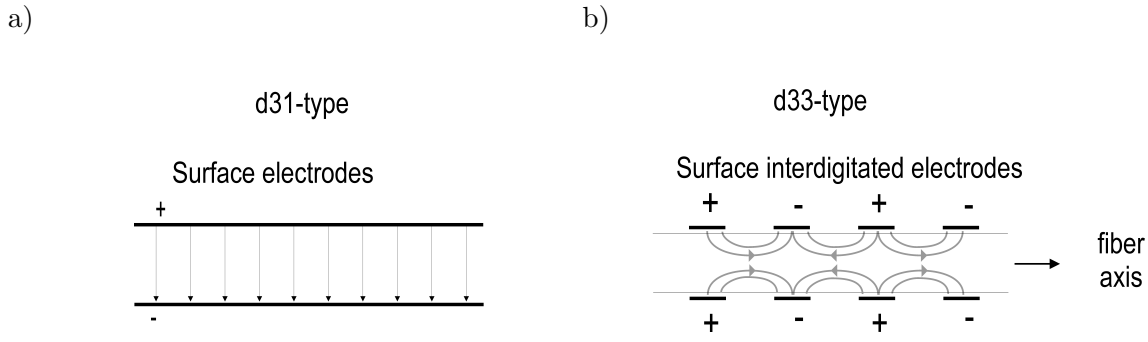

Figure 2.12: Electric fields in a) d_{31} and b) d_{33} piezocomposites

are aimed at exploiting the d_{33} actuation/sensing mode. This can be done by aligning the poling direction and the electric field with the fiber direction. The solution generally adopted is to use interdigitated electrodes (IDE) as shown in Figure 2.12b, which results in curved electric field lines, with the majority of the electric field aligned in the fiber direction. The general layout of both types of MFCs is represented in Figure 2.13. In the Smart Material documentation, the d_{33}-type is referred to as $P1$-type elongator (because $d_{33} > 0$) and the d_{31}-type is referred to as $P2$-type contractor (because $d_{31} < 0$). Piezoelectric plate elements implemented in SDT are based on the hypothesis

a) b)

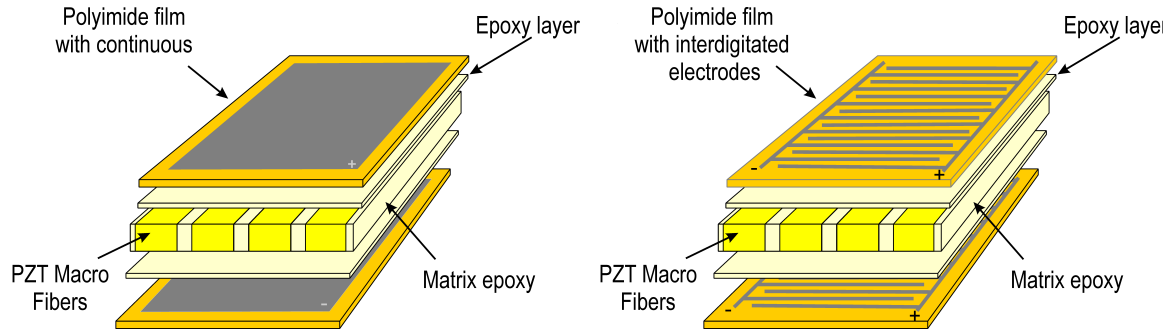

Figure 2.13: General layout of a) d_{31}-type MFCs and b) d_{33}-type MFCs

that the poling direction is through the thickness, which is suitable for the $P2$-type MFCs, but not for the $P1$-types. It is possible however with a simple analogy to model a $P1$-type MFC using the piezoelectric plate elements of SDT. The analogy is based on the equality of free in-plane strain of the transducer due to an applied voltage and capacitance. This requires two steps. The first one is to replace the curved electric field lines by a uniform field aligned with the poling direction, equal to $E = V/p$ where p is the distance between the fingers of the interdigitated electrodes (Figure 2.14).

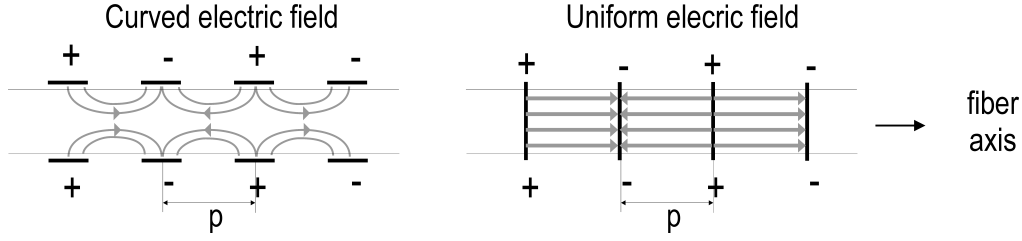

Figure 2.14: The curved electric field can be replaced by an equivalent electric field $E = V/p$

The second step is to express the equivalence in terms of free strains taking into account the difference

of local axes (this is because direction 3 is the poling direction which is different in both cases, see Figure 2.15).

$$\begin{array}{l} S_1|_{P2} = d_{31}|_{P2}\frac{V}{h} = S_3|_{P1} = d_{33}|_{P1}\frac{V}{p} \longrightarrow d_{31}|_{P2} = d_{33}|_{P1}\frac{h}{p} \\ S_2|_{P2} = d_{32}|_{P2}\frac{V}{h} = S_2|_{P1} = d_{32}|_{P1}\frac{V}{p} \longrightarrow d_{32}|_{P2} = d_{32}|_{P1}\frac{h}{p} \end{array} \tag{2.1}$$

As the thickness of the patch h is generally different from the distance between the fingers of the inter-digitated electrodes p, a h/p factor must be used. For MFCs, $h = 0.180mm$ and $p = 0.500mm$ so that $h/p = 0.36$. The PZT material used in MFCs has properties similar to the Ceramtec P502 material described in Section section 1.2.3 . If we assume that the active layer of the MFC is made of a bulk piezoceramic of that type, the equivalent d_{31} is given by :

$$S_1|_{P2} = d_{33}|_{P1}\frac{h}{p} = 440\frac{0.18}{0.5}(pC/N) = 158.4(pC/N) \tag{2.2}$$

This value is lower than the d_{31} coefficient of the bulk ceramic (185 pC/N). This shows that although the d_{33} coefficient is larger, the spacing of the fingers of IDE reduces the equivalent strain per Volt (ppm/V). This spacing cannot however be made much smaller as the part of the electric field aligned with the plane of the actuator would be significantly reduced. These findings are confirmed by the tabulated values of free strain per volt (ppm/V) in the fiber direction given in the datasheet of MFCs. Note that because the limiting value for actuation is the electric field and not the voltage, the $P1$-type MFCs have a much higher maximum voltage limit (1500 V) than the $P2$-type MFCs (360 V), leading to the possibility to achieve higher free strain, but at the cost of very high voltage values.

Similarly, the dielectric permittivity must be adapted to model $P1$-type MFCs using an equivalent $P2$-type MFC. This is done by expressing the equality of the capacitance:

$$C|_{P2} = \frac{\varepsilon_{33}^T|_{P2}\, b\, p}{h} = C|_{P1} = \frac{\varepsilon_{33}^T|_{P1}\, b\, h}{p} \longrightarrow \varepsilon_{33}^T|_{P2} = \varepsilon_{33}^T|_{P1}\left(\frac{h}{p}\right)^2 \tag{2.3}$$

The fact that piezoelectric fibers are mixed with an epoxy matrix introduces some orthotropy both at the mechanical and the piezoelectric levels. This means that all the parameters of the compliance matrix of an orthotropic material (1.29) must be identified, together with all piezoelectric coefficients (1.14). As we are integrating these transducers in plate structures, and assuming that the poling is in the direction of the thickness with electrodes on top and bottom of the piezoelectric layers, the compliance matrix reduces to:

$$\left[s^E\right] = \begin{bmatrix} \frac{1}{E_x} & \frac{-\nu_{yx}}{E_y} & 0 & 0 & 0 \\ \frac{-\nu_{xy}}{E_x} & \frac{1}{E_y} & 0 & 0 & 0 \\ 0 & 0 & \frac{1}{G_{yz}} & 0 & 0 \\ 0 & 0 & 0 & \frac{1}{G_{xz}} & 0 \\ 0 & 0 & 0 & 0 & \frac{1}{G_{xy}} \end{bmatrix} \tag{2.4}$$

a) b)

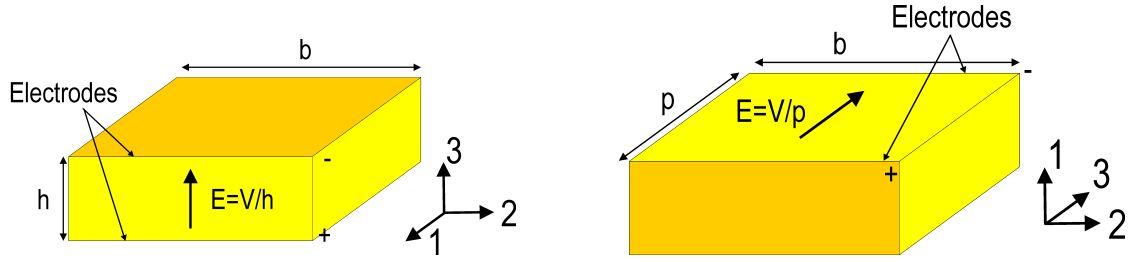

Figure 2.15: Electric fields and local axes used to model a $P1$-type MFC (b) with an equivalent $P2$-type MFC (a)

with $\frac{\nu_{yx}}{E_y} = \frac{\nu_{xy}}{E_x}$, the matrix of piezoelectric coefficients to:

$$[d] = \begin{bmatrix} d_{31} & d_{32} & 0 & 0 & 0 \end{bmatrix}; \tag{2.5}$$

and the matrix of dielectric permittivities to a scalar:

$$\left[\varepsilon^T\right] = \begin{bmatrix} \varepsilon_{33}^T \end{bmatrix} \tag{2.6}$$

In order to model such orthotropic transducers, it is therefore necessary to have access to 6 mechanical properties $E_x, E_y, \nu_{xy}, G_{xy}, G_{xz}, G_{yz}$, two piezoelectric coefficients d_{31}, d_{32}, and one dielectric constant ε_{33}^T. In the following, direction x will be replaced by L standing for 'longitudinal' (i.e. in the fiber direction) and y by T for 'transverse' (i.e. perpendicular to the fiber direction).

As there are no established and standardised techniques for testing piezocomposite transducers and identifying their full set of properties, it is common to find only a limited set of these coefficients in the datasheet of manufacturers. In addition, when such properties are given, they are measured on the full packaged piezocomposite transducer, which makes it difficult to translate them to the properties of each layer without making strong assumptions. The strategy adopted in this tutorial is to consider that an MFC is made of 5 layers (Figure 2.16). The electrode layer is slightly orthotropic due to the presence of the copper, but this effect can be neglected as it does not influence the overall behavior of the transducer. The 4 outer layers are therefore considered as homogeneous layers with the properties given in Table 2.2.

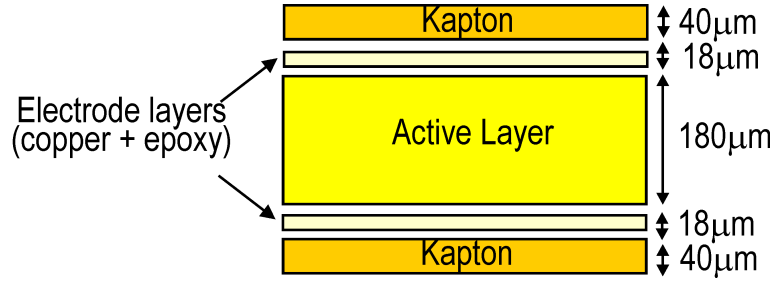

Figure 2.16: A MFC can be modeled as a 5-layer composite with an inner active layer and four passive layers

Material property	value	unit
Epoxy		
E	2.6	GPa
ν	0.33	
ρ	1500	kg/m^3
Kapton		
E	2.8	GPa
ν	0.3	
ρ	1580	kg/m^3

Table 2.2: Mechanical properties of the passive layers of MFCs

The mechanical, piezoelectric and dielectric properties of the active layers can be computed from their constituents using piezoelectric homogenization, assuming that the PZT material is Ceramtec P502, the matrix is epoxy with the properties given in Table 2.2, and the volume fraction of fibers is 86%. An analytical approach validated with detailed numerical computations has been developed in [3] and [5]. The homogenized properties found in these studies are given in Tables 2.3 and 2.4. They correspond to the *MFC_P2_AL* and *MFC_P1_AL* properties in `m_piezo Database`. For the $P1$-type MFCs, the values from Table 2.4 have been corrected with the h/p factor for the piezoelectric properties, and the $(h/p)^2$ factor for the dielectric constant. A value of $h/p = 0.36$ has been used.

$P2$ MFC Homogenized Properties	Symbol	Unit	Mixing rules
Young's modulus	E_L	GPa	47.17
	E_T	GPa	16.98
Shear Modulus	G_{LT}	GPa	6.03
	G_{Tz}	GPa	6.06
	G_{Lz}	GPa	17.00
Poisson's ratio	ν_{LT}	-	0.395
Piezoelectric charge constants	d_{31}	pC/N	-183
	d_{32}	pC/N	-153
Dieletric relative constant (free)	$\varepsilon_{33}^T/\varepsilon_0$	-	1600

Table 2.3: Homogenized properties of the active layer of $P2$-MFCs calculated using the analytical mixing rules of [5]

P_1 MFC Homogenized Properties	Symbol	Unit	Mixing rules
Young's modulus	E_L	GPa	42.18
	E_T	GPa	16.97
Shear Modulus	G_{LT}	GPa	6.03
	G_{Tz}	GPa	17
	G_{Lz}	GPa	6.06
Poisson's ratio	ν_{LT}	-	0.380
Piezoelectric charge constants	d_{32}	pC/N	-176
	d_{33}	pC/N	436
Dieletric relative constant (free)	$\varepsilon_{33}^T/\varepsilon_0$	-	1593

Table 2.4: Homogenized properties of the active layer of $P1$-MFCs calculated using the analytical mixing rules of [5] (correction factor not included)

2.2.2 Example of MFC transducers integrated in plate structures

This example deals with a cantilever aluminum plate with two $P1$-type MFCs (M8528-P1) attached on each side of the plate. The geometry is represented in Figure 2.17. The plate is meshed with

rectangular piezoelectric elements. The main part of the beam is made of one layer (aluminum), and the part where the two MFCs are attached is made of 11 layers (5 layers for each MFC and the central aluminum layer).

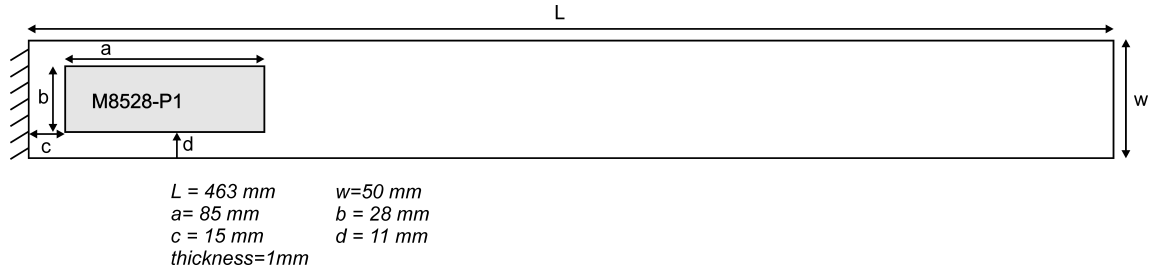

Figure 2.17: Geometric details of the aluminum plate with 2 $P1$-type MFCs

```
(d_piezo('TutoPlate_mfc-s1') )

% See full example as MATLAB code in d_piezo('ScriptPz_plate_MFC')
%% Step 1 - Build mesh and visualize
% Meshing script,open with sdtweb d_piezo('MeshMFCplate')
model=d_piezo('MeshMFCplate -cantilever')  % creates the model


cf=feplot(model); fecom('colordatagroup-EdgeAlpha.1');
```

Using the two MFCs as actuators, we define two combinations in order to induce bending or traction and compute and represent the static response (Figure 2.18):

```
(d_piezo('TutoPlate_mfc-s2') )

%% Step 2 - Define actuators and sensors
data.def=[1 -1;1 1]'; % Define combinations for actuators
data.lab={'V-bend';'V-Tract'};
data.DOF=[1682.21; 1683.21];
model=fe_case(model,'DofSet','V_{In}',data);
% Add tip displacement sensors in z
model=fe_case(model,'SensDof','Tipt-z',156.03); % Z-disp
model=fe_case(model,'SensDof','Tip-x',156.01); % X-disp
model=fe_case(model,'SensDof','Tipb-z',2964.03); % Z-disp

(d_piezo('TutoPlate_mfc-s3') )
```

```
%% Step 3 - Compute static response
d0=fe_simul('dfrf',stack_set(model,'info','Freq',0)); %
cf=feplot(model,d0); sens=fe_case(model,'sens');
C1=fe_case('SensObserve',sens,d0);
fecom(';view3;scd .1;colordataEvalA -edgealpha.1;undefline')
```

a) b)

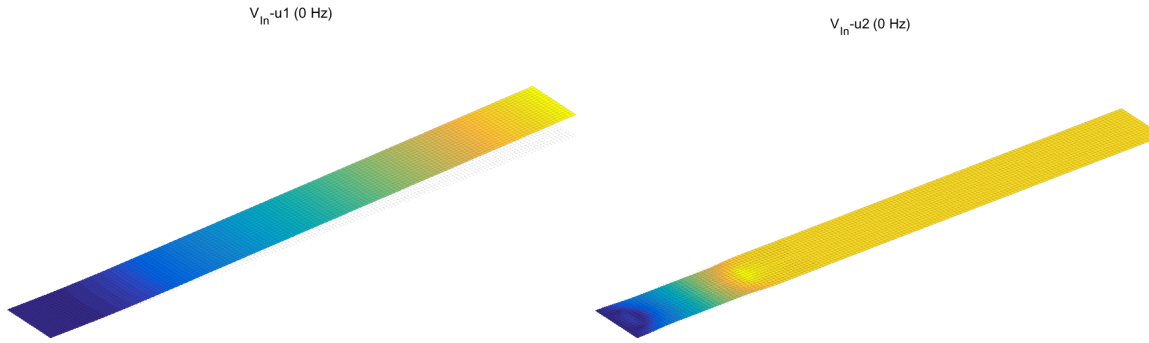

Figure 2.18: Static deformation under combined voltage actuation in a) bending, b) traction

The deformed shape under traction actuation highlights the fact that the induced strain in the lateral direction is of opposite sign with respect to the longitudinal direction, which is due to the fact that we are using a $P1$-type MFC. $F1$-type MFCs are based on the same layout as $P1$-types but the fibers are oriented with an angle of 45°. Such transducers can be easily modeled by changing the angle of the active layer in the multi-layer sequence. Assume that the bottom MFC makes an angle of 45° with respect to the axis of the beam and that the top MFC makes an angle of -45°. Each actuator induces both bending and torsion in the plate:
(`d_piezo('TutoPlate_mfc-s4')`)

```
%% Step 4 - Rotate fibers
model.il(2,[20 44])=[45 -45];
d1=fe_simul('dfrf',stack_set(model,'info','Freq',0)); % static response
cf.def=d1; fecom('scd 1e-2'); C2=fe_case('SensObserve',sens,d1);
```

The torsion can be easily seen by looking at the deformed shape resulting from the combination of the two MFCs with opposite signs which cancels the bending effect, as shown in Figure 2.19.

2.3 Using shaped orthotropic piezoelectric transducers

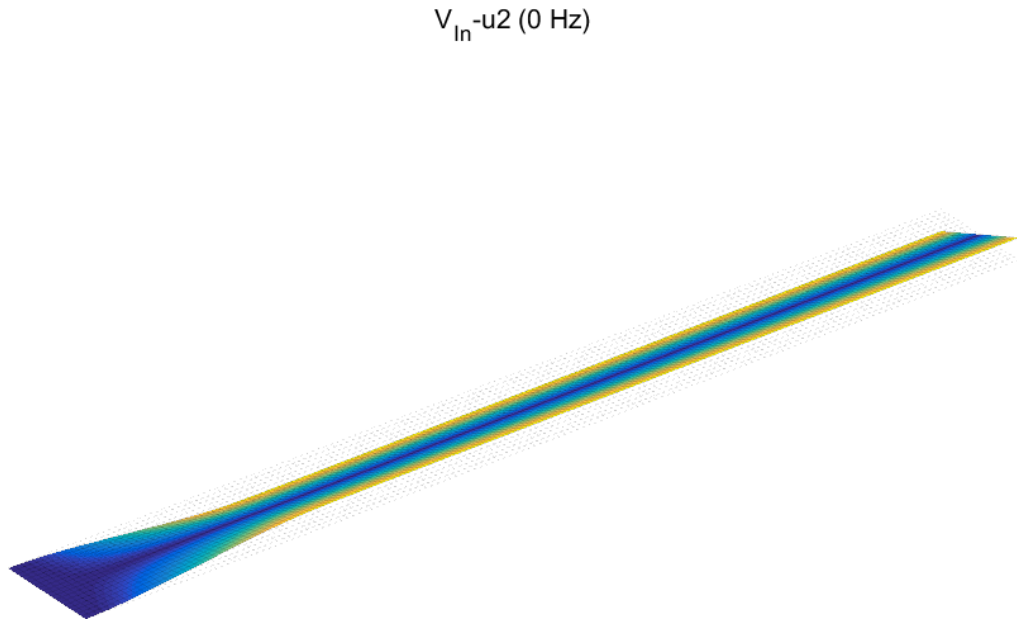

Figure 2.19: Static deformation under combined voltage with opposite sign using two $F1$-type MFCs

2.3.1 Introduction

Typical piezoelectric transducers found on the market are rectangular or circular. Different researchers have however studied the possibility to use more complex shapes. This idea was mainly driven by the active control applications. The first developments in this direction concern triangular actuators which will be used in the following example after recalling the theory behind the development of such transducers. When used as an actuator, an applied voltage on a piezoelectric patch results in a set of balanced forces on the supporting structure. The analytical expression of these so-called equivalent forces has been derived analytically in [6] in the general case of an orthotropic patch poled through the thickness with an arbitrary shape and attached to a supporting plate (assumed to follow Kirchhoff plate theory). The analytical expressions show that these forces are a function of the material properties of the piezo, as well as the expression of the normal to the contour of the patch. In the case of a triangular patch, the equivalent forces are illustrated on Figure 2.20. They consist in point forces P and $P/2$, and bending moments M_1 and M_2 whose expressions are:

$$\begin{aligned} P = &\quad -(e_{31}-e_{32})\frac{bl}{\frac{b^2}{4}+l^2} z_m V \\ M_1 = &\quad -e_{31} z_m V \\ M_2 = &\quad -\frac{\frac{b^2}{4}e_{31}+l^2 e_{32}}{\frac{b^2}{4}+l^2} z_m V \end{aligned} \tag{2.7}$$

These expressions show that the point forces are only present when the material is orthotropic ($e_{31} \neq e_{32}$). An interesting application of the triangular actuator is to design it to be a point-force actuator. This requires (i) to clamp the base of the triangle in order to cancel the bending moment M_1 and the two point forces $P/2$, (ii) to cancel M_2. The result is a single point-force P at the tip of the triangle. The cancelation of M_2 requires to have [7]:

$$M_2 = -\frac{\frac{b^2}{4}e_{31} + l^2 e_{32}}{\frac{b^2}{4} + l^2} z_m V = 0 \longrightarrow \frac{b}{l} = 2\sqrt{\frac{-e_{32}}{e_{31}}} \tag{2.8}$$

This expression shows that the point-force actuator can only be achieved when e_{31} and e_{32} are of opposite sign. With a PZT ceramic, this is possible using inter-digitated electrodes, which result in a compression in the lateral direction when the transducers elongates in the longitudinal direction. A possibility is to use a triangular transducer based on the same principle as the $P1-type$ MFC. The resulting force at the tip of the triangle is given by:

$$P = -e_{31}\frac{b}{l} z_m \, V \tag{2.9}$$

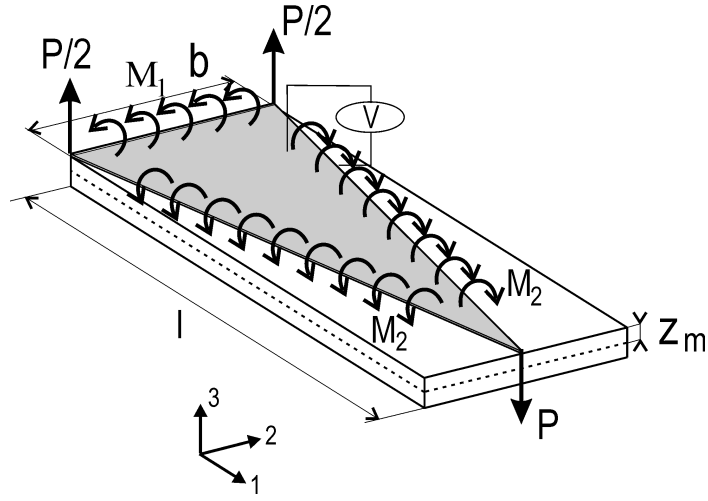

Figure 2.20: Equivalent loads for an orthotropic piezoelectric actuator

Given the material properties of the active layer of $P1$-MFCs in Table 2.4, the values of e_{31} and e_{32}

are:

$$\begin{aligned} e_{31} &= \left(\frac{E_L}{1-\nu_{TL}\nu_{LT}}\right) d_{31} + \left(\frac{\nu_{LT}E_T}{1-\nu_{TL}\nu_{LT}}\right) d_{32} = 18.32 C/m^2 \\ e_{32} &= \left(\frac{\nu_{TL}E_L}{1-\nu_{TL}\nu_{LT}}\right) d_{31} + \left(\frac{E_T}{1-\nu_{TL}\nu_{LT}}\right) d_{32} = -0.1859 C/m^2 \end{aligned} \tag{2.10}$$

and the b/l ratio leading to a point load actuator is

$$\frac{b}{l} = 2\sqrt{\frac{-e_{32}}{e_{31}}} = 0.2015 \tag{2.11}$$

Another possibility is to use a full piezoceramic instead of a composite, which is illustrated below.

2.3.2 Example of a triangular point load actuator

We consider an example similar to the one treated in [7] which consists in a $414mm$x$314mm$x$1mm$ aluminum plate clamped on its edges, on which a triangular piezoelectric transducer is fixed on the top surface in order to produce a point load, as illustrated in Figure 2.21. The piezoelectric material used is *SONOX P502* whose properties are given in Table 1.2 with the exception that the value of $\nu_p = 0.4$ in order to be in accordance with the value used in [7]. With these material properties, the b/l ratio to obtain a point load actuator is $b/l = 0.336$ (this will be verified in the example script). The triangular ceramic has a thickness of $180\mu m$ and is encapsulated between two layers of epoxy (see properties in Table 2.2) which have a thickness of $60\mu m$. The basis of the triangle is $33.6mm$ in order to obtain the point load actuator (the height has a length of $100mm$). One triangle is attached to the top surface, and one to the bottom, and the transducers are driven out of phase in order to induce pure bending of the plate and no in-plane motion.

2.3.3 Numerical implementation of the triangular point load actuator

The mesh used for the computations is shown in Figure 2.22 and is generated with:
(d_piezo('TutoPlate_triang-s1'))

```
% See full example as MATLAB code in d_piezo('ScriptPz_Plate_Triang')
%% Step 1 - Build Mesh using gmsh and visualize
% Meshing script can be viewed with sdtweb d_piezo('MeshTrianglePlate')
% --- requires gmsh
model=d_piezo('MeshTrianglePlate');


cf=feplot(model); fecom('colordatapro'); fecom('view2')
```

The static response due to an applied voltage on the piezo actuators is computed as follows:
(d_piezo('TutoPlate_triang-s2'))

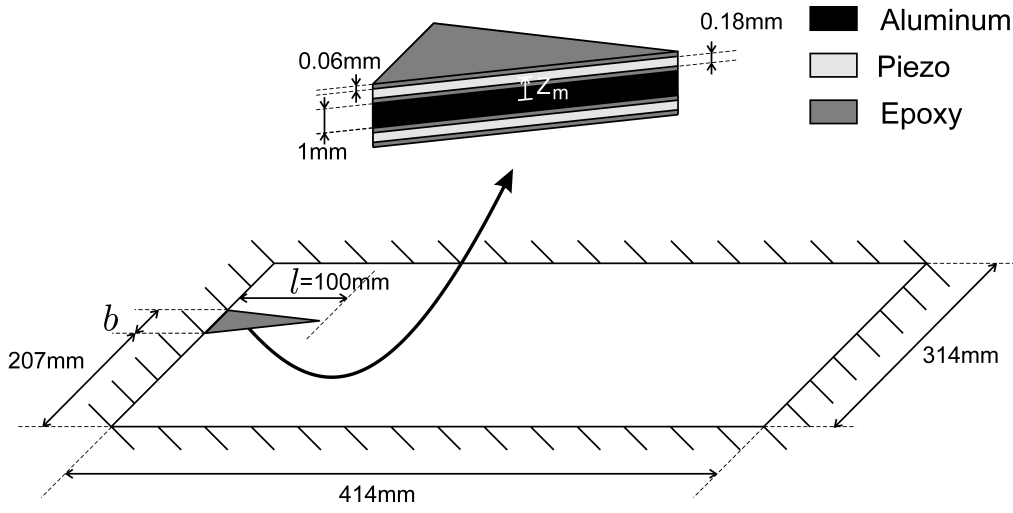

Figure 2.21: Description of the numerical case study for a point load actuator

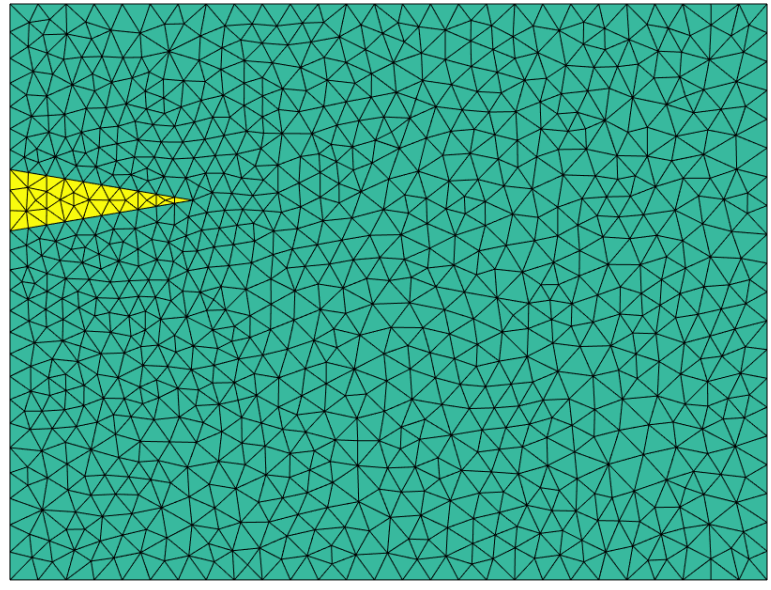

Figure 2.22: Mesh of the aluminum plate with a triangular piezoelectric actuator

```
%% Step 2 - Define actuators and sensors
model=fe_case(model,'SensDof','Tip',7.03); % Displ sensor
model=fe_case(model,'DofSet','V-Act',struct('def',[-1; 1],'DOF',[100001; 100002]+.21));
```

```
(d_piezo('TutoPlate_triang-s3') )
```

```
%% Step 3 - Compute static response to voltage actuation
d0=fe_simul('dfrf',stack_set(model,'info','Freq',0));
cf.def=d0; fecom('colordataz -alpha .8 -edgealpha .1')
fecom('scd -.03'); fecom('view3');
```

and represented on Figure 2.23.

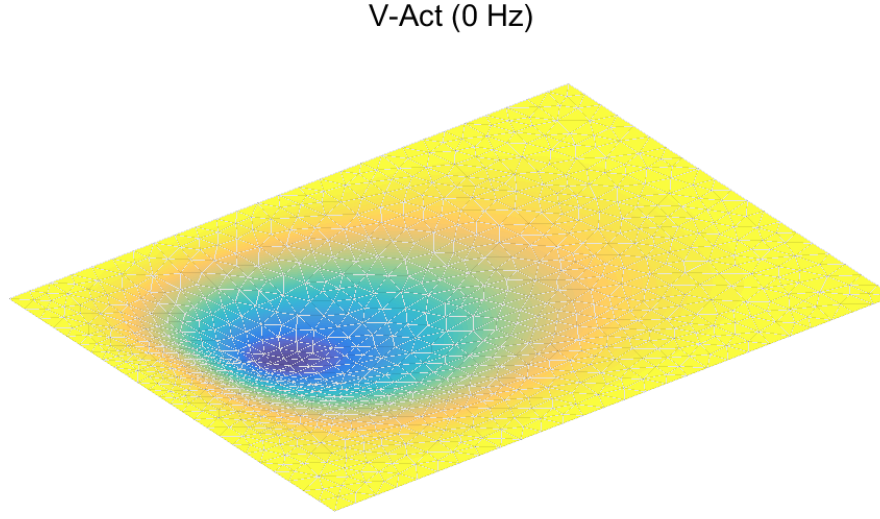

Figure 2.23: Static displacement due to voltage actuation on the triangular piezo

We now compute and compare the dynamic response of the plate excited with the triangular piezo and a point force whose amplitude is computed using Equation ((2.9)). The computation is performed with a reduced state-space model using 20 mode shapes:
(d_piezo('TutoPlate_triang-s4'))

```
%% Step 4 - Compute dynamic response with state-space model
[sys,TR]=fe2ss('free 5 20 0 -dterm',model);
C1=qbode(sys,linspace(0,500,1000)'*2*pi,'struct'); C1.name='.';
```

```
%% Point load actuation
```

```
model=fe_case(model,'Remove','V-Act'); % remove piezo actuator
model=fe_case(model,'FixDof','Piezos',[100001;100002]); %SC piezo electrodes

% Determine scaling factor, check b/l ratio and build point force
CC=p_piezo('viewdd -struct',model);
a=100; b=33.58;
zm=0.650e-3; V=1; e31=CC.e(1); A=-(e31*zm*V*b)/a; A=A*2; % Two triangles
bl= 2*sqrt(-CC.e(2)/CC.e(1));

data=struct('DOF',[7.03],'def',A); data.lab=fe_curve('datatype',13);
model=fe_case(model,'DofLoad','PointLoad',data);

% Static response to point load
d1=fe_simul('dfrf',stack_set(model,'info','Freq',0));
ind=fe_c(d1.DOF,7.03,'ind'); d1p=d1.def(ind);

% Dynamic response (reduced modal model)
[sys,TR]=fe2ss('free 5 20 0 -dterm',model);
C2=qbode(sys,linspace(0,500,1000)'*2*pi,'struct'); C2.name='-';


% Compare frequency responses
ci=iiplot;
iicom(ci,'curveinit',{'curve',C1.name,C1;'curve',C2.name,C2});
iicom('submagpha');
```

The amplitude and phase of the vertical displacement at the tip of the triangle are represented for both cases in Figure 2.24, showing the excellent agreement.

2.4 Vibration damping using a tuned resonant shunt circuit

2.4.1 Introduction

The idea of damping a structure via a resonant shunt circuit is very similar to the mechanical *tuned mass damper* (TMD) concept. The mechanical TMD is replaced by a 'RL' shunt circuit which, together with the capacitance of the piezoelectric element to which it is attached, acts as a resonant 'RLC' circuit. By tuning the resonance frequency of this circuit to the open-circuit (OC) resonance frequency of the structure equipped with a piezoelectric transducer, one can achieve vibration reduction around the resonant peak of interest. The mechanism is based on the conversion of part of

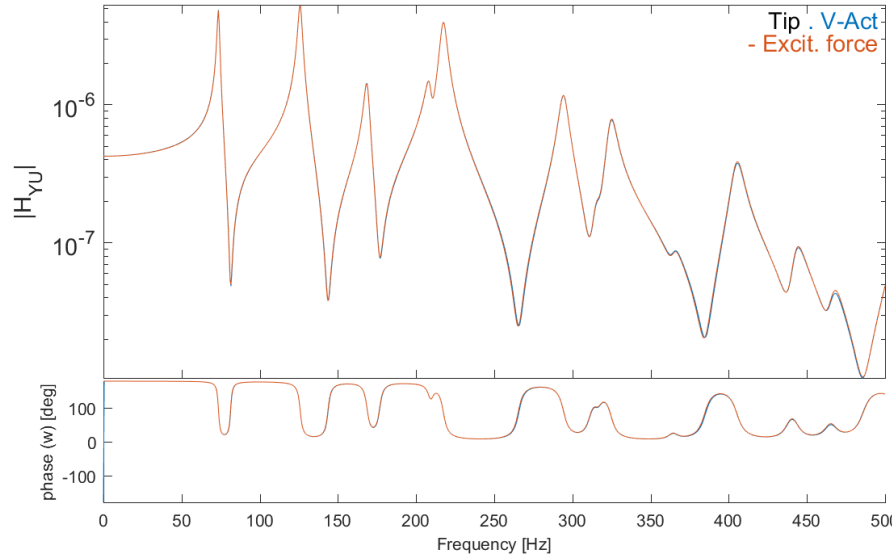

Figure 2.24: Dynamic response at the tip of the triangle due to (i) voltage actuation on the piezo and (ii) point force at the tip of the triangle

the mechanical energy to electrical energy which is then dissipated in the resistive component of the circuit.

The part of mechanical energy which is converted into electrical energy is given by the generalized electro-mechanical coupling coefficient α_i of the mode i of interest. In practice, this generalized coupling coefficient can be computed based on the open-circuit (OC) and short-circuit (SC) frequencies Ω_i and ω_i of the piezoelectric structure. Experimentally, these frequencies are usually obtained via the measurement of the impedance (V/I) or the capacitance (Q/V) of the piezoelectric structure, and one has:

$$\alpha_i = \frac{\Omega_i^2 - \omega_i^2}{\Omega_i^2} \tag{2.12}$$

Once α_i is known for the mode of interest, the values of R and L can be computed. Several rules exist to compute the optimal values of R and L [8]. We adopt here Yamada's tuning rules which are equivalent to Den Hartog's tuning rules for the mechanical TMD. The first rule aims at tuning the resonant circuit to the OC frequency Ω_i of the piezoelectric structure:

$$\delta = \frac{\Omega_i}{\omega_e} = 1 \tag{2.13}$$

with

$$\omega_e = \sqrt{\frac{1}{LC_{i2}}} \tag{2.14}$$

where C_{i2} is the capacitance of the piezoelectric element attached to the structure taken after the resonant frequency of interest. Note that this value is in practice difficult to measure with precision. In this example, we will take the value which is at the frequency corresponding to the mean value between the SC resonant frequencies ω_i and ω_{i+1}. This first tuning rule allows to compute the value of L. For different values of R, one can show that when plotting the response of the structure to which the resonant shunt has been added for different values of R, all curves cross at two points P and Q which are at the same height (Figure 2.25). The second tuning rule is aimed at finding the optimal value of R which minimizes the response of the structure for the range of frequencies around the natural frequency of interest and is given by:

$$R = \sqrt{\frac{3\alpha_i^2}{2-\alpha_i^2}}\frac{1}{C_{i2}\Omega_i} \tag{2.15}$$

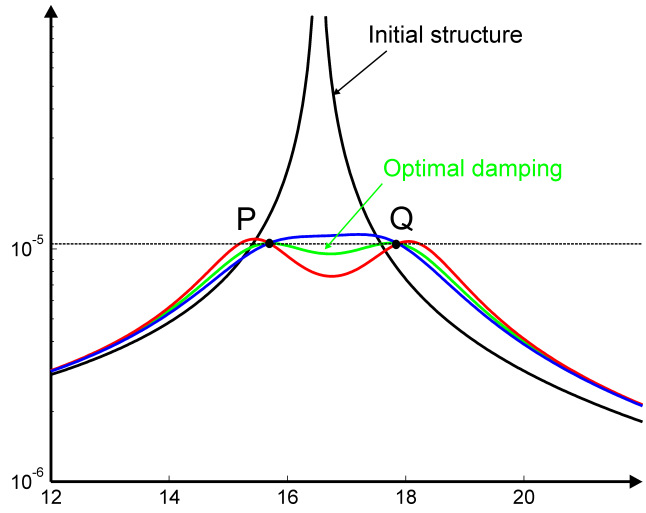

Figure 2.25: Response of the structure with and without and RL shunt : P and Q are at the same height when $\delta = 1$

2.4.2 Resonant shunt circuit applied to a cantilever beam

We illustrate the use of a resonant shunt with the following example of a cantilever beam. The beam is has a length of *350 mm*, a width of *25 mm* and a height of *2 mm* (Figure 2.26). Two pairs of piezoelectric *PIC 255* patches of dimensions *50 mm X 25 mm X 0.5 mm* are glued on each side of the beam starting at the cantilever side . The nodes associated to the electrical dofs of the

four patches are numbered respectively [10001 10002] for the patches next to the clamping side, and [20001 20002] for the other pair situated next to it.

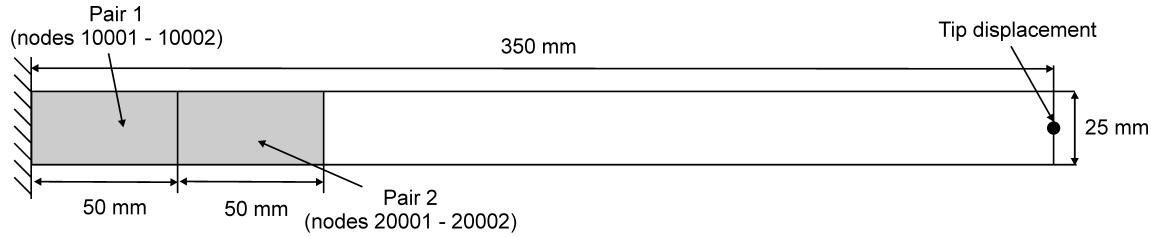

Figure 2.26: Cantilever beam with two pairs of piezoelectric patches

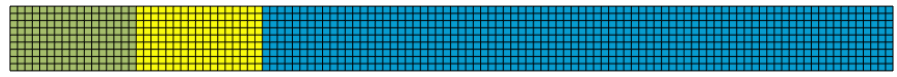

Figure 2.27: Mesh of the cantilever beam showing the two pairs of piezoelectric patches on the left, next to the clamp

We start by generating the mesh (Figure 2.27) and setting the damping in the model.
(d_piezo('TutoPz_shunt-s1'))

```
% See full example as MATLAB code in d_piezo('ScriptPz_Shunt')
%% Step 1 - Build mesh and visualize
% Meshing script can be viewed with sdtweb d_piezo('MeshShunt')
model=d_piezo('meshshunt');
model=stack_set(model,'info','DefaultZeta',1e-4)


feplot(model); cf=fecom; fecom('colordatapro')
```

In order to implement the shunt, we will compute the capacitance curve of the first set of patches used in phase opposition (bending) and extract the OC and SC first natural frequency of the cantilever beam. In order to do that, we define two combinations of patches for actuation (bending using the first pair in opposition of phase, and bending using the second pair in opposition of phase), one combination of charge sensors in opposition of phase (to compute the capacitance of the first pair), and one sensor for tip displacement (Figure 2.26).

(d_piezo('TutoPz_shunt-s2'))

```
%% Step 2 - Define actuators and sensors
% Actuators
data.def=[1 -1 0 0; 0 0 1 -1]'; % Define combinations for actuators
data.DOF=[10001 10002 20001 20002]';
model=fe_case(model,'DofSet','V_In',data);
% Sensors
r1=struct('cta',[1 -1],'DOF',[10001;10002]+.21,'name','QS3+4');
model=p_piezo('ElectrodeSensQ',model,r1);
model=fe_case(model,'SensDof','Tip',1185.03);
sens=fe_case(model,'sens');
```

We can now compute the response of the structure to the two bending actuators using a reduced state-space model with 30 modes. The response of the combination of charge sensors is the capacitance curve (Figure 2.28) of the first pair of piezo patches used in opposition of phase from which ω_1 and Ω_1 are extracted to compute α_1, and C_{12} is computed.

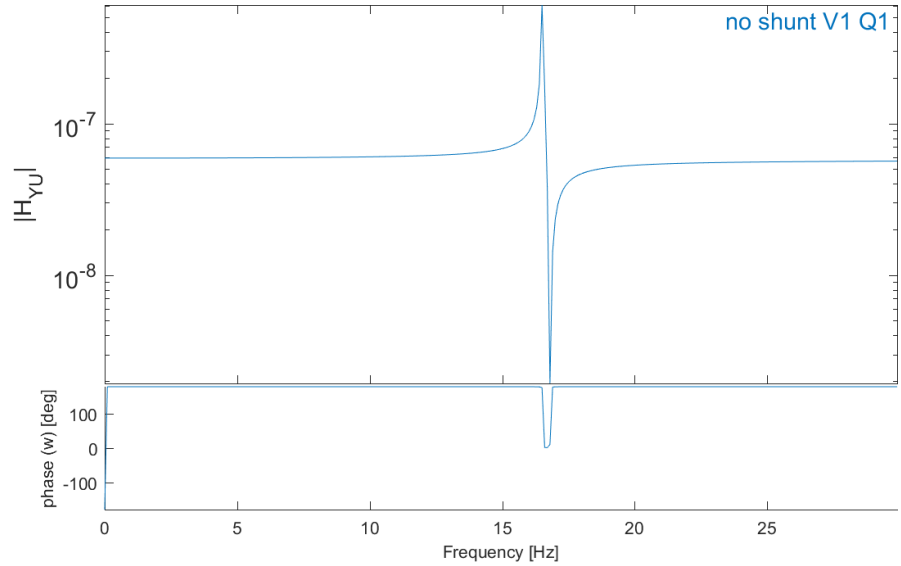

Figure 2.28: Capacitance (Q/V) of the first pair of piezo patches in bending. The resonance corresponds to ω_1 and the anti-resonance to Ω_1. C_{12} is the capacitance in the flat part after the anti-resonance

```
w=linspace(0,1e3,1e4)'*2*pi;
[sys,TR]=fe2ss('free 5 30 0 -dterm',model);
```

```
 C1=qbode(sys,w,'struct'); C1.name='no shunt';
 C1.X{2}={'V1';'V2'}; C1.X{3}={'Q1';'Tip'}



 ci=iiplot;
 iicom('CurveReset');iicom('curveinit',C1)
 iicom(ci,'xlim[0 30]') %

(d_piezo('TutoPz_shunt-s3') )

%% Step 3 - Determine parameters for shunt tuning
 % Extract w1 and W1 and compute alpha_1
C=C1.Y(:,1);
% Find poles and zeros of impedance (1/jwC)
if exist('findpeaks','file'); % requires findpeaks
[pksPoles,locsPoles]=findpeaks(abs(1./C)); Wi=w(locsPoles);
[pksZeros,locsZeros]=findpeaks(abs(C)); wi=w(locsZeros);
% concentrate on mode of interest (mode 1)
 W1=w(locsPoles(1)); w1=w(locsZeros(1));
% Compute alpha for mode of interest
a1=sqrt((W1^2-w1^2)/W1^2);


% Compute Cs2 for mode of interest
i1=1; i2=locsZeros(1); i3=locsZeros(2);
dw2=w(i3)-w(i2); wCs2=w(i2)+dw2/2;
[y,i]=min(abs(w-wCs2)); Cs2=abs(C(i));
```

We can now use Yamada's tuning rules to find R and L:

```
%% Determine shunt parameters (R and L) and apply it to damp 1st mode
% Tuning using Yamada's rule
d=1; r=sqrt((3*a1^2)/(2-a1^2));
L_Yam=1/d^2/Cs2/W1^2; R_Yam=r/Cs2/W1;
```

and represent the FRF of the tip displacement due to bending actuation on the second pair of piezos for the initial system and the system with the shunt (Figure 2.29). The shunt is implemented using the *feedback* function of the *Control toolbox*.
(d_piezo('TutoPz_shunt-s4'))

```
%% Step 4 - Compute dynamic response with optimal shunt
w=linspace(0,40,1e3)*2*pi; sys2=ss(sys.a,sys.b,sys.c,sys.d);
C1=qbode(sys2,w,'struct'); C1.name='no shunt';
C1.X{2}={'V1';'V2'}; C1.X{3}={'Q1';'Tip'}

% Implement shunt using feeback - requires control toolbox - compute FRF
A=tf([L_Yam R_Yam 0],1); % RL shunt in tf form
sys3=feedback(sys2,A,1,1,1);
C=freqresp(sys3,w); a=C(:); C2=C1; C2.Y=reshape(a,4,1000)';
C2.name='RL shunt';

% Plot and compare curves
iicom('CurveReset');
iicom(ci,'curveinit',{'curve',C1.name,C1;'curve',C2.name,C2});
iicom(ci,'ch 4')
end
```

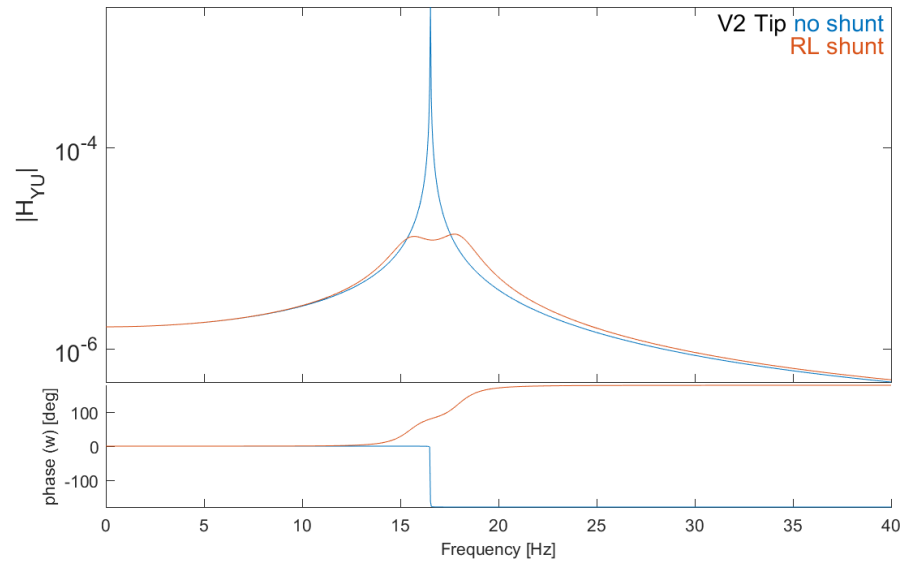

Figure 2.29: Tip displacement due to the bending actuator of the second pair of piezo patches with and without shunt

2.5 Piezo volumes and transfers: accelerometer example

This application example deals with the determination of the sensitivity of a piezoelectric sensor to base excitation.

2.5.1 Working principle of an accelerometer

By far the most common sensor for measuring vibrations is the accelerometer. The basic working principle of such a device is presented in Figure 2.30(a). It consists of a moving mass on a spring and dashpot, attached to a moving solid. The acceleration of the moving solid results in a differential movement x between the mass M and the solid. The governing equation is given by,

$$M\ddot{x} + c\dot{x} + kx = -M\ddot{x_0} \tag{2.16}$$

In the frequency domain $x/\ddot{x_0}$ is given by,

$$\frac{x}{\ddot{x_0}} = \frac{-1}{-\omega^2 + \omega_n^2 + 2j\xi\omega\omega_n} \tag{2.17}$$

with $\omega_n = \sqrt{\frac{k}{m}}$ and $\xi = b/2\sqrt{km}$ and for frequencies $\omega << \omega_n$, one has,

$$\frac{x}{\ddot{x_0}} \simeq \frac{-1}{\omega_n^2} \tag{2.18}$$

showing that at low frequencies compared to the natural frequency of the mass-spring system, x is proportional to the acceleration $\ddot{x_0}$. Note that since the proportionality factor is $\frac{-1}{\omega_n^2}$, the sensitivity of the sensor is increased as ω_n^2 is decreased. At the same time, the frequency band in which the accelerometer response is proportional to $\ddot{x_0}$ is reduced.

The relative displacement x can be measured in different ways among which the use of piezoelectric material, either in longitudinal or shear mode (Figure 2.31). In such configurations, the strain applied to the piezoelectric material is proportional to the relative displacement between the mass and the base. If no amplifier is used, the voltage generated between the electrodes of the piezoelectric material is directly proportional to the strain, and therefore to the relative displacement. For frequencies well below the natural frequency of the accelerometer, the voltage produced is therefore proportional to the absolute acceleration of the base.

2.5.2 Determining the sensitivity of an accelerometer to base excitation

A basic design of a piezoelectric accelerometer working in the longitudinal mode is shown in Figure 2.32. In this example, the casing of the accelerometer is not taken into account, so that the

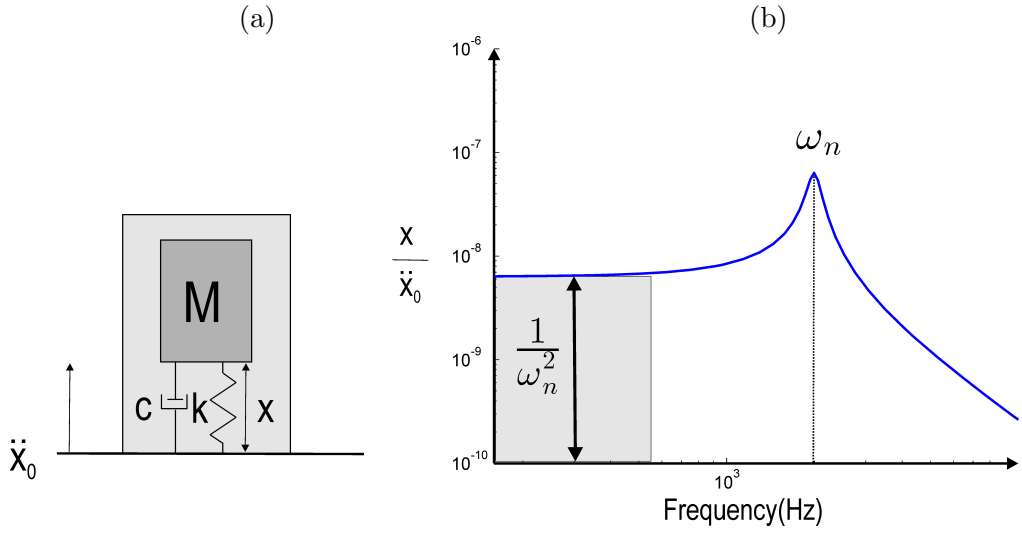

Figure 2.30: Working principle of an accelerometer

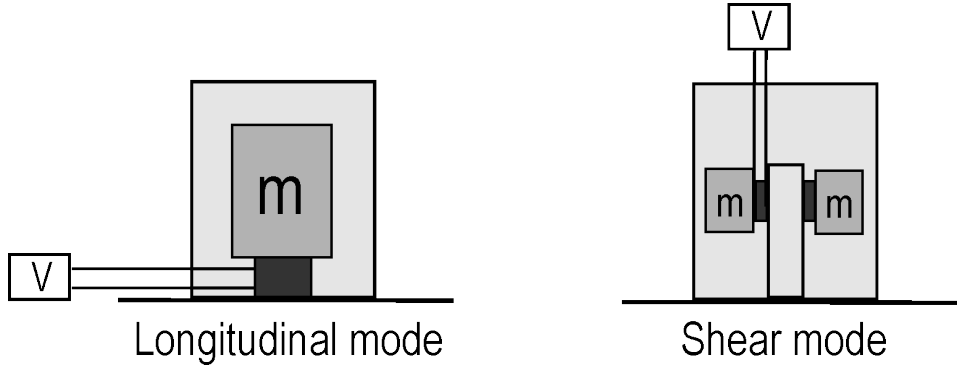

Figure 2.31: Different sensing principles for standard piezoelectric accelerometers

device consists in a $3mm$ thick rigid wear plate ($10mm$ diameter), a $1mm$ thick piezoelectric element ($5mm$ diameter), and a $10mm$ thick ($10mm$ diameter) steel proof mass. The mechanical properties of the three elements are given in Table 2.5. The piezoelectric properties of the sensing element are given in Table 2.6 and correspond to *SONOX_P502_iso* property in `m_piezo Database`. The sensing element is poled through the thickness and the two electrodes are on the top and bottom surfaces.

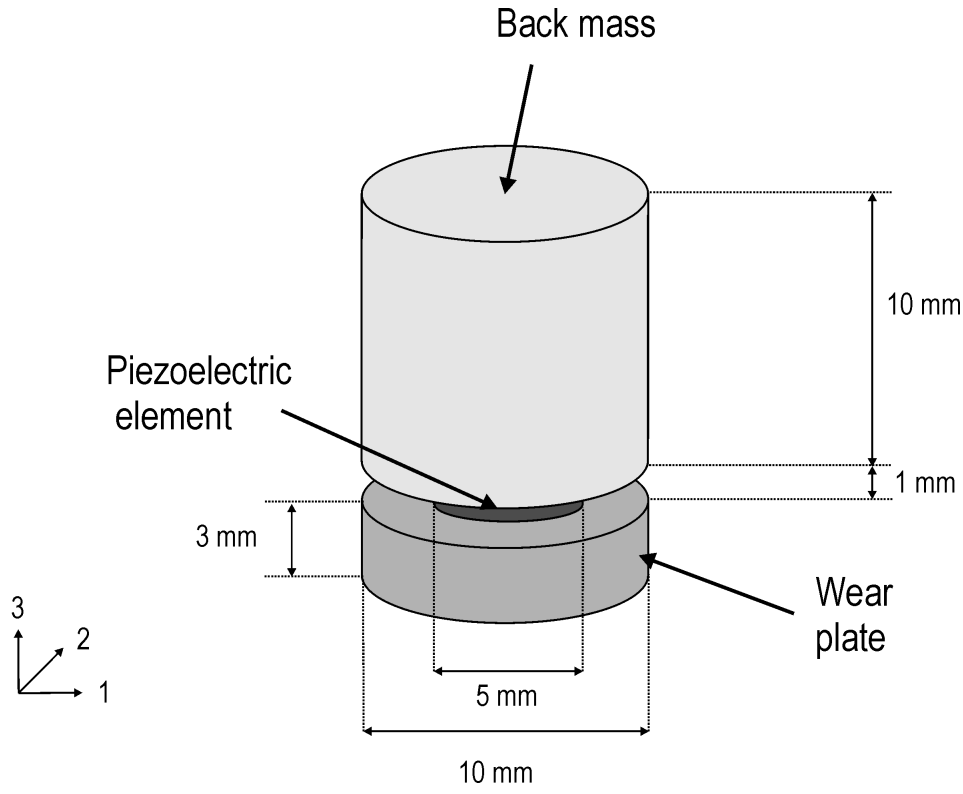

Figure 2.32: Basic design of a piezoelectric accelerometer working in the longitudinal mode

Part	Material	E (GPa)	ρ (kg/m^3)	ν
Wear plate	Al_2O_3	400	3965	0.22
Sensing element	Piezo	54	7740	0.44
Proof mass	Steel	210	7800	0.3

Table 2.5: Mechanical properties of the wear plate, sensing element and proof mass

Property	Value
$d_{31} = d_{32}$	-185 $10^{-12} pC/N$ (or m/V)
d_{33}	440 $10^{-12} pC/N$ (or m/V)
$d_{15} = d_{24}$	560 $10^{-12} pC/N$ (or m/V)
$\varepsilon_{33}^T = \varepsilon_{22}^T = \varepsilon_{11}^T$	1850 ε_0
ε_0	8.854 $10^{-12} Fm^{-1}$

Table 2.6: Piezoelectric properties of the sensing element

The sensitivity curve of the accelerometer, expressed in $V/m/s^2$ is used to assess the response of the sensor to a base acceleration in the sensing direction (here vertical). In order to compute this sensitivity curve, one needs therefore to apply a uniform vertical base acceleration to the sensor and to compute the response of the sensing element as a function of the frequency.

This can be done in different ways. The following scripts compare two approaches. The first one consists in applying a uniform pressure on the base to excite the accelerometer. In this case, the pressure is constant, but the acceleration of the base is not strictly constant due to the flexibility of the wear plate. The second one consists in enforcing a constant vertical acceleration of all the nodes at the bottom of the base. In this case the acceleration is constant over the whole bottom surface of the accelerometer. The two approaches are compared in the following illustrative scripts.
(`d_piezo('TutoAccel-s1')`)
The mesh of the accelerometer is produced with the following call to `d_piezo` . It is shown in Figure 2.33

```
% See full example as MATLAB code in d_piezo('ScriptPz_accA')
%% Step 1 - Build Mesh and visualize
% Meshing script can be viewed with sdtweb d_piezo('MeshBaseAccel')
model=d_piezo('MeshBaseAccel');


cf=feplot(model); fecom('colordatagroup');
set(gca,'cameraposition',[-0.0604   -0.0787    0.0139])
```

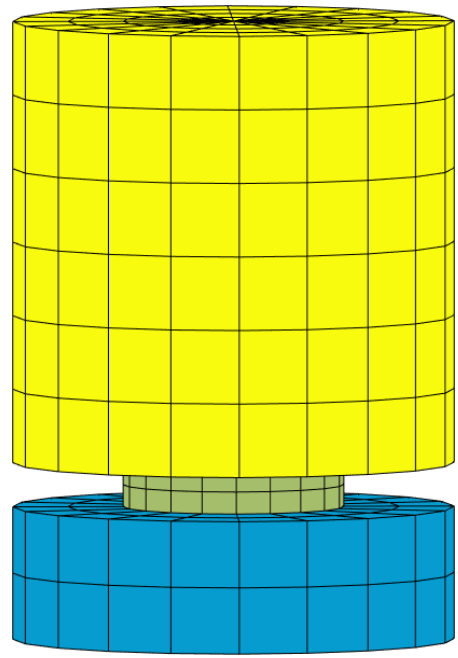

Figure 2.33: Mesh of the piezoelectric accelerometer. The different colors represent the different groups

The call includes the meshing of the accelerometer, the definition of material properties, as well as the definition of electrodes. In addition, the bottom electrode is grounded, and both a voltage and a charge sensor are defined for the top electrode. A displacement sensor at the center of the base is defined in order to compute the sensitivity. The different calls used are:
(d_piezo('TutoAccel-s2'))

```
%% Step 2 - Define sensors and actuators
% -MatID 2 requests a charge resultant sensor
% -vout requests a voltage sensor
model=p_piezo('ElectrodeMPC Top sensor -matid 2 -vout',model,'z==0.004');
% -ground generates a v=0 FixDof case entry
model=p_piezo('ElectrodeMPC Bottom sensor -ground',model,'z==0.003');
% Add a displacement sensor for the basis
model=fe_case(model,'SensDof','Base-displ',1.03);
```

The sensitivity for the sensor used in a voltage mode is then computed using the following script:

```
% Remove the charge sensor (not needed)
model=fe_case(model,'remove','Q-Top sensor');
% Normal surface force (pressure) applied to bottom of wear plate for excitation:
data=struct('sel','z==0','eltsel','groupall','def',1e4,'DOF',.19);
model=fe_case(model,'Fsurf','Bottom excitation',data);

% Other parameters
model=stack_set(model,'info','Freq',logspace(3,5.3,200)'); % freq. for computation
```

(d_piezo('TutoAccel-s3'))

```
%% Step 3 - Compute dynamic response (full) and plot Bode diagram
ofact('silent'); d1=fe_simul('dfrf',model);

% Project on sensor
sens=fe_case(model,'sens');

% Build a clean "curve" for iiplot display
C1=fe_case('SensObserve -DimPos 2 3 1',sens,d1);C1.name='DFRF';C1.Ylab='Base-Exc';
C1.X{2}={'Sensor output(V)';'Base Acc(m/s^2)';'Sensitivity (V/m/s^2)'};
C1.Y(:,2)=C1.Y(:,2).*(-(C1.X{1}(:,1)*2*pi).^2); % Base acc =disp.*-w.^2
C1.Y(:,3)=C1.Y(:,1)./C1.Y(:,2);                 % Sensitivity=V/acc
C1=sdsetprop(C1,'PlotInfo','sub','magpha','scale','xlog;ylog');
C1.name='Free-Voltage';
```

```
ci=iiplot;
iicom(ci,'curveInit',C1.name,C1);iicom ch3; iicom('submagpha');
```

The second approach consists in imposing a uniform displacement to the base of the accelerometer. The script is:
(d_piezo('TutoAccel-s4'))

```
%% Step 4 - Response with imposed displacement
% Remove pressure
 model=fe_case(model,'remove','Bottom excitation')

% Link dofs of base and impose unit vertical displacement
rb=feutilb('geomrb',feutil('getnode z==0',model),[0 0 0], ...
     feutil('getdof',model));
rb=fe_def('subdef',rb,3); % Keep vertical displacement
model=fe_case(model,'DofSet','Base',rb);

 % compute
 ofact('silent'); model.DOF=[]; d1=fe_simul('dfrf',model);

 % Project on sensor and create output
 sens=fe_case(model,'sens');
 C2=fe_case('SensObserve -DimPos 2 3 1',sens,d1);C2.name='DFRF';C2.Ylab='Imp-displ';

 % Build a clean "curve" for iiplot display
 C2.X{2}={'Sensor output(V)';'Base Acc(m/s^2)';'Sensitivity (V/m/s^2)'};
 C2.XLab{3}={'Freq','[Hz]',[]};
 C2.Y(:,2)=C2.Y(:,2).*(-(C2.X{1}*2*pi).^2); % Base acc
 C2=sdsetprop(C2,'PlotInfo','sub','magpha','scale','xlog;ylog');
 C2.Y(:,3)=C2.Y(:,1)./C2.Y(:,2);% Sensitivity
 C2.name='Imp-Voltage';
 C2=feutil('rmfield',C2,'Ylab'); C1=feutil('rmfield',C1,'Ylab');
 ci=iiplot; iicom(ci,'curveinit',{'curve',C1.name,C1;'curve',C2.name,C2});
 iicom('submagpha');
```

The two curves are compared in Figure 2.34. The behavior described in Figure 2.30 is clearly reproduced in both cases in the frequency band of interest, showing the flat part before the resonance. The sensitivities are comparable, but as the mechanical boundary conditions are slightly different, the eigenfrequencies do not match exactly.

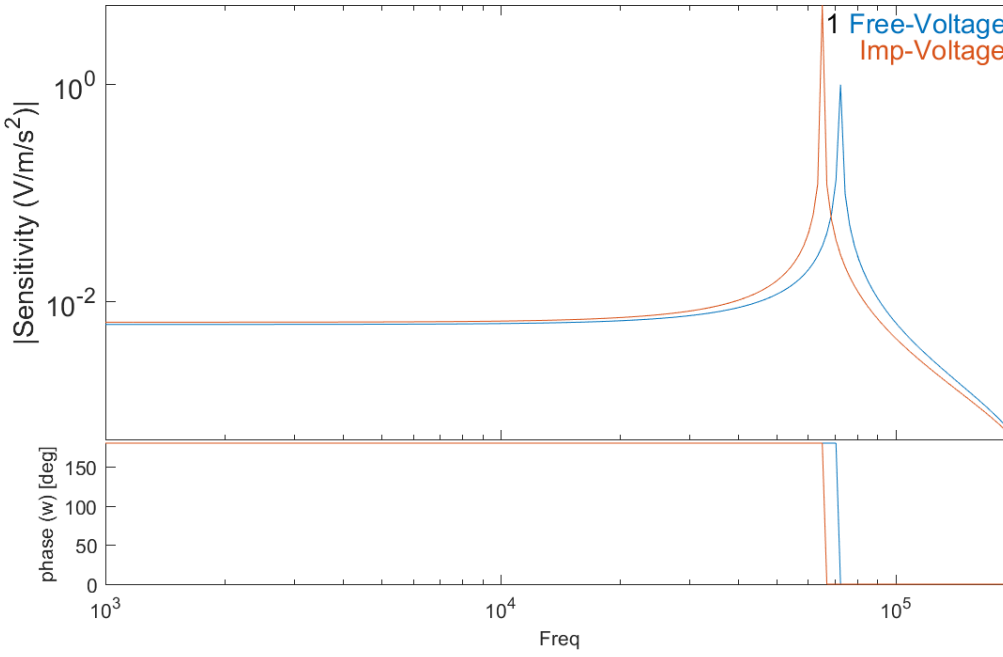

Figure 2.34: Comparison of the sensitivities computed with a uniform base acceleration, and a uniform base pressure

The sensor can also be used in the charge mode. The following scripts compares the sensitivity of the sensor used in the voltage and charge modes. The sensitivities are normalized to the static sensitivity in order to be compared on the same graph, as the orders of magnitude are very different (Figure 2.35). The charge sensor corresponds to a short-circuit condition which results in a lower resonant frequency than the sensor used in a voltage mode where the electric field is present in the piezoelectric material which results in a stiffening due to the piezoelectric coupling, as already illustrated in Section 2.1 for a plate. Here the difference of eigenfrequency is however higher (about 10%) due to the fact that there is more strain energy in the piezoelectric element, and that it is used in the d_{33} mode which has a higher electromechanical coupling factor than the d_{31} mode.
(d_piezo('TutoAccel-s5'))

```
%% Step 5 - Compare charge and voltage mode for sensing
 % Meshing script,open with sdtweb d_piezo('MeshBaseAccel')
model=d_piezo('MeshBaseAccel');
model=fe_case(model,'remove','V-Top sensor');

% Short-circuit electrodes of accelerometer
model=fe_case(model,'FixDof','V=0 on Top Sensor', ...
    p_piezo('electrodedof Top sensor',model));

% Other parameters
  model=stack_set(model,'info','Freq',logspace(3,5.3,200)');

% Link dofs of base and impose unit vertical displacement
rb=feutilb('geomrb',feutil('getnode z==0',model),[0 0 0], ...
     feutil('getdof',model));
rb=fe_def('subdef',rb,3); % Keep vertical displacement
model=fe_case(model,'DofSet','Base',rb);

 % compute
 ofact('silent'); model.DOF=[]; d1=fe_simul('dfrf',model);

 % Project on sensor and create output
 sens=fe_case(model,'sens');
 C4=fe_case('SensObserve -DimPos 2 3 1',sens,d1);
 C4.name='DFRF';C4.Ylab='Imp-displ';

 % Build a clean "curve" for iiplot display
 C4.X{2}={'Sensor output(C)';'Base Acc(m/s^2)';'Sensitivity (C/m/s^2)'};
 C4.XLab{3}='Freq [Hz]';
```

```
C4.Y(:,2)=C4.Y(:,2).*(-(C4.X{1}*2*pi).^2); % Base acc
C4=sdsetprop(C4,'PlotInfo','sub','magpha','show','abs','scale','xlog;ylog');
C4.Y(:,3)=C4.Y(:,1)./C4.Y(:,2);% Sensitivity
C4.name='Imp-Charge';

% Normalize the sensitivities to plot on same graph
C6=C2; % save C6 as non-normalized
C2.Y(:,3)=C2.Y(:,3)./C2.Y(1,3);C4.Y(:,3)=C4.Y(:,3)./C4.Y(1,3);
C2=feutil('rmfield',C2,'Ylab'); C4=feutil('rmfield',C4,'Ylab');
iicom(ci,'curvereset');
iicom(ci,'curveinit',{'curve',C2.name,C2;'curve',C4.name,C4});
iicom('ch 3'); iicom('submagpha');
```

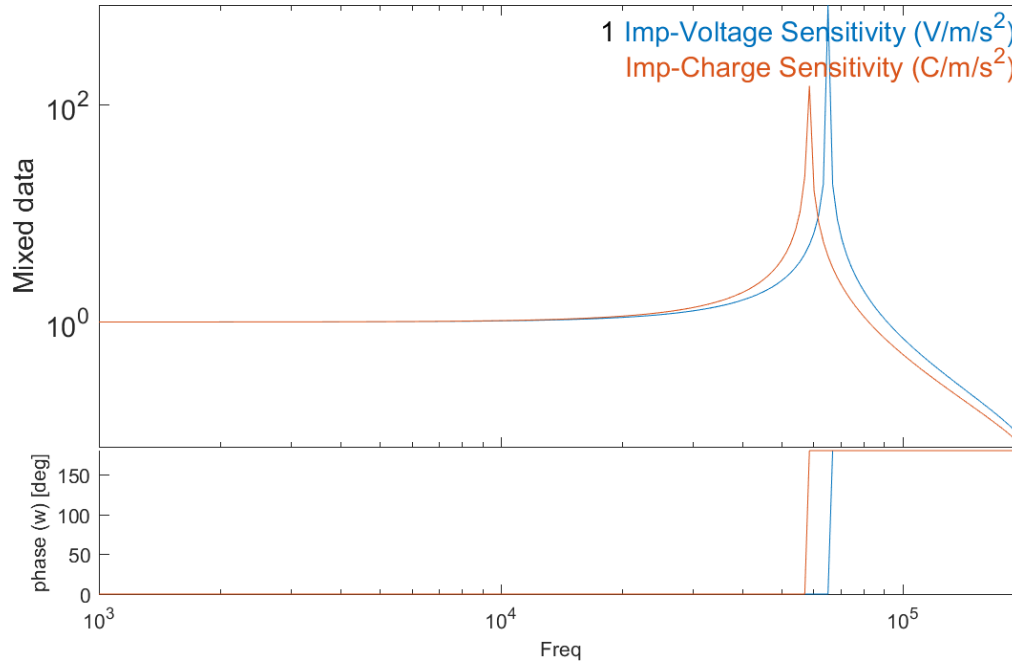

Figure 2.35: Comparison of the normalized sensitivities of the sensor used in the charge and voltage mode

2.5.3 Computing the sensitivity curve using a piezoelectric shaker

Experimentally, the sensitivity curve can be measured by attaching the accelerometer to a shaker in order to excite the base. Usually, this is done with an electromagnetic shaker, but we illustrate in the following example the use of a piezoelectric shaker for sensor calibration. The piezoelectric shaker consists of two steel cylindrical parts with a piezoelectric disc inserted in between. The base of the shaker is fixed and the piezoelectric element is used as an actuator: imposing a voltage difference between the electrodes results in the motion of the top surface of the shaker to which the accelerometer is attached (Figure 2.36).

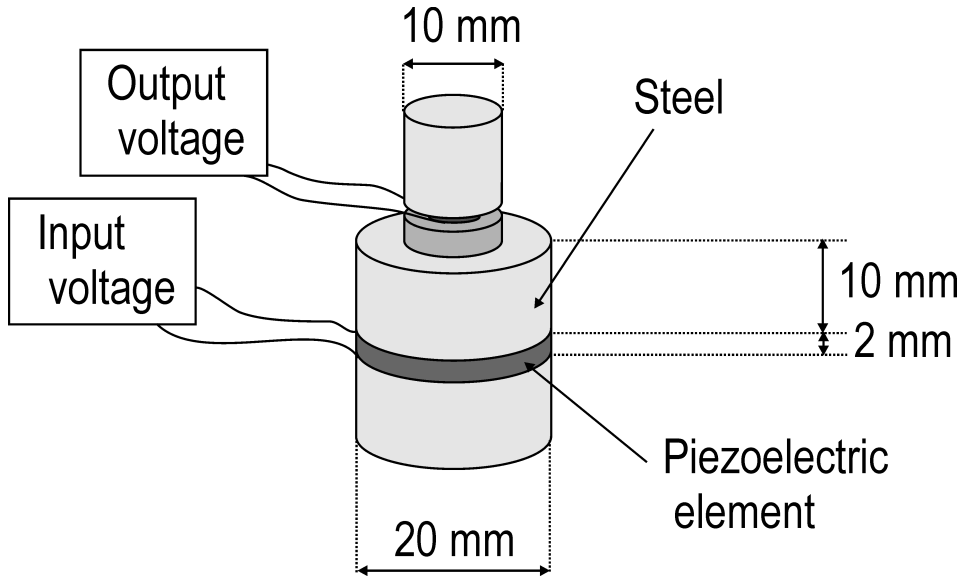

Figure 2.36: Piezoelectric accelerometer attached to a piezoelectric shaker for sensor calibration

The piezoelectric properties for the actuating element in the piezoelectric shaker are identical to the ones of the sensing element given in Table 2.6 and it is poled through the thickness. A voltage is applied to the actuator and the resulting voltage on the sensing element is computed. The sensitivity is then computed by dividing the sensor response by the acceleration at the center of the wear plate as a function of the excitation frequency. The mesh is represented in Figure 2.37 and is obtained with:

(d_piezo('TutoAcc_shaker-s1'))

```
% See full example as MATLAB code in d_piezo('ScriptPz_acc_shaker')
%% Step 1 - Build mesh and visualize
% Meshing script,open with sdtweb d_piezo('MeshPiezoShaker')
model=d_piezo('MeshPiezoShaker');
```

```
cf=feplot(model); fecom('colordatapro');
set(gca,'cameraposition',[-0.0604   -0.0787    0.0139])
```

In the meshing script, a voltage actuator is defined for the piezoelectric disk in the piezo shaker by setting the bottom electrode potential to zero, and defining the top electrode potential as an input: (d_piezo('TutoAcc_shaker-s2'))

```
%% Step 2 - Define actuators and sensors
  % -input "In" says it will be used as a voltage actuator
model=p_piezo('ElectrodeMPC Top Actuator -input "Vin-Shaker"',model,'z==-0.01');
  % -ground generates a v=0 FixDof case entry
model=p_piezo('ElectrodeMPC Bottom Actuator -ground',model,'z==-0.012');
```

and the shaker is mechanically attached at the bottom.

After meshing, the script to obtain the sensitivity is:

```
% Voltage sensor will be used - remove charge sensor
model=fe_case(model,'remove','Q-Top sensor');

% Frequencies for computation
model=stack_set(model,'info','Freq',logspace(3,5.3,200)');
```

(d_piezo('TutoAcc_shaker-s3'))

```
 %% Step 3 - Compute response, voltage input on shaker
 ofact('silent'); model.DOF=[]; d1=fe_simul('dfrf',model);

 % Project on sensor and create output
 sens=fe_case(model,'sens');
 C5=fe_case('SensObserve -DimPos 2 3 1',sens,d1);
 C5.name='DFRF';C5.Ylab='Shaker-Exc';

 % Build a clean "curve" for iiplot display
 C5.X{2}={'Sensor output(V)';'Base Acc(m/s^2)';'Sensitivity (V/m/s^2)'};
 C5.Xlab{1}='Freq [Hz]';
 C5.Y(:,2)=C5.Y(:,2).*(-(C5.X{1}*2*pi).^2); % Base acc
 C5=sdsetprop(C5,'PlotInfo','sub','magpha','show','abs','scale','xlog;ylog');
 C5.Y(:,3)=C5.Y(:,1)./C5.Y(:,2);% Sensitivity
 C5.name='Shaker-Voltage'; ci=iiplot;
 C5=feutil('rmfield',C5,'Ylab');
```

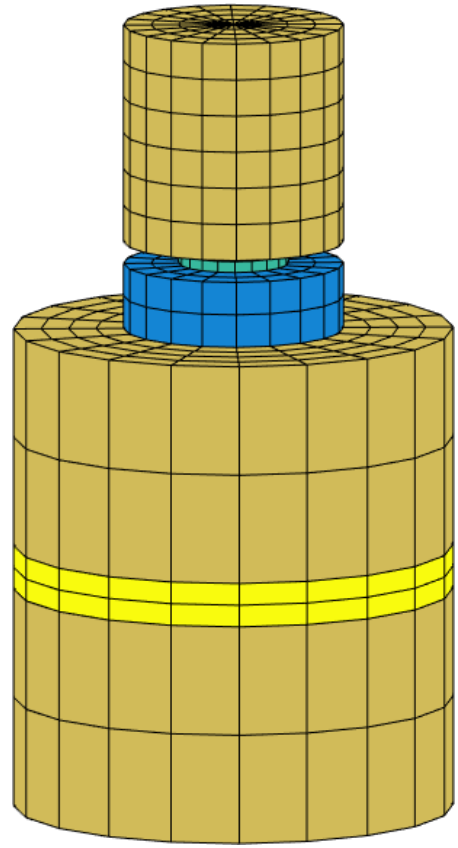

Figure 2.37: Mesh of the piezoelectric accelerometer attached to a piezoelectric shaker

```
ci=iiplot;
iicom(ci,'curveinit',C5); iicom('ch 3'); iicom('submagpha');
```

The sensitivity curve obtained is shown in Figure 2.38. It is comparable around the natural frequency of the accelerometer, but at low frequencies, the flat part is not correctly represented and a few spurious peaks appear at high frequencies. These differences are due to the fact that the piezoelectric shaker does not impose a uniform acceleration of the base of the sensor.

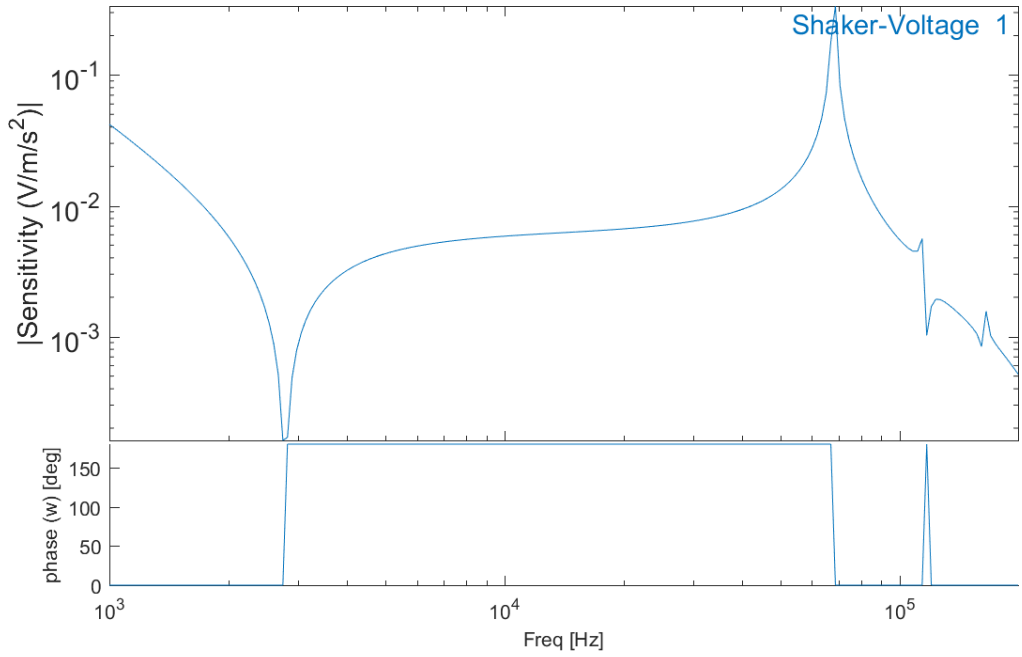

Figure 2.38: Sensitivity curve obtained with a piezoelectric shaker

2.6 Piezo volumes and advanced views : IDE example

This second example deals with a piezoelectric patch with inter-digitated electrodes (IDE). The principle of such electrodes is illustrated in Figure 2.39 [9]. The continuous electrodes are replaced by thin electrodes in the form of a comb with alternating polarity. This results in a curved electric field. Except close to the electrodes, the electric field is aligned in the plane of the actuator. In doing so, the extension of the patch in the plane is due to both the d_{31}-mode and d_{33}-mode. The d_{33}-mode is interesting because the value of d_{33} is 2 to 3 times higher than the d_{31}, d_{32} coefficients.

In addition, as d_{33} and d_{31} have opposite sign, the application of a voltage across the IDE will lead to an expansion in the longitudinal direction, and a contraction in the lateral direction, and the amplitudes will be different.

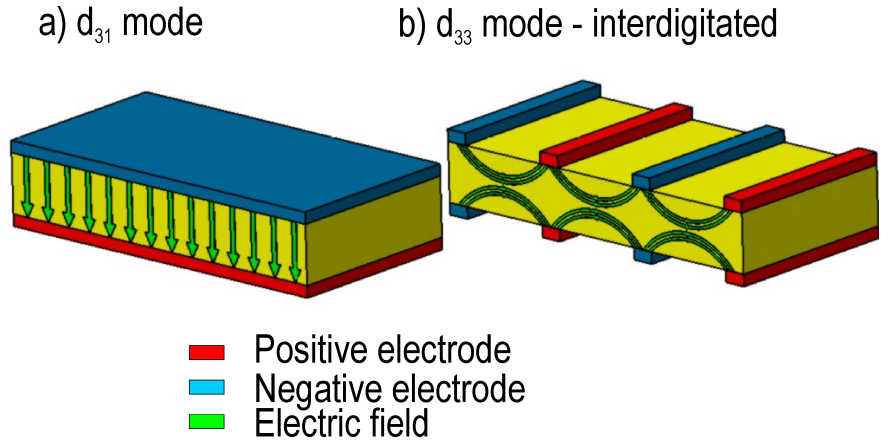

Figure 2.39: Electric field for a) continuous electrodes b) Inter-digitated electrodes

The behavior of a piezoelectric patch with interdigitated electrodes can be studied by considering a representative volume element as shown in Fig 2.40.

Let us consider such a piezoelectric patch whose geometrical properties are given in Table 2.7. The default material considered is again *SONOX_P502_iso* (Table 2.6).

Property	Value
l_x	0.4 mm
l_y	0.3 mm
p	0.7 mm
e	0.05 mm

Table 2.7: Geometrical properties of the piezoelectric patch

We compute the static response due to a unit voltage applied across the electrodes, and represent the curved electric field:
(`d_piezo('TutoPatch_num_IDE-s1')`)

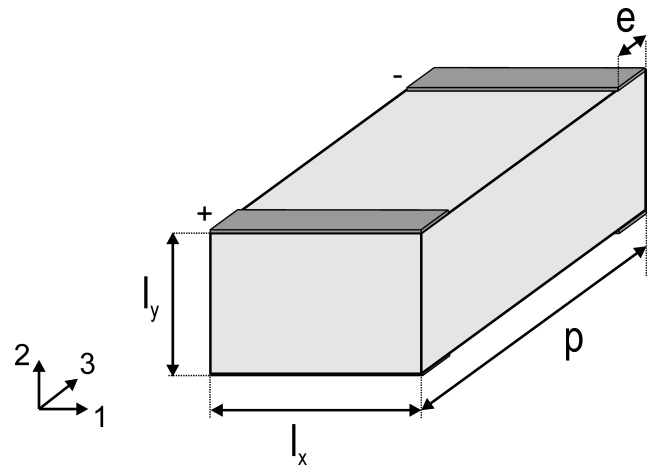

Figure 2.40: Definition of a representative volume element to study the behavior of a piezoelectric patch with IDEs

```
% See full example as MATLAB code in d_piezo('ScriptPz_Patch_Num_IDE')
%% Step 1 - Build mesh
% Meshing script can be viewed with sdtweb d_piezo('MeshIDEPatch')
% Build mesh, electrodes and actuation
model=d_piezo(['MeshIDEPatch nx=10 ny=5 nz=14 lx=2000e-6' ...
 'ly=1500e-6 p0=3500e-6 e0=250e-6']);

(d_piezo('TutoPatch_num_IDE-s2') )

%% Step 2 - Compute response due to V and visualize
% low freq response to avoid rigid body modes
model=stack_set(model,'info','Freq',10);
def=fe_simul('dfrf',model);


% Plot deformed shape
cf=feplot(model,def); fecom('view3'); fecom('viewy-90'); fecom('viewz+90')
fecom('undef line'); fecom('triax') ; iimouse('zoom reset')

(d_piezo('TutoPatch_num_IDE-s3') )

%% Step 3 - visualize electric field
cf.sel(1)={'groupall','colorface none -facealpha0 -edgealpha.1'};
```

```
p_piezo('viewElec EltSel "matid1" DefLen 250e-6 reset',cf);
fecom('scd 1e-10')
p_piezo('electrodeview -fw',cf); % to see the electrodes on the mesh
iimouse('zoom reset')
```

The resulting deformation and electric field are represented in Fig 2.41. The mean strains S_1, S_2 and S_3 and the mean electric field in direction 3 (poling direction) are then computed. In this example, the electric field is aligned with the poling direction, but is of opposite direction, resulting in a negative value of the mean strain S_3 (d_{33} is positive). Because d_{31} and d_{32} are negative, the mean values of S_1 and S_2 are positive: when the patch contracts in direction 3, it is elongated in directions 1 and 2. By dividing the mean strains by the mean electric field in the poling direction, one should recover the d_{31}, d_{32} and d_{33} coefficients of the material. The mean value of E_3 is however different from the value which would be obtained if the electric field was uniform (continuous electrodes on the sides of the patch). This value is considered here as the reference analytical value given by $E_3 = \frac{V}{p}$.

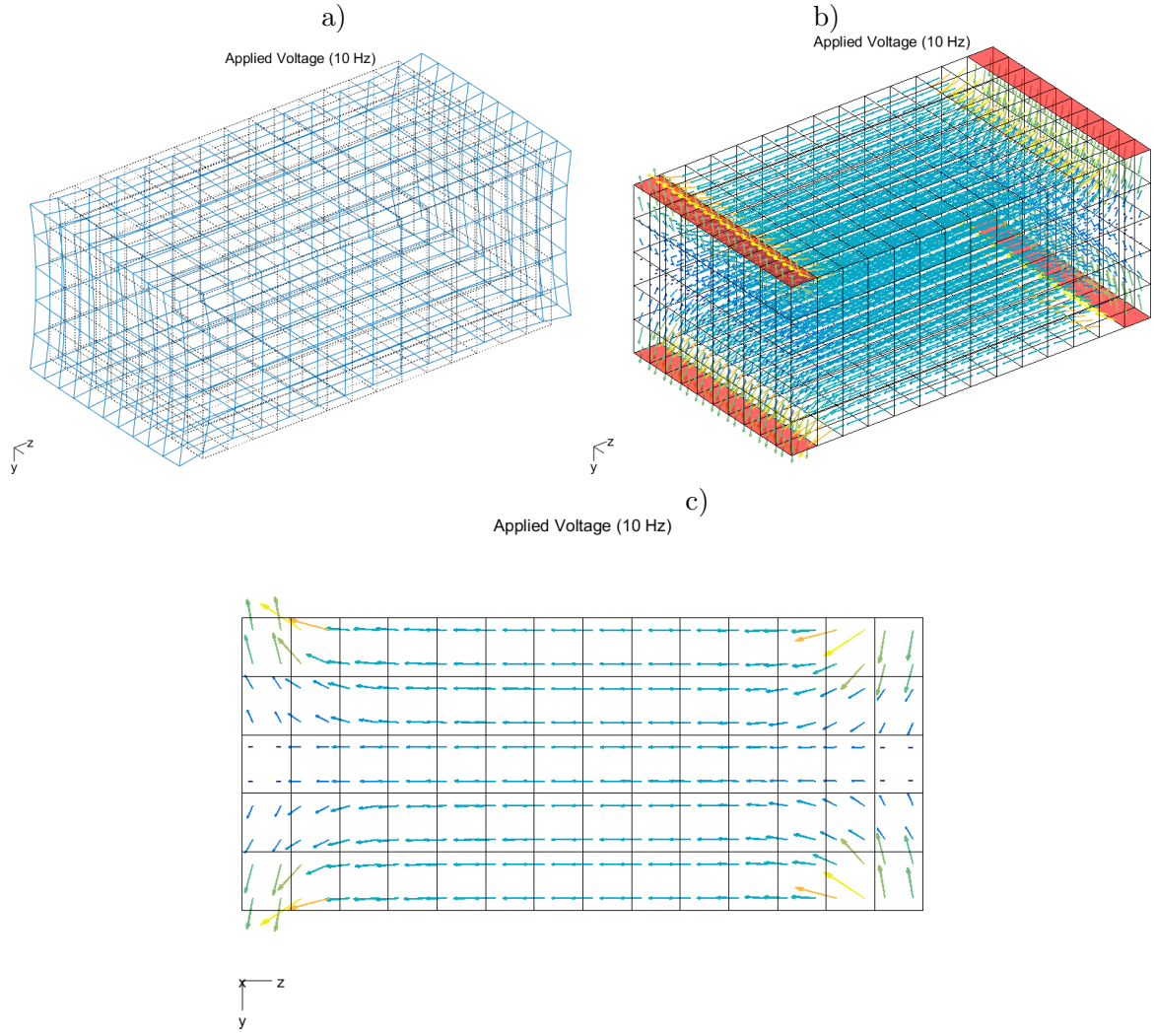

Figure 2.41: a) Free deformation of the IDE patch under unit voltage actuation b) 3D Electric field distribution and c) 2D Electric field

```
(d_piezo('TutoPatch_num_IDE-s4') )
```

```
%% Step 4 - Compare efective values of constitutive law
% Decompose constitutive law
CC=p_piezo('viewdd -struct',cf); %
% Compute mean value of fields and deduce equivalent d_ij
% Uniform field is assumed for analytical values
```

```
a=p_piezo('viewstrain -curve -mean',cf); % mean value of S1-6 and E1-3
fprintf('Relation between mean strain on free structure and d_3i\n');
E3=a.Y(9,1); disp({'E3 mean' a.Y(9,1) -1/3500e-6 'E3 analytic'})
disp([a.X{1}(1:3) num2cell([a.Y(1:3,1)/E3 CC.d(3,1:3)']) ...
{'d_31';'d_32';'d_33'}])
```

The ratio between the mean of E_3 and the analytical value is about 0.80, which means that the free strain of an IDE patch with the geometrical properties considered in this example will be about 20 % lower than if the electric field was uniform. In fact, the spacing of the electrodes in an IDE patch is a compromise between the loss of performance due to the part of the piezoelectric material in which the electric field is not aligned with the poling direction, and the distance between the electrodes which, when increased, decreases the effective electric field for a given applied voltage. The total charge on the electrodes and the charge density are then computed.
(d_piezo('TutoPatch_num_IDE-s5'))

```
%% Step 5 - Charge visualisation and total on electrodes
p_piezo('electrodeTotal',cf)
% charge density on the electrodes
feplot(model,def);
cut=p_piezo('electrodeviewcharge',cf,struct('EltSel','matid 1'));
fecom('view3'); fecom('viewy-90'); fecom('viewz+90'); iimouse('zoom reset');
iimouse('trans2d 0 0 0 1.6 1.6 1.6')
```

Figure 2.42 shows the distribution of the charge density on the electrodes.

The capacitance of the patch can be computed and compared to the analytical value (for a uniform field) given by $C^T = \frac{\varepsilon^T (l_x\, l_y)}{p}$:
(d_piezo('TutoPatch_num_IDE-s6'))

```
%% Step 6 - Theoretical capacitance for uniform field
Ct=CC.epst_r(3,3)*8.854e-12*2000e-6*1500e-6/3500e-6;
% total charge on the electrodes = capacitance (unit voltage)
C=p_piezo('electrodeTotal',cf);
% Differences are due to non-uniform field, this is to be expected
disp({'C_{IDE}' cell2mat(C(2,2)) Ct 'C analytic'})
```

The capacitance of the IDE patch is about 10% lower than the analytical value.
It is also interesting to plot color maps of strain and stress components in the patch , which can be done using `fe_stress` .
(d_piezo('TutoPatch_num_IDE-s7'))

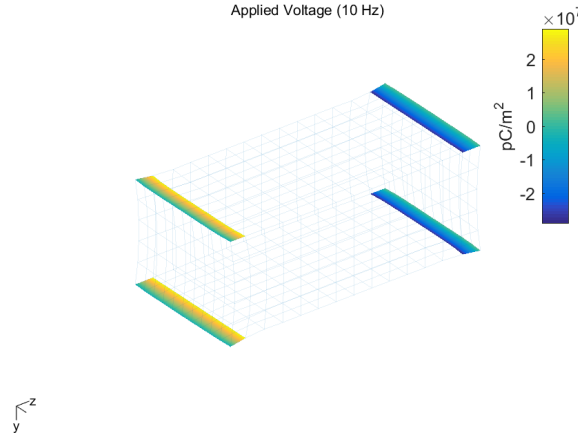

Figure 2.42: Charge density on the electrodes resulting from a static unit voltage applied to the IDEs

```
%% Step 7 - Stress and strain visualisation
% Stress field using fe_stress
c1=fe_stress('stressAtInteg -gstate',model,def);
cf.sel='reset';cf.def=fe_stress('expand',model,c1);
cf.def.lab={'T11';'T22';'T33';'T23';'T13';'T12';'D1';'D2';'D3'}; %
fecom('colordata 99 -edgealpha.1');
fecom('colorbar',d_imw('get','CbTR','String','Stress/V [MPa/V]'));
iimouse('trans2d 0 0 0 1.6 1.6 1.6')
```

Figure 2.43 shows the colormap of T_1, T_2 and T_3. It is clear that the curved electrical field induces important stress concentrations in the area close to the electrodes

The strains and electrical displacement can also be computed with `fe_stress` , but this requires to replace the piezoelectric material with a 'PiezoStrain' material:

```
% Replace with 'PiezoStrain' material
mo2=model; mo2.pl=m_piezo('dbval 1 PiezoStrain')
% Now represent strain fields using fe_stress
c1=fe_stress('stressAtInteg -gstate',mo2,def);
cf.sel='reset';cf.def=fe_stress('expand',mo2,c1);
cf.def.lab={'S11';'S22';'S33';'S23';'S13';'S12';'E1';'E2';'E3'};
fecom('colordata 99 -edgealpha.1');
fecom('colorbar',d_imw('get','CbTR','String','Strain/V [m/mV]'));
```

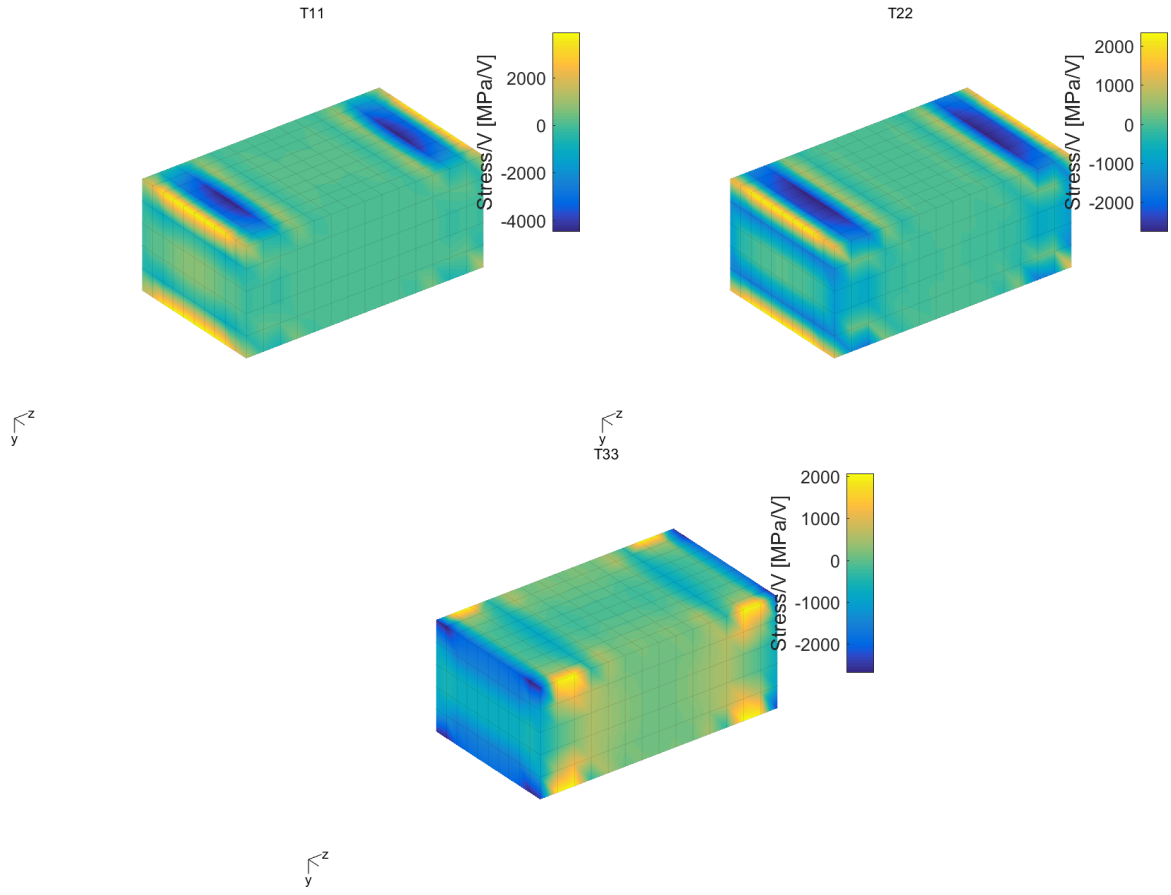

Figure 2.43: Colormap of stresses T_1, T_2 and T_3 due to applied voltage on the patch with IDE

```
iimouse('trans2d 0 0 0 1.6 1.6 1.6')
```

Figure 2.44 shows the colormap of S_1, S_2 and S_3. The strain is uniform in the central regio, but there are strong variations in the areas under the electrodes

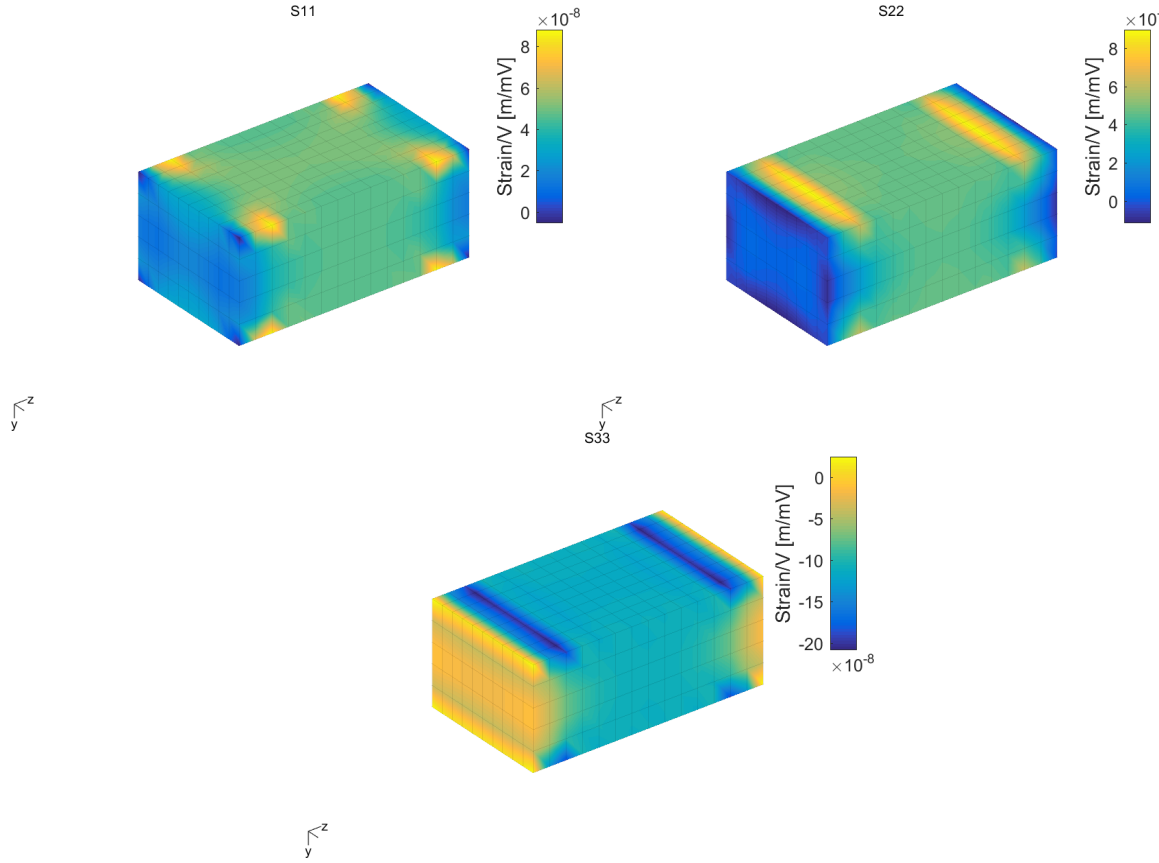

Figure 2.44: Colormap of strains S_1, S_2 and S_3 due to applied voltage on the patch with IDE

Note that in this example, the poling direction has been considered to be aligned with the z-axis. In practice, as the IDE patch is usually poled using the IDE electrodes, the poling direction is aligned with the curved electric field lines. This difference of poling only concerns a few elements in the mesh, and from a global point of view, it does not have an important impact on the assessment of the performance of the patch, but it may have an important impact on the prediction of strains and stresses around the electrode areas. Aligning the poling direction with the curved electric field lines is possible but requires the handling of local basis which are oriented based on the computed electric

field lines.

2.7 Periodic homogenization of piezocomposite transducers

In this example, we will show how to compute the homogeneous equivalent mechanical, piezoelectric and dielectric properties of both $P1$ and $P2$-type MFCs. The methodology is general and can be extended to other types of piezocomposites.

2.7.1 Constitutive equations

For d_{31} patches, the poling direction (conventionally direction 3) is normal to the plane of the patches (Figure 2.45a) and according to the plane stress assumption $T_3 = 0$. The electric field is assumed to be aligned with the polarization vector ($E_2 = E_1 = 0$). The constitutive equations reduce to:

$$\begin{Bmatrix} T_1 \\ T_2 \\ T_4 \\ T_5 \\ T_6 \\ D_3 \end{Bmatrix} = \begin{bmatrix} c_{11}^{E*} & c_{12}^{E*} & 0 & 0 & 0 & -e_{31}^{*} \\ c_{12}^{E*} & c_{22}^{E*} & 0 & 0 & 0 & -e_{32}^{*} \\ 0 & 0 & c_{44}^{E*} & 0 & 0 & 0 \\ 0 & 0 & 0 & c_{55}^{E*} & 0 & 0 \\ 0 & 0 & 0 & 0 & c_{66}^{E*} & 0 \\ e_{31}^{*} & e_{32}^{*} & 0 & 0 & 0 & \varepsilon_{33}^{S*} \end{bmatrix} \begin{Bmatrix} S_1 \\ S_2 \\ S_4 \\ S_5 \\ S_6 \\ E_3 \end{Bmatrix} \tag{2.19}$$

where the superscript * denotes the properties under the plane stress assumption (which are not equal to the properties in 3D).

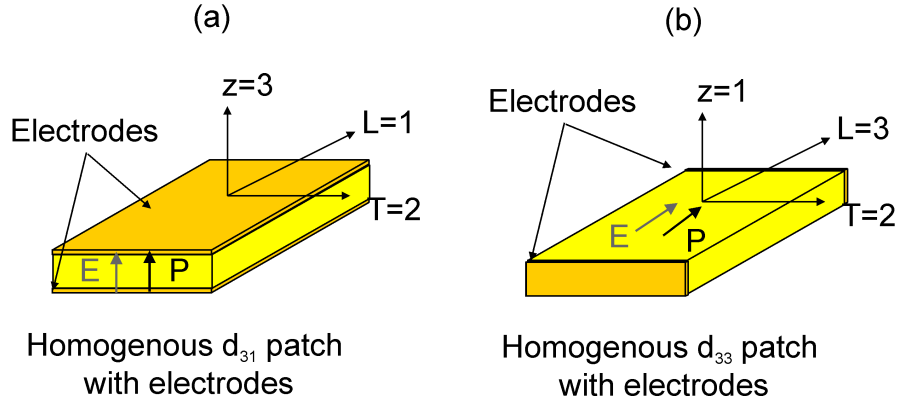

Figure 2.45: Homogeneous models of the piezoelectric layers with electrodes : d_{31} and d_{33} piezoelectric layers

For d_{33} patches, although the electric field lines do not have a constant direction, when replacing the active layer by an equivalent homogeneous layer, we consider that the poling direction is that of the fibers (direction 3, Figure 2.45b), and that the electric field is in the same direction. With

this reference frame, the plane stress hypothesis implies that $T_1 = 0$. The constitutive equations are given by

$$\begin{Bmatrix} T_2 \\ T_3 \\ T_4 \\ T_5 \\ T_6 \\ D_3 \end{Bmatrix} = \begin{bmatrix} c_{22}^{E*} & c_{23}^{E*} & 0 & 0 & 0 & -e_{32}^{*} \\ c_{32}^{E*} & c_{33}^{E*} & 0 & 0 & 0 & -e_{33}^{*} \\ 0 & 0 & c_{44}^{E*} & 0 & 0 & 0 \\ 0 & 0 & 0 & c_{55}^{E*} & 0 & 0 \\ 0 & 0 & 0 & 0 & c_{66}^{E*} & 0 \\ e_{32}^{*} & e_{33}^{*} & 0 & 0 & 0 & \varepsilon_{33}^{S*} \end{bmatrix} \begin{Bmatrix} S_2 \\ S_3 \\ S_4 \\ S_5 \\ S_6 \\ E_3 \end{Bmatrix} \tag{2.20}$$

2.7.2 Homogenization of piezocomposites

Homogenization techniques are widely used in composite materials. They consist in computing the homogeneous, equivalent properties of multi-phase heterogeneous materials. The homogenization is performed on a so-called representative volume element (RVE) which is a small portion of the composite which, when repeated in 1, 2 or 3 directions forms the full composite. In the case of flat transducers considered here, the composite is periodic in 2 directions (the directions of the plane of the composite) Equivalent properties are obtained by writing the constitutive equations (Equation ((2.19)) or ((2.20)) in this case) in terms of the average values of T_i, S_i, D_i, E_i on the RVE:

$$\begin{array}{ll} \overline{T_i} = \frac{1}{V}\int_V T_i dV & \overline{D_i} = \frac{1}{V}\int_V D_i dV \\ \overline{S_i} = \frac{1}{V}\int_V S_i dV & \overline{E_i} = \frac{1}{V}\int_V E_i dV \end{array}$$

where $\overline{\ }$ denotes the average value.

For both types of piezocomposites, matrix $\left[c^{E*}\right]$ is a function of the longitudinal (in the direction of the fibers) and transverse in-plane Young's moduli (E_L and E_T), the in plane Poisson's ratio ν_{LT}, the in-plane shear modulus G_{LT}, and the two out-of-plane shear moduli G_{Lz} and G_{Tz}. Matrix $[e^*]$ is given by

$$[e^*] = [d]\left[c^{E*}\right]$$

where

$$[d] = \begin{bmatrix} d_{31} & d_{32} & 0 & 0 & 0 \end{bmatrix}$$

in the case of d_{31} piezocomposites and

$$[d] = \begin{bmatrix} d_{32} & d_{33} & 0 & 0 & 0 \end{bmatrix}$$

in the case of d_{33} piezocomposites. Note that the coefficients d_{ij} are unchanged under the plane stress hypothesis.

When used as sensors or actuators, piezocomposite transducers are typically equipped with two electrodes. These electrodes impose an equipotential voltage on their surfaces, and the electrical

variables are the voltage difference V across the electrodes, and the electrical charge Q. These two variables are representative of the electrical macro variables which will be used in the numerical models of structures equipped with such transducers : transducers are used either in open-circuit conditions ($Q = 0$ or imposed) or short-circuit conditions ($V = 0$ or imposed). Instead of the average values of D_i and E_i, the macro variables Q and V are therefore used in the homogenization process. For a homogeneous d_{33} transducer (Figure 2.46), the constitutive equations can be rewritten in terms of these macro variables:

$$\begin{Bmatrix} T_2 \\ T_3 \\ T_4 \\ T_5 \\ T_6 \\ Q \end{Bmatrix} = \begin{bmatrix} c_{22}^{(SC*)} & c_{23}^{(SC*)} & 0 & 0 & 0 & -e_{32}^*/p \\ c_{32}^{(SC*)} & c_{33}^{(SC*)} & 0 & 0 & 0 & -e_{33}^*/p \\ 0 & 0 & c_{44}^{(SC*)} & 0 & 0 & 0 \\ 0 & 0 & 0 & c_{55}^{(SC*)} & 0 & 0 \\ 0 & 0 & 0 & 0 & c_{66}^{(SC)*} & 0 \\ e_{32}^*A & e_{33}^*A & 0 & 0 & 0 & \varepsilon_{33}^{s*}A/p \end{bmatrix} \begin{Bmatrix} S_2 \\ S_3 \\ S_4 \\ S_5 \\ S_6 \\ -V \end{Bmatrix} \tag{2.21}$$

where SC stands for 'short-circuit' ($V = 0$), p is the length of the transducer, A is the surface of the electrodes of the equivalent homogeneous transducer and Q is the charge collected on the electrodes.

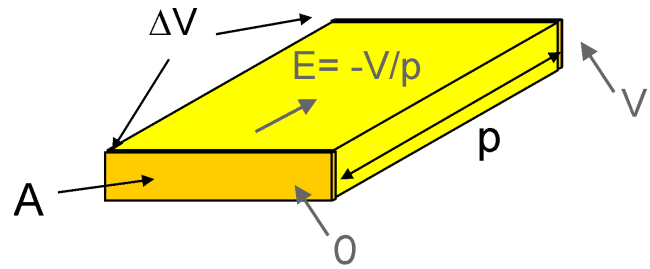

Figure 2.46: Homogeneous model of the d_{33} piezocomposite and definition of the macro variables

For d_{31}-piezocomposites, the approach is identical.

2.7.3 Definition of local problems

The RVE is made of two different materials. In order to find the homogeneous constitutive equations, Equation ((2.21)) is written in terms of the average values of the mechanical quantities S_i and T_i in the RVE and the electrical variables Q and V defined on the electrodes:

$$\begin{Bmatrix} \overline{T_2} \\ \overline{T_3} \\ \overline{T_4} \\ \overline{T_5} \\ \overline{T_6} \\ Q \end{Bmatrix} = \begin{bmatrix} \overline{c_{22}}^{(SC*)} & \overline{c_{23}}^{(SC*)} & 0 & 0 & 0 & -\overline{e_{32}}^{*}/p \\ \overline{c_{32}}^{(SC*)} & \overline{c_{33}}^{(SC*)} & 0 & 0 & 0 & -\overline{e_{33}}^{*}/p \\ 0 & 0 & \overline{c_{44}}^{(SC*)} & 0 & 0 & 0 \\ 0 & 0 & 0 & \overline{c_{55}}^{(SC*)} & 0 & 0 \\ 0 & 0 & 0 & 0 & \overline{c_{66}}^{(SC*)} & 0 \\ \overline{e_{32}}^{*}A & \overline{e_{33}}^{*}A & 0 & 0 & 0 & \overline{\varepsilon_{33}}^{S*}A/p \end{bmatrix} \begin{Bmatrix} \overline{S_2} \\ \overline{S_3} \\ \overline{S_4} \\ \overline{S_5} \\ \overline{S_6} \\ -V \end{Bmatrix} \tag{2.22}$$

The different terms in Equation ((2.22)) can be identified by defining local problems on the RVE. The technique consists in imposing conditions on the different strain components and V and computing the average values of the stress and the charge in order to find the different coefficients. For the electric potential, two different conditions ($V = 0, 1$) are used. For the mechanical part, we assume that the displacement field is periodic in the plane of the transducer: on the boundary of the RVE, the displacement can be written :

$$u_i = \overline{S}_{ij}\, x_j + v_i \tag{2.23}$$

where u_i is the i^{th} component of displacement, $\overline{S}_{ij}$ is the average strain in the RVE (tensorial notations are used), x_j is the j^{th} spatial coordinate of the point considered on the boundary, and v_i is the periodic fluctuation on the RVE. The fluctuation v is periodic in the plane of the transducer so that between two opposite faces (noted A^-/A^+, B^-/B^+ and C^-/C^+, Figure 2.47), one can write ($v(x_j^{K+}) = v(x_j^{K-})$, $K = A, B, C$) :

$$u_i^{K+} - u_i^{K-} = \overline{S}_{ij}\,(x_j^{K^+} - x_j^{K-}) \qquad K = A, B, C \tag{2.24}$$

Because we consider a plate with the plane stress hypothesis $T_1 = 0$, equation (2.24) should not be satisfied for $K = A$ and $j = 1$ (no constraint on the normal displacement on faces A^+ and A^-). For a given value of the average strain tensor ($\overline{S}_{ij}$), equation ((2.24)) defines constraints between the points on each pair of opposite faces. This is illustrated in Figure 2.48, where an average strain S_2 is imposed on the RVE and the constraints are represented for u_2 on faces B^- and B^+.

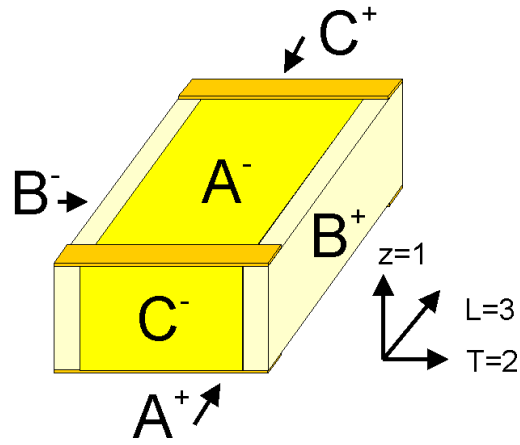

Figure 2.47: Definition of pairs of opposite faces on the RVE

Note that these constraints do not impose that the faces of the RVE remain plane, which is important for the evaluation of the shear stiffness coefficients.

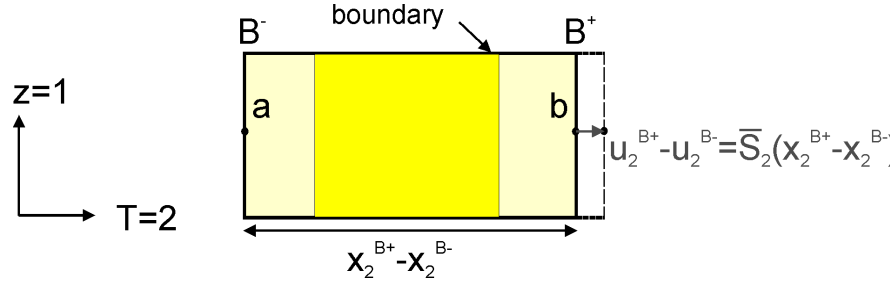

Figure 2.48: Example of an average strain S_2 imposed on the RVE and associated periodic conditions

In total, six local problems are needed to identify all the coefficients in ((2.22)) (Figure 2.49). The first problem consists in applying a difference of potential V to the electrodes of the RVE and imposing zero displacement on all the faces (except the top and bottom). In the next five local problems, the difference of potential is set to 0 (short-circuited condition), and five deformation mechanisms are induced. Each of the deformation mechanisms consists in a unitary strain in one of the directions (with zero strain in all the other directions). For each case, the average values of T_i and S_i, and the charge accumulated on the electrodes Q, are computed, and used to determine all the coefficients in ((2.22)), from which the engineering constants are determined.

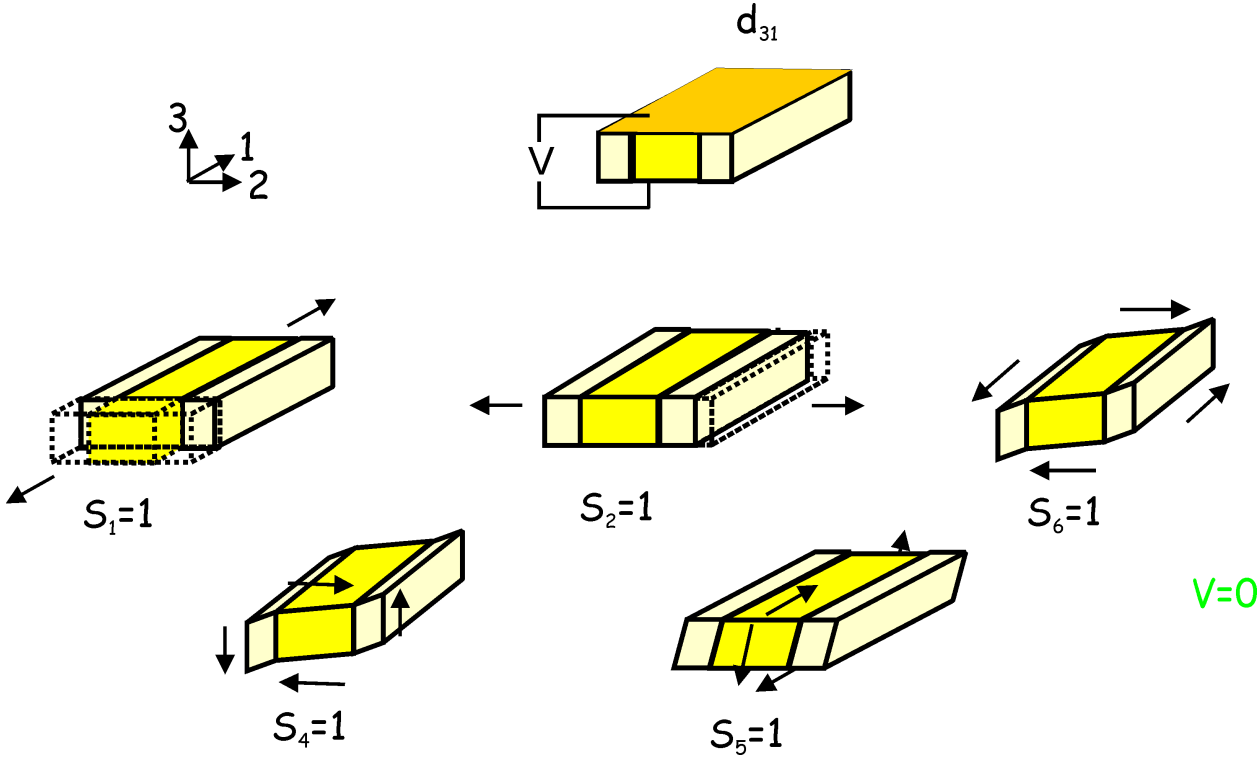

Figure 2.49: The six local problems solved by the finite element method in order to compute the homogenized properties of d_{31}-MFCs

2.7.4 Application of periodic piezoelectric homogenization to $P2$-MFCs

We are going to compute the homogeneous properties of a $P2$-type MFC with varying volume fraction of piezoelectric fibers. We first define the range of volume fractions to compute the homogeneous properties and the dimensions of the RVE.

```
(d_piezo('TutoPz_P2_homo-s1') )
```

```
% See full example as MATLAB code in d_piezo('ScriptPz_P2_homo')
%% Step 1 - Meshing of RVE
% Meshing script can be viewed with sdtweb d_piezo('MeshHomoMFCP2')
Range=fe_range('grid',struct('rho',[0.001 linspace(0.1,0.9,9) .999], ...
  'lx',.300,'ly',.300,'lz',.180,'dd',0.04));
```

Then for each value of the volume fraction of piezoelectric fibers ρ, we compute the solution of the six local problems, the average value of stress, strain and charge. From these values we extract the

engineering mechanical properties, the piezoelectric and dielectric properties.

```
(d_piezo('TutoPz_P2_homo-s2') )

%% Step 2 - Loop on volume fraction and compute homogenize properties
for jPar=1:size(Range.val,1)

RO=fe_range('valCell',Range,jPar,struct('Table',2));% Current experiment

% Create mesh
model= ...
d_piezo(sprintf(['meshhomomfcp2 rho=%0.5g lx=%0.5g ly=%0.5g' ...
  'lz=%0.5g dd=%0.5g'],[RO.rho RO.lx RO.ly RO.lz RO.dd]));


% Define the six local problems
RB=struct('CellDir',[max(model.dx) max(model.dy) max(model.dz)],'Load', ...
       {{'e11','e22','e12','e23','e13','vIn'}});
 % Periodicity on u,v,w on x and y face
 % periodicity on u,v only on the z face
  RB.DirDofInd={[1:3 0],[1:3 0],[1 2 0 0]};
 % Voltage DOFs are always eliminated from periodic conditions

 % Compute the deformation for the six local problems
 def=fe_homo('RveSimpleLoad',model,RB);
 % Represent the deformation of the RVE
 cf=comgui('guifeplot-reset',2);cf=feplot(model,def); fecom('colordatamat')


% Compute stresses, strains and electric field
a1=p_piezo('viewstrain -curve -mean -EltSel MatId1 reset',cf); % Strain epoxy
a2=p_piezo('viewstrain -curve -mean -EltSel MatId2 reset',cf); % Strain piezo
b1=p_piezo('viewstress -curve -mean- EltSel MatId1 reset',cf); % Stress epoxy
b2=p_piezo('viewstress -curve -mean- EltSel MatId2 reset',cf); % Stress piezo

% Compute charge on electrodes
 mo1=cf.mdl.GetData;
  i1=fe_case(mo1,'getdata','Top Actuator');i1=fix(i1.InputDOF);
  mo1=p_piezo('electrodesensq TopQ2',mo1,struct('MatId',2,'InNode',i1));
  mo1=p_piezo('electrodesensq TopQ1',mo1,struct('MatId',1,'InNode',i1));
```

```
  c1=fe_case('sensobserve',mo1,'TopQ1',cf.def); q1=c1.Y;
  c2=fe_case('sensobserve',mo1,'TopQ2',cf.def); q2=c2.Y;


% Compute average values:
a0=a1.Y(1:6,:)*(1-RO.rho)+a2.Y(1:6,:)*RO.rho;
b0=b1.Y(1:6,:)*(1-RO.rho)+b2.Y(1:6,:)*RO.rho;
q0=q1+q2; % Total charge is the sum of charges on both parts of electrode


% Compute C matrix
C11=b0(1,1)/a0(1,1); C12=b0(1,2)/a0(2,2); C22=b0(2,2)/a0(2,2);
C44=b0(4,4)/a0(4,4); C55=b0(5,5)/a0(5,5); C66=b0(6,3)/a0(6,3);
sE=inv([C11 C12; C12 C22]);

% Extract mechanical engineering constants
E1(jPar)=1/sE(1,1); E2(jPar)=1/sE(2,2); nu12(jPar)=-sE(1,2)*E1(jPar);
nu21(jPar)=-sE(1,2)*E2(jPar);G12(jPar)=C66; G23(jPar)=C44; G13(jPar)=C55;

% Extract piezoelectric properties
e31(jPar)=b0(1,6)*RO.lz; e32(jPar)=b0(2,6)*RO.lz;
d=[e31(jPar) e32(jPar)]*sE; d31(jPar)=d(1); d32(jPar)=d(2);

% Extract dielectric properties
eps33(jPar)=-q0(6)*RO.lz/(RO.lx*RO.ly);
eps33t(jPar)=eps33(jPar)+ [d31(jPar) d32(jPar)]*[e31(jPar); e32(jPar)];

end % Loop on rho0 values
```

Figure 2.50 represents the solution of the six local problems for $\rho = 0.6$.
We can now plot the evolution of the homogeneous properties of the $P2$-type MFC as a function of the volume fraction ρ:
(d_piezo('TutoPz_P2_homo-s3'))

```
%% Step 3 - Homogeneous properties as a function of volume fraction
rho0=Range.val(:,strcmpi(Range.lab,'rho'));

out=struct('X',{{rho0,{'E_T','E_L','nu_{LT}','G_{LT}','G_{Tz}','G_{Lz}', ...
    'e_{31}','e_{32}','d_{31}','d_{32}','epsilon_{33}^T'}},'Xlab',...
    {{'\rho','Component'}},'Y',[E1' E2' nu21' G12' G13' G23' e32' e31' ...
```

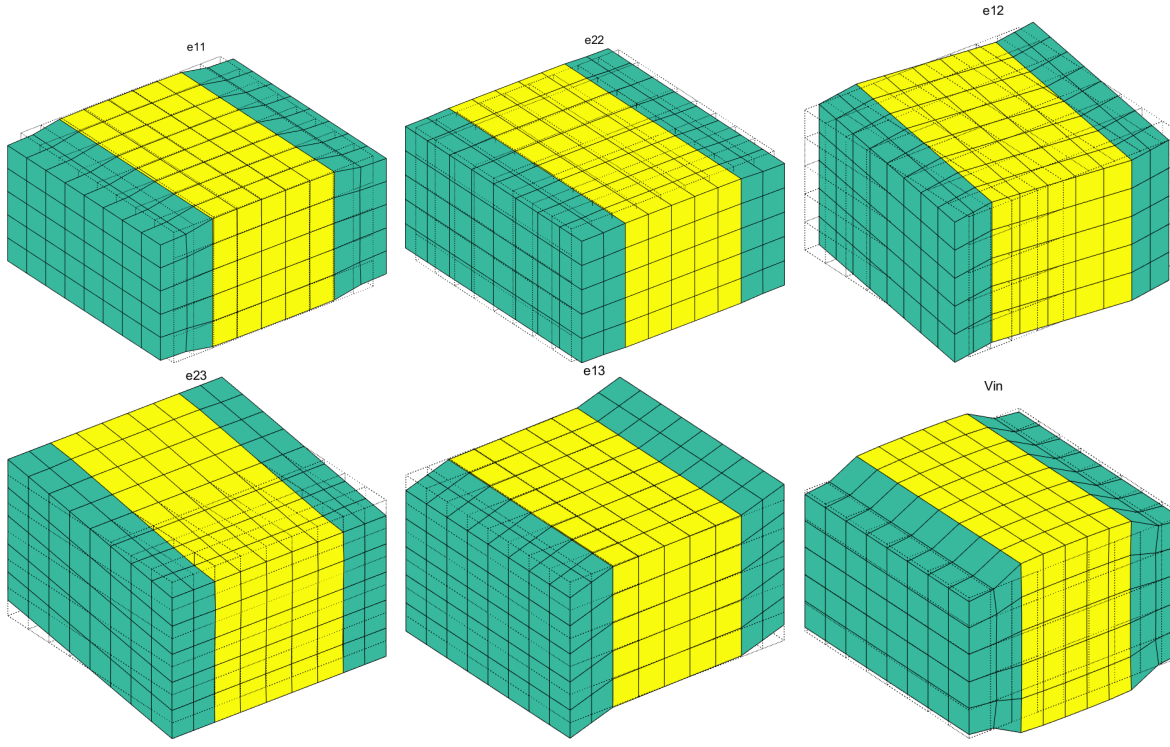

Figure 2.50: Solutions of the six local problems on the RVE for $\rho = 0.6$ for a $P2$-type MFC

```
    d32' d31' eps33t'/8.854e-12]);

ci=iiplot; iicom('CurveReset');
iicom(ci,'CurveInit','P2-MFC homogenization',out);
```

Figure 2.51 represents the evolution of the mechanical properties and Figure 2.52 represents the evolution of the piezoelectric and dielectric properties as a function of ρ. The properties of MFC transducers correspond to the value of $\rho = 0.86$.

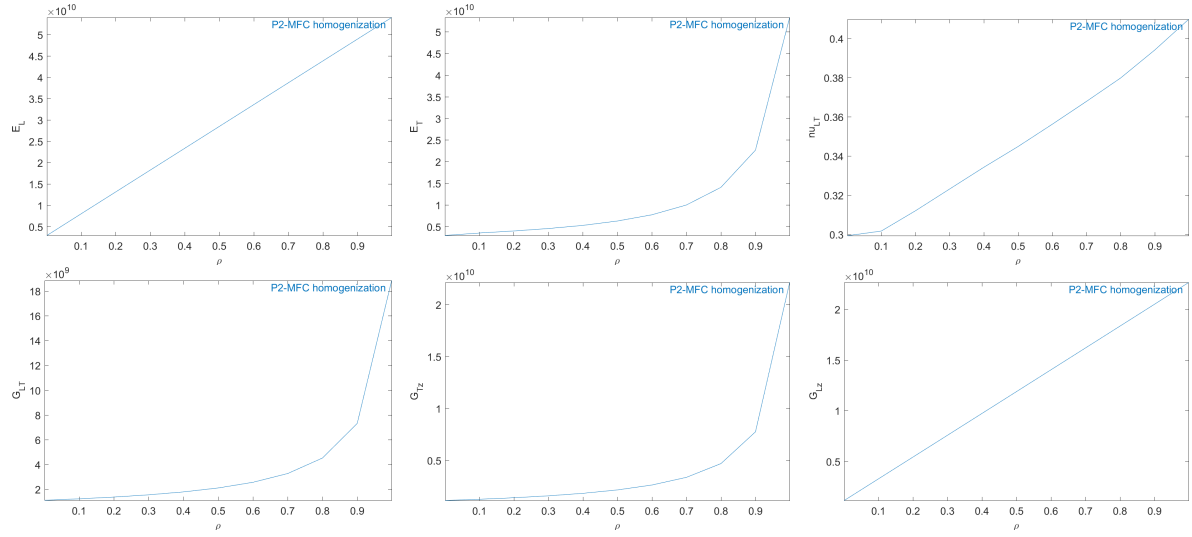

Figure 2.51: Evolution of the homogeneous mechanical properties of a $P2$-type piezocomposite as a function of ρ

2.7.5 Application of periodic piezoelectric homogenization to $P1$-MFCs

We are now going to compute the homogeneous properties of a $P1$-type MFC with varying volume fraction of piezoelectric fibers. We first define the range of volume fractions to compute the homogeneous properties and the dimensions of the RVE.

```
(d_piezo('TutoPz_P1_homo-s1') )

% See full example as MATLAB code in d_piezo('ScriptPz_P1_homo')
%% Step 1 - Meshing or RVE and definition of volume fractions
% Meshing script can be viewed with sdtweb d_piezo('MeshHomoMFCP1')
```

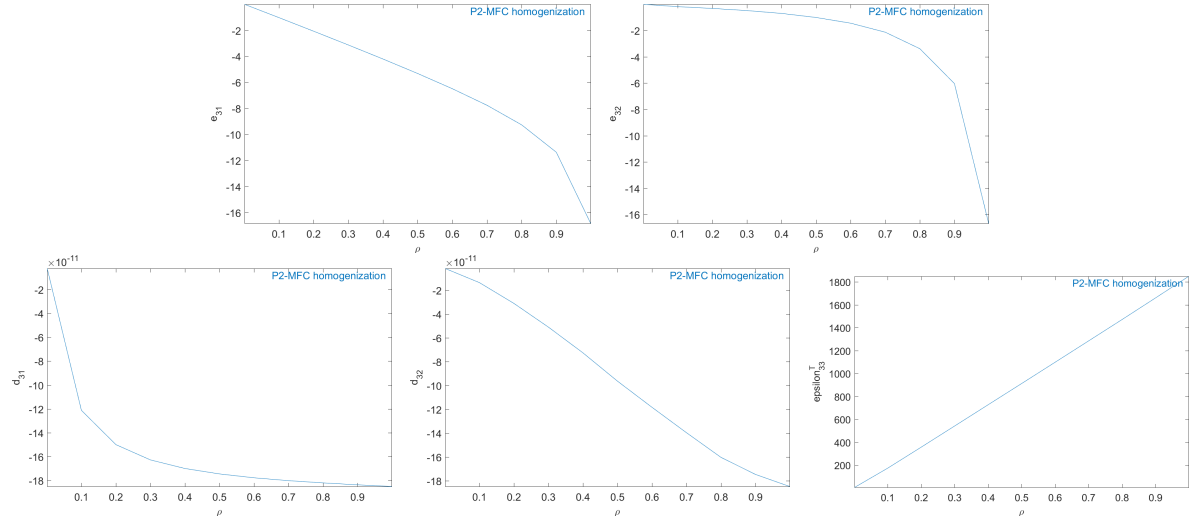

Figure 2.52: Evolution of the homogeneous piezoelectric and dielectric properties of a $P2$-type piezocomposite as a function of ρ

```
Range=fe_range('grid',struct('rho',[0.001 linspace(0.1,0.9,9) .999], ...
  'lx',.18,'ly',.18,'lz',1.080,'e',0.09,'dd',0.04));
```

Then for each value of the volume fraction of piezoelectric fibers ρ, we compute the solution of the six local problems, the average value of stress, strain and charge. From these values we extract the engineering mechanical properties, the piezoelectric and dielectric properties.

```
(d_piezo('TutoPz_P1_homo-s2') )

%% Step 2 - Loop on volume fractions and computation of homogenized properties
for jPar=1:size(Range.val,1)

RO=fe_range('valCell',Range,jPar,struct('Table',2));% Current experiment

% Create mesh
model=...
d_piezo(sprintf(['meshhomomfcp1 rho=%0.5g lx=%0.5g ly=%0.5g lz=%0.5g' ...
   ' e=%0.5g dd=%0.5g'],[RO.rho RO.lx RO.ly RO.lz RO.e RO.dd]));

%%
RB=struct('CellDir',[max(model.dx) max(model.dy) max(model.dz)],'Load', ...
```

```
           {{'e33','e11','e23','e12','e13','vIn'}});
 % It seems fe_homo reorders the strains
 % Periodicity on u,v,w on x and z face
 % periodicity on u,w only on the y face
 % Voltage DOFs are always eliminated from periodic conditions
 RB.DirDofInd={[1:3 0],[1 0 3 0],[1:3 0]};
 def=fe_homo('RveSimpleLoad',model,RB);

cf=comgui('guifeplot-reset',2);
cf=feplot(model,def); fecom('colordatamat'); fecom('triax')


% Electric field for Vin
p_piezo('electrodeview -fw',cf); % to see the electrodes on the mesh
cf.sel(1)={'groupall','colorface none -facealpha0 -edgealpha.1'};
p_piezo('viewElec EltSel "matid1:2" DefLen 0.07 reset',cf);
fecom('scd 1e-10')


% Compute stresses, strains and electric field
a1=p_piezo('viewstrain -curve -mean -EltSel MatId1 reset',cf); % Strain S epoxy
a2=p_piezo('viewstrain -curve -mean -EltSel MatId2 reset',cf); % Strain S piezo
b1=p_piezo('viewstress -curve -mean- EltSel MatId1 reset',cf); % Stress T
b2=p_piezo('viewstress -curve -mean- EltSel MatId2 reset',cf); % Stress T

% Compute charge
 mo1=cf.mdl.GetData;
  i1=fe_case(mo1,'getdata','Top Actuator');i1=fix(i1.InputDOF);
  mo1=p_piezo('electrodesensq TopQ2',mo1,struct('MatId',2,'InNode',i1));
  mo1=p_piezo('electrodesensq TopQ1',mo1,struct('MatId',1,'InNode',i1));
  c1=fe_case('sensobserve',mo1,'TopQ1',cf.def); q1=c1.Y;
  c2=fe_case('sensobserve',mo1,'TopQ2',cf.def); q2=c2.Y;

% Compute average values:
a0=a1.Y(1:6,:)*(1-RO.rho)+a2.Y(1:6,:)*RO.rho;
b0=b1.Y(1:6,:)*(1-RO.rho)+b2.Y(1:6,:)*RO.rho;
q0=q1+q2; %total charge is the sum of charges

% Compute C matrix
C11=b0(3,2)/a0(3,2); C12=b0(3,1)/a0(1,1); C22=b0(1,1)/a0(1,1);
C44=b0(5,5)/a0(5,5); C55=b0(4,4)/a0(4,4); C66=b0(6,3)/a0(6,3);
```

```
sE=inv([C11 C12; C12 C22]);
E1(jPar)=1/sE(1,1); E2(jPar)=1/sE(2,2); nu12(jPar)=-sE(1,2)*E1(jPar);
nu21(jPar)=-sE(1,2)*E2(jPar);
e33(jPar)=b0(3,6)*RO.lz;
e31(jPar)=b0(1,6)*RO.lz;
eps33(jPar)=-q0(6)*RO.lz/(RO.ly*RO.lx);
d=[e33(jPar) e31(jPar)]*sE; d33(jPar)=d(1); d31(jPar)=d(2);
eps33t(jPar)=eps33(jPar)+ [d33(jPar) d31(jPar)]*[e33(jPar); e31(jPar)];
G12(jPar)=C44;
G23(jPar)=C66;
G13(jPar)=C55;

end % loop on Rho values
```

Figure 2.53 represents the solution of the six local problems for $\rho = 0.6$.

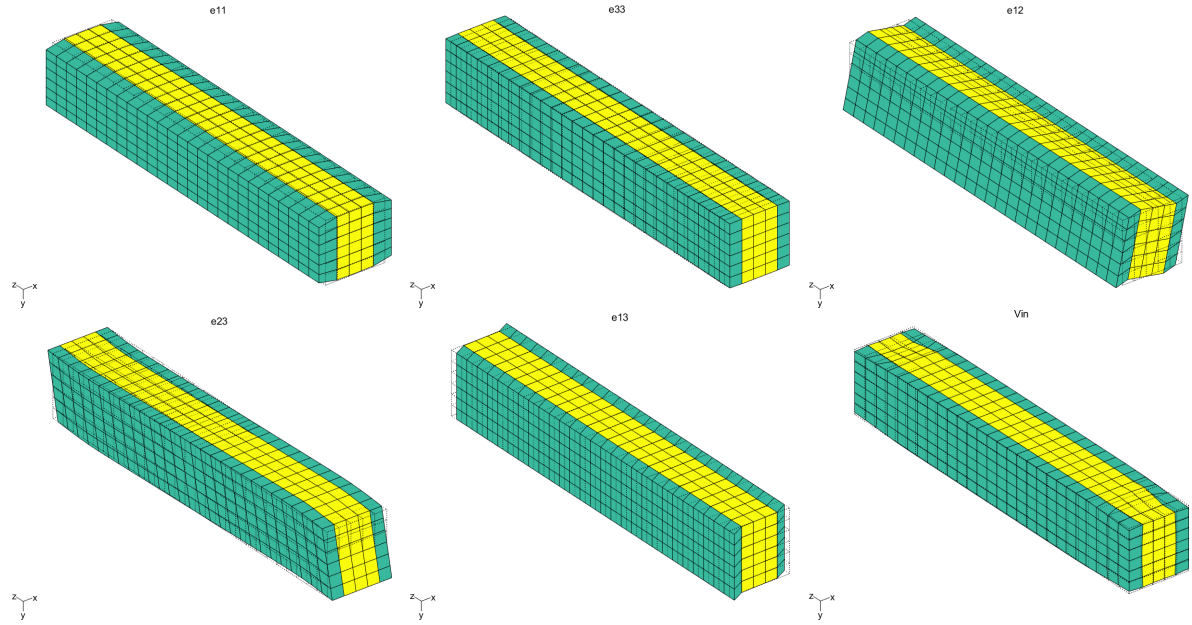

Figure 2.53: Solutions of the six local problems on the RVE for $\rho = 0.6$

Figure 2.54 represents the inhomogeneous electric field for the sixth local problem (applied voltage) and $\rho = 0.6$.

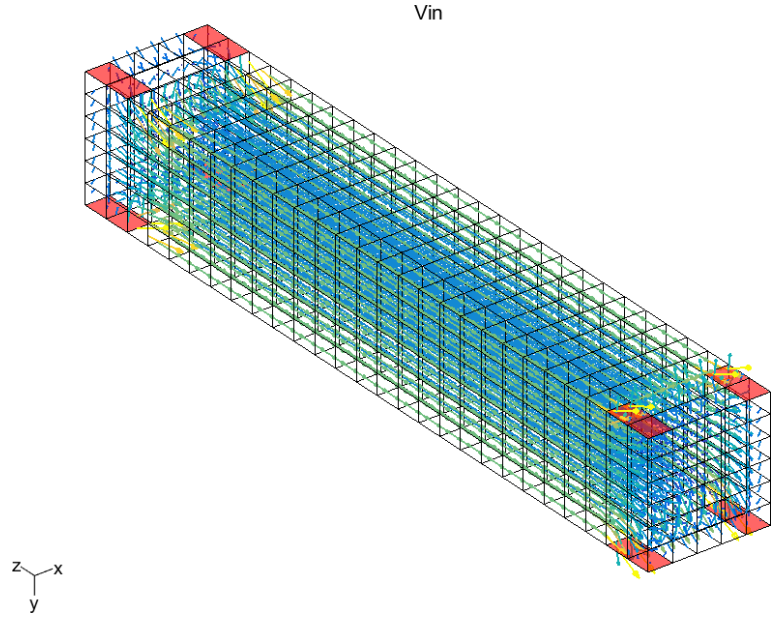

Figure 2.54: Electric field for the sixth local problem (applied voltage) on the RVE of a $P1$-type MFC for $\rho = 0.6$

We can now plot the evolution of the homogeneous properties of the $P1$-type MFC as a function of the volume fraction ρ

```
(d_piezo('TutoPz_P1_homo-s3') )

%% Step 3 - Plot homogeneous properties as a function of volume fraction
rho0=Range.val(:,strcmpi(Range.lab,'rho'));

out=struct('X',{{rho0,{'E_L','E_T','nu_{LT}','G_{LT}','G_{Lz}','G_{Tz}', ...
    'e_{31}','e_{33}','d_{31}','d_{33}','epsilon_{33}^T'}}},'Xlab',...
    {{'\rho','Component'}},'Y',[E1' E2' nu12' G12' G13' G23' e31' e33' ...
    d31' d33' eps33t'/8.854e-12]);
ci=iiplot;
iicom('CurveReset');
iicom(ci,'CurveInit','P1-MFC homogenization',out);
```

Figure 2.55 represents the evolution of the mechanical properties and Figure 2.56 represents the evolution of the piezoelectric and dielectric properties as a function of ρ. The properties of MFC transducers correspond to the value of $\rho = 0.86$.

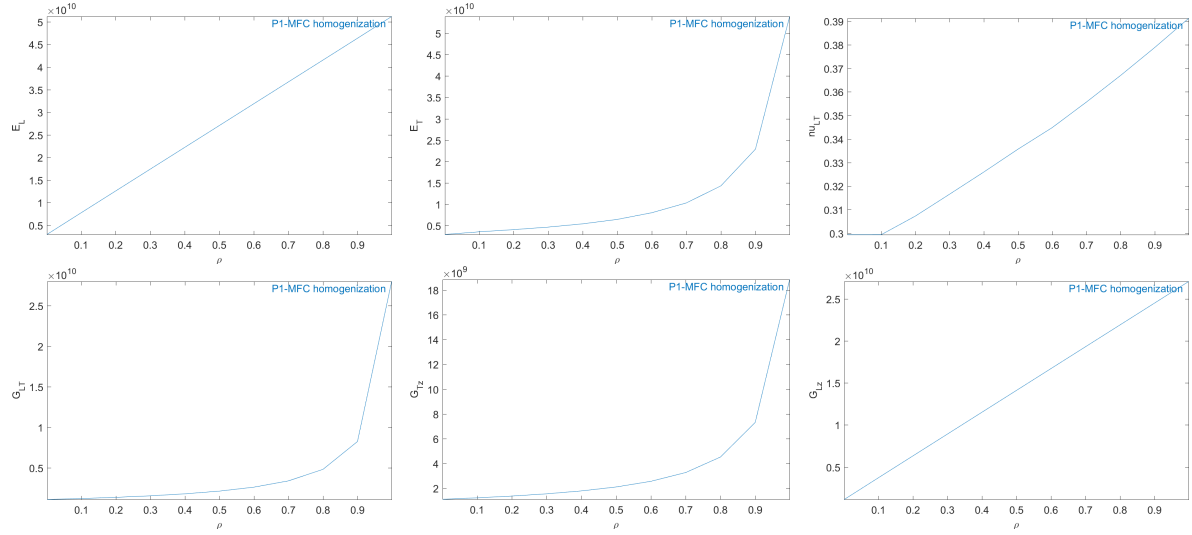

Figure 2.55: Evolution of the homogeneous mechanical properties of a $P1$-type piezocomposite as a function of ρ

All the properties match well the results presented in [3]

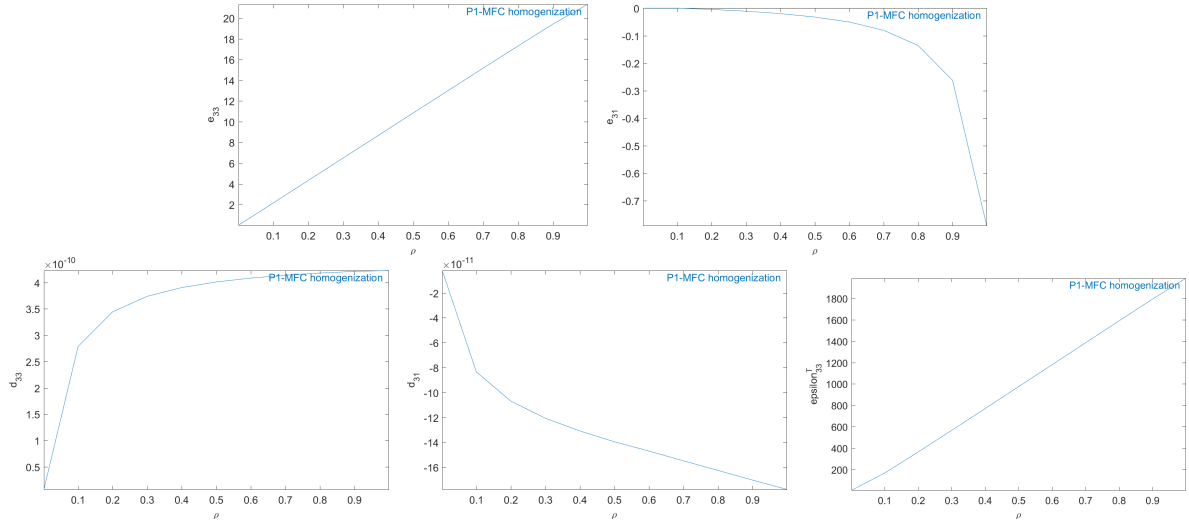

Figure 2.56: Evolution of the homogeneous piezoelectric and dielectric properties of a $P1$-type piezocomposite as a function of ρ

2.8 External links

References to external documents. In SDT use `sdtweb('ref')` to open the page.

- `hexa8` element function in SDT see `hexa8`.
- `feplot` SDT function of mesh display, see `feplot`.
- `FindNode` SDT help on node selection, see `findnode`.
- `fe2ss` building of state space models `fe2ss`.
- `DofSet` SDT entry for enforced displacement. See `fe_case#DofSet`.
- `SensDOF` SDT entry sensors See `fe_case#SensDOF`.
- `2` documentation of composite shell, see `p_shell#2`.
- `p_solid` element property function for volumes, `p_solid`
- `m_elastic` material property function , `m_elastic`
- `resultant` `sensor#resultant`

- `fe_simul` access to base solvers `fe_simul`
- end

Function reference

Contents

Piezo related functions	
d_piezo	support for demonstration of piezo capabilities
p_piezo	piezoelectric volume and shell property handling
m_piezo	piezoelectric material property handling

d_piezo

Purpose

Support function for piezoelectric demos

Syntax

```
sdtweb('_taglist','d_piezo')  % display contents
```

Accepted commands are

Script

These commands group sample scripts. Use d_piezo to display tag list and see available contents.

MeshPlate

Meshing utilities for the placement of piezoelectric patches on a supporting structure (flat plate for now).
The options are specified in a structure with fields

- .list : defines a list of features to be introduced with columns giving name,LamSpec,Geo, name laminate specification and shape options.
- .unit : gives the model unit (needed since patch dimensions are always given in mm).

The laminate specification string is composed of the following

- BaseId*i* gives the ProId of the base laminate which is then used to figure out the position of patches.
- +Patch or -Patch to place a patch above or below the base laminate.
- Patch itself is a specification of a patch material and geometry. The list of implemented patch can be obtained using m_piezo Patch
- .In to specify that the patch has an enforced voltage.

The geometry/position specification string Geo can be

- a specification of the patch corner and orientation such as xc=.03 yc=.05 ang=30 if the patch geometry is specified using the laminate specification.
- rect shapes [xc lx nx yc ly ny alpha MatId ProId] where MatId and ProId are filled automatically if not provided.

- `circ` shapes `[xc yc rc lc (MatId ProId)]`
- `global lx=.4 ly=.3 lc=.02 -Sens`. The option `-Sens` generates a sensor entry corresponding to normal displacement of the initial mesh. Alternatively you can add a sensor configuration `SensDOF` entry see `sdtweb('sensor#scell')` or `sdtweb('sensor#sstruct')`.

```
% Start by defining properties of the underlying laminate
mdl=struct('Node',[],'Elt',[], ... % empty model
    'pl', ... % composite layer property
      [1 fe_mat('m_elastic','SI',1) 42.5e9 .042 1490 3.35e9 .01], ...
     'il', ... % laminate definition (6 layers at 0,90,0,90,0,90)
     p_shell(['dbval 1 laminate    1 2.167e-4 0    1 2.167e-4 90 ' ...
         '1 2.167e-4 0 1 2.167e-4 90 1 2.167e-4 0 1 2.167e-4 90']), ...
     'unit','SI');
RG=struct;
RG.list={'Name','Lam','shape'
   'Main_plate', mdl,'global lx=.4 ly=.3 lc=.02'
   'Act1','BaseId1 +SmartM.MFC-P1.2814 -SmartM.MFC-P1.2814.in','xc=.35 yc=.25 ang=30'
   'Sen2','BaseId1 +SmartM.MFC-P1.2814','xc=.03 yc=.05 ang=30'
   'Sen3','BaseId1 +Noliac.NCE51.OD25TH1','xc=.05 yc=.25'
   };
cf=feplot;d_piezo('MeshPlate',RG);cf.mdl.name='Plate with piezo';
p_piezo('electrodeinfo',cf.mdl.GetData)
matgui('jil',cf);matgui('jpl',cf); % Display properties
```

The following illustrates transient simulation to a load on a specific piezo

```
model=cf.mdl.GetData; model=p_piezo('electrode2case',model);
opt=fe_time('TimeOpt Newmark .25 .5 0 .3e-6 200');
opt.AssembleCall='assemble -fetime Load';
%opt.FinalCleanupFcn='out.DOF=model.DOF;
%out.def=[Case.T*out.def+Case.TIn*[0 ft(1:end-1)'']];';
model=stack_set(model,'info','Rayleigh',[0 2*.0025/200e3]);
def=fe_time(opt,cf.mdl);def.name=model.name;
cf.def=def; fecom('colordataevalRadZ-edgealpha0');fecom('scc1e-10');
```

Mesh

`Patch` Simple volume patch.

`Plate` Generic script for arbitrary placement of patches on a flat plate. A list of shapes can be given as a cell array. This is considered as a demo since it currently only supports a rectangular base plate.
`GammaS` build a weighting for surface control.

m_piezo

Purpose

Material function for piezoelectric solids

Syntax

```
mat= m_piezo('database name')
pl = m_piezo('dbval MatId  -elas 12 Name');
```

See section 2 for tutorial calls. Accepted commands are

`[ Database, Dbval] [-unit TY] [,MatiD]] Name`

m_piezo contains a number of defaults obtained with the database and dbval commands which respectively return a structure or an element property row. You can select a particular entry of the database with using a name matching the database entries.
Piezoelectric materials are associated with two material identifiers, the main defines the piezoelectric properties and contains a reference ElasMatId to an elastic material used for the elastic properties of the material (see m_elastic for input formats).

```
m_piezo('info') % List of materials in data base
% database piezo and elastic properties
pl=m_piezo('dbval 3 -elas 12 Sample_ULB')
```

Theoretical details on piezoelectric materials are given in chapter 1. The m_piezo Const and BuildConstit commands support integration constant building for piezo electric volumes integrated in the standard volume elements. Element properties are given by p_solid entries, while materials formats are detailed here.

Patch

Supports the specification of a number of patches available on the market. The call uses an option structure with fields

- .name of the form ProId*val+patchName*. For example ProId1+SmartM.MFC-P1.2814.
- MatId value for the initial MatId.

m_piezo('patch') lists currently implemented geometries. In particular

- Noliac.Material.Geometry is used for circular patches by Noliac. Fields for the geometry are
  - OD outer diameter (mm).

- TH Thickness (mm). To specify a milimiter fraction replace the . by and _. For example TH0_7 is used for TH=0.7 mm.
- ID inner diameter (mm) (optional for piezo rings).

- SmartM.Material.Geometry is used for circular patches by Noliac. The geometry is coded assuming a rectangle in mm. Thus 2814 corresponds to an 28 x 14 mm active rectangle.

The piezoelectric constants can be declared using the following sub-types

1 : Simplified 3D piezoelectric properties

[ProId Type ElasMatId d31 d32 d33 eps1T eps2T eps3T EDType]
These simplified piezoelectric properties (1.54) can be used for PVDF, but also for PZT if shear mode actuation/sensing is not considered ($d_{24} = d_{15} = 0$). For EDType==0 on assumes d is given. For EDType==1, e is given. Note that the values of ε^T (permitivity at zero stress) should be given (and not ε^S).

2 : General 3D piezo

[ProId Type ElasMatId d_1:18 epsT_1:9]
d_1:18 are the 18 constants of the $[d]$ matrix (see section 1.2.1), and epsT_1:9 are the 9 constants of the $\left[\varepsilon^T\right]$ matrix. One reminds that strains are stored in order xx, yy, zz, yz, zx, yx.

3 : General 3D piezo, e matrix

[ProId Type ElasMatId e_1:18 epsT_1:9]
e_1:18 are the 18 constants of the $[d]$ matrix, and epsT_1:9 are the 9 constants of the $\left[\varepsilon^T\right]$ matrix in the constitutive law (see section 1.2.1).

See also

p_piezo.

p_piezo

Purpose

Property function for piezoelectric shells and utilities associated with piezoelectric models.

Syntax

```
mat= m_piezo('database name')
pl = m_piezo('dbval MatId  -elas 12 Name');
```

See section 2 for tutorial calls. Accepted commands are

ElectrodeMPC

`[model,InputDOF(end+1,1)]=p_piezo('ElectrodeMPC Name',model,'z==5e-5');` defines the isopotential constraint as a case entry `Name` associated with `FindNode` command `z==5e-5`. An illustration is given in section 2.5 .
Accepted command options are

- `-Ground` defines a fixed voltage constraint `FixDof,V=0 on` *Name*.
- `-Input"InName"` defines an enforced voltage `DofSet,`*InName* entry for voltage actuation.
- `MatId`*i* is used to define a resultant sensor to measure the charge associated with the electrode. Note that the electrode surface must not be inside the volume with `MatId`*i*. If that is the case, you must arbitrarily decompose your mesh in two parts with different `MatId`. You can also generate this sensor a posteriori using `ElectrodeSensQ`, which attempts to determine the `MatId`*i* based on the search of a piezoelectric material connected to the MPC.

ElectrodeSensQ

`model=p_piezo('ElectrodeSensQ 1682 Q-Base',model);` adds a charge sensor (`resultant`) called `Q-Base` on node `1682`. (See (1.59) for theory).
For **shells**, the node number is used to identify the `p_piezo` shell property and thus the associated elements. It is reminded that `p_piezo` entries must be duplicated when multiple patches are used.
For **volumes**, the `p_piezo ElectrodeMPC` should be first defined, so that it can be used to obtain the electrode surface information.
Note that the command calls `fe_case('SensMatch')` so that changes done to material properties after this call will not be reflected in the observation matrix of this sensor.
To obtain sensor combinations (add charges of multiple sensors as done with specific wiring), specify a data structure with observation `.cta` at multiple `.DOF` as illustrated below.
For a voltage sensor, you can simply use a DOF sensor
`model=fe_case(model,'SensDof','V-Base',1682.21)`.

```
model=d_piezo('meshULBPlate cantilever');  % creates the model
% If you don't remember the electrode node numbers
p_piezo('ElectrodeDOF',model)
% Combined charge
r1=struct('cta',[1 1],'DOF',[1684;1685]+.21,'name','QS2+3');
model=p_piezo('ElectrodeSensQ',model,r1);
sens=fe_case(model,'sens');
% Combined voltage
r1=struct('cta',[1 1],'DOF',[1684;1685]+.21,'name','VS2+3');
model=fe_case(model,'SensDof',r1.name,r1);
sens=fe_case(model,'sens');sens.lab
```

ElectrodeDOF

`p_piezo('ElectrodeDof Bottom',model)` returns the DOF the bottom electrode. With no name for selection `p_piezo('ElectrodeDof',model)` the command returns the list of electrode DOFs based on MPC defined using the `ElectrodeMPC` command or `p_piezo` shell entries. Use `ElectrodeDof.*` to get all DOFs.

ElectrodeView ...

`p_piezo('electrodeview',cf)` outlines the electrodes in the model and prints a clear text summary of electrode information. To only get the summary, pass a model `model` rather than a pointer `cf` to a `feplot` figure.

`p_piezo('electrodeviewCharge',cf)` builds a `StressCut` selection allowing the visualization of charge density. You should be aware that only resultant charges at nodes are known. For proper visualization a transformation from charge resultant to charge density is performed, this is known to have problem in certain cases so you are welcome to report difficulties.

Electrode2Case

`Electrode2Case` uses electrode information defined in the obsolete `Electrode` stack entry to generate appropriate case entries : `V_In` for enforced voltage actuators, `V_Out` for voltage measurements, `Q_Out` for charge sensors.

ElectrodeInit

`ElectrodeInit` analyses the model to find electric master DOFs in piezo-electric shell properties or in MPC associated with volume models.

Tab

Tab commands are used to generate tabulated information about model contents. The calling format is p_piezo('TabDD',model). With no input argument, the current feplot figure is used. Currently generated tabs are

- TabDD constitutive laws
- TabPro material and element parameters shown as java tables.

View

p_piezo('ViewDD',model) displays information about piezoelectric constitutive laws in the current model.
p_piezo('ViewElec ...',model) is used to visualize the electrical field. An example is given in section 2.6 . Command options are DefLen*val* to specify the arrow length, EltSel*val* for the selection of elements to be viewed, Reset to force reinit of selection.
ViewStrain and ViewStress follow the same calling format.

Shell element properties

Piezo shell elements with electrodes are declared by a combination of a mechanical definition as a layered composite, see p_shell 2, and an electrode definition with element property rows of the form
[ProId Type MecaProId ElNodeId1 LayerId1 UNU1 ElNodeId2...]

- Type typically fe_mat('p_piezo','SI',1)
- MecaProId : ProId for mechanical properties of element p_shell 2 composite entry. The MatId*i* for piezo layers must be associated with piezo electric material properties.
- ElNodId1 : NodeId for electrode 1. This needs to be a node declared in the model but its position is not used since only the value of the electric potential (DOF 21) is used. You may use a node of the shell but this is not necessary.
- LayerId : layer number as declared in the composite entry.
- UNU1 : currently unused property (angle for polarization)

The constitutive law for a piezoelectric shell are detailed in section 1.3.2 . The following gives a sample declaration.

```
model=femesh('testquad4'); % Shell MatId 100 ProdId 110

% MatId 1 : steel, MatId 12 : PZT elastic prop
```

```
model.pl=m_elastic('dbval 1  Steel');
% Sample ULB piezo material, sdtweb m_piezo('sample_ULB')
model.pl=m_piezo(model.pl,'dbval 3 -elas 12 Sample_ULB');

% ProId 111 : 3 layer composite (mechanical properties)
model.il=p_shell(model.il,['dbval 111 laminate ' ...
    '3 1e-3 0 ' ...  % MatID 3 (PZT),   1 mm piezo, 0
    '1 2e-3 0  ' ... % MatID 1 (Steel), 2 mm
    '3 1e-3 0']);    % MatID 3 (PZT),   1 mm piezo, 0
% ProId 110 : 3 layer piezo shell with electrodes on nodes 1682 and 1683
model.il=p_piezo(model.il,'dbval 110 shell 111 1682 1 0 1683 3 0');

p_piezo('viewdd',model) % Details about the constitutive law
p_piezo('ElectrodeInfo',model) % Details about the layers
```

Bibliography

[1] J. Yang, *An introduction to the theory of piezoelectricity.* Springer, 2010.

[2] "IEEE standards on piezoelectricity, ans n° 176-187, IEEE," 1988.

[3] A. Deraemaeker and H. Nasser, "Numerical evaluation of the equivalent properties of Macro Fiber Composite (MFC) transducers using periodic homogenization," *International Journal of Solids and Structures*, vol. 47, pp. 3272–3285, 2010.

[4] W. Wilkie, R. Bryant, J. High, R. Fox, R. Hellbaum, A. Jalink, B. Little, and P. Mirick, "Low-cost piezocomposite actuator for structural control applications," in *Proc. SPIE 7th Annual Int. Symp. Smart. Struct. Mater.*, (Newport Beach, USA), 2000.

[5] A. Deraemaeker, H. Nasser, A. Benjeddou, and A. Preumont, "Mixing rules for the piezoelectric properties of Macro Fiber Composites," *Journal of Intelligent Material Systems and Structures*, vol. 20(12), pp. 1391–1518, 2009.

[6] A. Deraemaeker, G. Tondreau, and F. Bourgeois, "Equivalent loads for two-dimensional distributed anisotropic piezoelectric transducers with arbitrary shapes attached to thin plate structures," *Journal of the Acoustical Society of America*, vol. 129(2), pp. 681–690, 2011.

[7] G. Tondreau, S. Raman, and A. Deraemaeker, "Point load actuation on plate structures based on triangular piezoelectric patches," *Smart Structures and Systems*, vol. 13(4), pp. 547–565, 2014.

[8] P. Soltani, G. Kerschen, G. Tondreau, and A. Deraemaeker, "Piezoelectric vibration damping using resonant shunt circuits: an exact solution," *Smart Materials and Structures*, vol. 23, 2014. 125014.

[9] N. Hagood, R. Kindel, K. Ghandi, and P. Gaudenzi, "Improving transverse actuation of piezoceramics using interdigitated surface electrodes," in *Proc. SPIE Vol. 1917, p. 341-352, Smart Structures and Materials 1993: Smart Structures and Intelligent Systems, Nesbitt W. Hagood; Ed.* (N. W. Hagood, ed.), vol. 1917, pp. 341–352, 1993.